INDEPENDENT PARTICLE THEORY WITH ELECTRON CORRELATION

By

ARIANA BESTE

A DISSERTATION PRESENTED TO THE GRADUATE SCHOOL
OF THE UNIVERSITY OF FLORIDA IN PARTIAL FULFILLMENT
OF THE REQUIREMENTS FOR THE DEGREE OF
DOCTOR OF PHILOSOPHY

UNIVERSITY OF FLORIDA

2004

ACKNOWLEDGMENTS

I would like to express my gratitude to my advisor, Dr. Rodney J. Bartlett, for all his guidance and support during the past few years. I would also like to thank Dr. Ajith Perera and Dr. Monika Musial for their help, and for all the interesting conversations we had.

I thank the members of my committee, Dr. Samuel B. Trickey, Dr. Jeffrey L. Krause, Dr. Philip J. Brucat, and Dr. Dmitrii Maslov. My thanks also go to the members of our research group (in particular Igor Schweigert and Thomas Henderson) for the exchange of scientific ideas and fruitful conversations. I would also like to thank my parents (Gudrun and Herbert Beste) for their never-ending support through all the stages of my life.

I thank the Air Force Office of Scientific Research for funding.

TABLE OF CONTENTS

LIST OF TABLES

LIST OF FIGURES

Abstract of Dissertation Presented to the Graduate School
of the University of Florida in Partial Fulfillment of the
Requirements for the Degree of Doctor of Philosophy

INDEPENDENT PARTICLE THEORY WITH ELECTRON CORRELATION

By

Ariana Beste

May 2004

Chair: Rodney J. Bartlett
Major Department: Chemistry

A correlated independent particle (CIP) model is formulated where the effective Hamiltonian is composed of the Fock operator and a correlation potential. The CIP model can be regarded as a generalized Hartree-Fock model that includes correlation, or as an approximation to density matrix functional theory, where the density matrix is restricted to be idempotent. Within the model, the kinetic energy and the exchange energy can be expressed exactly, leaving the correlation energy functional as the remaining unknown. Inspired by the extended Koopman's theorem, the condition of exactness of the ionization potentials and electron affinities as the eigenvalues of the effective one-particle operator is chosen on the correlation potential.

If no truncation is introduced, the equation-of-motion coupled-cluster method for ionization potentials and electron affinities (IP-EOM-CC/EA-EOM-CC) yields exact ionization potentials and electron affinities. An energy-dependent correlation potential is obtained from a partitioned equation-of-motion approach which reproduces IP-EOM-CC and EA-EOM-CC results as orbital energies. As a consequence of the energy dependence of the correlation potential, a different effective Hamiltonian corresponds to each orbital and each eigenvalue. The equivalence of the correlation

potential to the energy-dependent self-energy used in the propagator method with respect to the eigenvalues is shown if the coupled-cluster wave function is used for the ground state.

The energy dependence is regarded as a disadvantage, but can be removed by using the Fock space coupled-cluster method in the one-hole and the one-particle space (which is equivalent to the IP-EOM-CC and EA-EOM-CC method) to extract a correlation potential. The resultant correlation potential is energy-independent and universal for all orbitals. In a one-step procedure, the exact FS-CC results for ionization potentials and electron affinities are obtained within the CIP model.

Further, the infinite-order correlation potential derived from the Fock space coupled-cluster approach is approximated by a potential correct through second-order in perturbation. To improve the orbitals compared to the Hartree-Fock method, the Brillouin-Brueckner condition correct through second-order in perturbation is superimposed. Results for ionization potentials, and electron affinities and properties are given for some sample molecules.

CHAPTER 1
INTRODUCTION

Because of their conceptional simplicity, independent particle models play an essential role in electronic structure theory. Their solutions (molecular orbitals) provide the conceptional framework for much of chemistry. Different independent particle models emphasize different criteria in their generation and their solutions; and associated eigenvalues form the basis for elements ranging from photoelectronic spectra to frontier molecular-orbital theories.

The most widely used independent particle models are density functional theory and Hartree-Fock theory. Theoretical justification for the former was given by Hohenberg and Kohn [1]. It is a density-based theory that is formally exact and incorporates correlation effects. Today's popular version of DFT was initialized by Kohn and Sham [2]. In it orbitals were introduced to describe the kinetic energy and the exact density. In the resultant model, eigenvalue equations for one-electron functions and their corresponding energies are solved. Correlation is included through an unknown (but often approximated [3, 4]) potential. This potential also has to account for the kinetic energy correction, because the kinetic energy in the Kohn Sham model is that of a noninteracting system. Since the functional dependence of the exchange energy on the density is not known either, exchange potentials can also only be approximated [5–7]. The main disadvantage in DFT is that the exchange correlation potential has to describe different kinds of energy corrections that even scale differently [8]. That makes the functional and the potential difficult to approximate, and systematic improvements of the various potentials are generally not available. Recently, exact local exchange potentials and second-order ab initio perturbation

correlation potentials were developed [9–11] that are orbital-dependent and guarantee convergence to the exact result in the correlation and basis set limit. Some of the traditional problems in DFT (like the self interaction, the wrong asymptotic behavior of the potential, the integer-discontinuity condition, and even the inability to obtain weak interactions) are removed by the use of orbital-dependent potentials in ab initio dft.

The second well-known independent particle model is the Hartree-Fock theory. It is a wave-function theory that uses the variational principle to determine the energetically best wave-function given by a single determinant [12]. From the variation, a set of eigenvalue equations for the orbitals and the corresponding orbital energies is obtained. By making the ansatz of a determinant of orbitals for the wave-function, the Pauli principle is fulfilled and, therefore, within the model, the exchange is treated exactly. Similarly, within this independent particle model, the kinetic energy is exact. Koopmans' theorem [13] also gives meaning to all the orbital energies, while Kohn Sham theory only assigns the highest orbital energy to an ionization potential. But correlation is not included in Hartree-Fock theory. Correlation corrections can be added to the wave-function and the energy through many-body perturbation theory [14, 15], coupled-cluster theory [16] and configuration interaction [17] for instance, at the cost of losing the simplicity of the independent particle wave-function.

An alternative route to an exact one-electron picture is based on electron-propagator theory [18, 19]. The Dyson equation leads to a pseudo-eigenvalue equation for energy-dependent orbitals (Dyson orbitals). The corresponding one-electron operator has an energy-independent Hartree-Fock part, and an energy-dependent part (namely the self-energy that accounts for correlation effects [20]). The self-energy can be expanded in different orders of perturbation theory. Therefore, the theory provides a way to systematic improvement. Independent particle models

based on ab initio electron-propagator methods have been successfully applied to calculate ionization potentials and Dyson orbitals for different systems [21–23]. To each ionization potential there corresponds a Dyson orbital and a self-energy, dependent on that ionization potential (which makes it necessary to solve the pseudo-eigenvalue problem for each ionization potential and each orbital separately, making the Dyson orbitals an overdetermined, non-orthogonal set). However, their diagonalization leads to natural orbitals [24]. The same, of course, holds for electron affinities and the corresponding orbitals.

Gilbert's [25] extensions to the Hohenberg-Kohn theorems made the recent formulation of density matrix functional theory possible. Natural orbital functionals were developed in which the density matrix is expressed in natural orbitals and corresponding occupation numbers. Natural orbital functionals can be divided into corrected Hartree models and corrected Hartree-Fock [26] models. Buijse and Baehrends [27] developed a corrected Hartree scheme, which was extended by Gödecker and Umrigar [28] to include an additional correction term for the self interaction. Though extremely simple, natural orbital functionals show surprising success in calculating correlation energies for atoms and small molecules. Analyzed by various authors [29–33] the major drawbacks of such models are overcorrelation, inability to describe the limiting case of the high-density homogeneous electron gas, and violation of the N-representability condition of the implicitly defined second-order reduced density matrix. Other authors proposed density matrix functionals based on the contracted Schroedinger equation [34–37] and the hypervirial theorem [38, 39].

A highly desirable model would be a generalized independent particle model that retains the advantage of the Hartree-Fock theory in being able to describe the kinetic energy and the exchange energy exactly, but which incorporates correlation effects. This could be achieved by applying the Brillouin-Brueckner condition

or equivalently, the maximum overlap condition that requires that a single determinant of Brueckner orbitals has maximum overlap with the exact wave-function. The Brueckner method originated in nuclear physics [40] and became known in some quantum chemistry circles from its generalization by Löwdin to an exact self consistent field theory [41]. Larsson [42, 43] developed a Hartree-Fock-like model that includes correlation using the Brillouin-Brueckner condition. Chiles and Dykstra [44], Purvis and Bartlett [45] and Adamowicz and Bartlett [46], and Handy et al. [47] obtained Brueckner orbitals in coupled-cluster theory. Stolarczyk and Monkhorst formulated an effective Hamiltonian that has the form of the Fock operator plus a correlation potential [48] by applying the maximum overlap condition to a coupled-cluster reference wave-function. Scuseria [49, 50] implemented the Brueckner coupled-cluster method, using the effective Brueckner Hamiltonian in a self consistent scheme. Recently, Lindgren and Salomonson [51] made valuable contributions to the field. Minimizing the energy with respect to the partitioning of the Hamiltonian lead them to a Brueckner effective Hamiltonian, which they expressed in different orders perturbation.

Our goal was to formulate a correlated independent particle (CIP) model that has the general form $(f + v_c)\phi_p = \varepsilon_p\phi_p$, where f is either the Fock operator or a Fock-like operator, and v_c is the correlation potential to be determined, while the ϕ_p are the one-particle solutions. However, the question is what condition is reasonable to impose to obtain v_c. We chose to impose the condition of exactness of the ionization potentials (IP's) and electron affinities (EA's) as the negative of the orbital energies, ε_p. This, of course, is closely related to Dyson theory, if the potential has an energy-dependent form as is the case for potentials constructed in Section 3.1.3. This choice is justified by the extended Koopmans' theorem (EKT) in which the eigenvalues of two distinct effective one-particle operators represent the IP's and the EA's respectively. The EKT method was independently developed by Day, Smith

and Garrod [52] for single ionization and attachment processes and a generalization of it for ionization that includes double and higher ionizations by Morrell, Parr, and Levy [53]. Several authors argued [53–55] that at least the lowest IP is exact if the exact wave-function is used. Numerical support was given by Morrison [56] and Sundholm and Olsen [57, 58]. The energy-independent effective one-electron operator formulated in Section 3.4 can be viewed as a realization of the extended Koopmans' theorem Fock operator [59], where the ground state wave-function is represented by the coupled-cluster wave-function and where the assumption that ionization and electron capture can be described by the creation or annihilation of a single spin orbital is relaxed, and additional excitations are allowed.

Our study explored different ways to obtain a correlation potential for a generalized Hartree-Fock model that includes electron correlation: the correlated independent particle (CIP) model. The CIP model can also be viewed as an approximation to density matrix functional theory. The correlation potential is chosen such that the eigenvalues of the effective one-particle method represent the exact IP's and EA's. Chapter 2 gives basic theorems and ideas leading to the formulation of the CIP model. The Chapter 3 describes different realizations of the correlation potential yielding exact IP's and EA's as eigenvalues of an effective Hamiltonian. Equivalence and similarities among the methods used to obtain the correlation potential (i.e. the equation-of-motion coupled-cluster method, the Fock space coupled-cluster method and the coupled-cluster Green's function method) are shown. In Chapter 4 the energy-independent correlation potential constructed in Section 3.4 is approximated through second-order in perturbation, and results are given for some sample molecules. To improve the orbitals of the CIP model compared to Hartree-Fock orbitals, an additional condition is applied: the Brillouin-Brueckner condition. Results for dipole moments of sample molecules using those orbitals are listed in Chapter 4. Chapter 5 presents the conclusions.

CHAPTER 2
CORRELATED INDEPENDENT PARTICLE MODEL AS AN APPROXIMATION TO DENSITY MATRIX FUNCTIONAL THEORY

In this chapter the basic ideas and theorems used and developed to formulate the correlated independent particle (CIP) model are outlined. The CIP model is an independent particle model that includes correlation through a correlation potential. The eigenvalues of the employed effective Hamiltonian are orbital energies, which are associated with formally exact IP's and EA's. The CIP model is viewed as an extension to the Hartree-Fock model or as an approximation to density matrix functional theory where the first-order density matrix is restricted to be idempotent.

Since the Hartree-Fock theory is a special case of the CIP model and density matrix functional theory, the Hartree-Fock model is briefly summarized in Section 2.1. In Section 2.2 the necessary theorems and proofs to establish the existence of a universal energy functional of the first-order reduced-density matrix are reported and the validity of the variational principle is shown. Hartree-Fock theory is shown to be a special case of density matrix functional theory. In Section 2.3 the CIP model is introduced. The condition of exactness of the ionization potentials (IP's) and electron affinities (EA's) as the eigenvalues of the one-particle operator employed in the CIP model is used to determine the correlation potential. This choice is inspired by the extended Koopmans' theorem, which is described in Section 2.4. Finally in Section 2.5 wesummarize the different density matrix functionals developed in the past.

2.1 Hartree-Fock Theory

The Hartree-Fock approximation [12] is one of the most widely used independent particle theories in quantum chemistry. It is a wave-function method attempting to solve the many-electron problem by finding an approximate solution to the nonrelativistic time-independent electronic Schroedinger equation. The simplicity of the wave-function allows for a direct chemical interpretation. The eigenfunctions of the Fock operator are orbitals with corresponding orbital energies that play a vital role in explaining and determining chemical reaction mechanisms. However, the lack of accuracy of the Hartree-Fock approximation prevents the prediction of reaction energies and other electronic properties within a few kcal/mole. To reach higher accuracy, correlated methods like many-body perturbation theory [14, 15], coupled-cluster theory [16] and configuration interaction [17] have to be used. But since the Hartree-Fock approximation usually accounts for most of the total energy, it is often used as a starting point for correlated methods.

At first glance the Hartree-Fock approximation does not use the density matrix as its basic variable, but rather the wave-function. However, the particular ansatz for the wave-function leads to eigenvalue equations that are, as seen later, the equations of a special case in density matrix functional theory: namely, when the correlation energy is zero (i.e., the Hartree-Fock energy can be written in terms of the first-order density matrix only).

The nonrelativistic time-independent Schroedinger equation is given by

$$H\Psi = E\Psi, \tag{2.1}$$

where H is the Hamiltonian operator for a system of nuclei and electrons described by position vectors. The distance between the ith electron and the Ath nucleus is r_{iA}, the distance between the ith electron and the jth electron is r_{ij}. In the Born-Oppenheimer approximation, the electrons move in a field of fixed nuclei. The

Hamiltonian (in Hartree atomic units) is then

$$H = -\sum_{i=1}^{N} \frac{1}{2}\nabla_i^2 - \sum_{i=1}^{N}\sum_{A=1}^{M} \frac{Z_A}{r_{iA}} + \sum_{i=1}^{N}\sum_{j>i}^{N} \frac{1}{r_{ij}}. \tag{2.2}$$

N is the number of electrons and M is the number of nuclei. Z_A is the atomic number of nucleus A. The first term on the right-hand side is the operator for the kinetic energy of the electrons, the second term is the nuclear-electron attraction operator, and the third term is the operator for electron-electron repulsion.

The variational principle states that the exact energy is always lower than or equal to the expectation value of the Hamiltonian with respect to a trial normalized wave-function Φ

$$E_{\text{exact}} \leq \langle \Phi | H | \Phi \rangle. \tag{2.3}$$

The Dirac notation [60] is used to denote integral expressions. A reasonable ansatz for the wave-function can be used and the energy minimized to obtain the best wave-function of that particular form.

The simplest antisymmetric wave-function of an N-electron system that is composed of one-electron functions is a Slater determinant

$$\Phi_0(x_1, x_2, \ldots, x_N) = \frac{1}{\sqrt{N!}} \begin{vmatrix} \phi_1(x_1) & \phi_2(x_1) & \ldots & \phi_N(x_1) \\ \phi_1(x_2) & \phi_2(x_2) & \ldots & \phi_N(x_2) \\ \ldots & \ldots & \ldots & \ldots \\ \phi_1(x_N) & \phi_2(x_N) & \ldots & \phi_N(x_N) \end{vmatrix}.$$

The one-electron functions ϕ_i depend on the space-spin coordinates x_i of the electrons. For orthonormal spin orbitals, the expectation value of the Hamiltonian with respect to the Slater determinant is given by

$$E_0 = \sum_i \langle \phi_i | h | \phi_i \rangle + \frac{1}{2} \sum_{ij} \langle \phi_i \phi_j || \phi_i \phi_j \rangle. \tag{2.4}$$

h is the one-electron operator part of the Hamiltonian and includes the kinetic energy operator and the nuclear-electron attraction. The double bar $||$ denotes the sum of the coulomb and the exchange contributions to the two-electron integral $\langle\phi_i\phi_j||\phi_i\phi_j\rangle = \langle\phi_i\phi_j|\phi_i\phi_j\rangle - \langle\phi_i\phi_j|\phi_j\phi_i\rangle$.

In the Hartree-Fock model, the spin orbitals ϕ_i are varied under the orthogonality constraint $\langle\phi_i|\phi_j\rangle = \delta_{ij}$ to obtain the Slater determinant that corresponds to the lowest energy. The problem of minimizing a functional under constraints can be solved by the Lagrangian multiplier method. The functional to be minimized is

$$\mathcal{L} = E_0 - \sum_{ij}^{N} \epsilon_{ji}(\langle\phi_i|\phi_j\rangle - \delta_{ij}), \tag{2.5}$$

where the ϵ_{ij} are the Lagrange multipliers. Variation of the orbitals leads to the Hartree-Fock equations

$$f|\phi_i\rangle = \sum_{j}^{N} \epsilon_{ji}|\phi_j\rangle. \tag{2.6}$$

f is the Fock operator, defined as

$$f(x_1) = h(x_1) + \sum_{j}^{N} \int \phi_j^*(x_2) r_{12}^{-1}(1 - \mathcal{P}_{12})\phi_j(x_2)dx_2. \tag{2.7}$$

The operator $\mathcal{P}_{12}$ permutes electron one and electron two.

For a single determinant wave-function, any expectation value is invariant under a unitary transformation of the spin orbitals. Since ϵ is a Hermitian matrix, it is always possible to find a unitary transformation that diagonalizes ϵ. The transformed Hartree-Fock equations

$$f|\phi_i\rangle = \epsilon_i|\phi_i\rangle \tag{2.8}$$

are known as canonical Hartree-Fock equations. The eigenfunctions of the canonical Hartree-Fock equations are the canonical spin orbitals, and the eigenvalues are the orbital energies.

The Fock operator has a functional dependence on the occupied spin orbitals but once the spin orbitals are known, the Fock operator becomes a well-defined Hermitian operator with an infinite number of eigenfunctions. The N orbitals with the lowest orbital energies are the occupied orbitals in Φ_0 labeled $i, j, \ldots$, the remaining spin orbitals are the virtual orbitals with indices $a, b, \ldots$. Labels $p, q, \ldots$ refer to general orbitals. The orbital energy is given by

$$\begin{aligned} \epsilon_p &= \langle \phi_p | f | \phi_p \rangle \\ &= \langle \phi_p | h | \phi_p \rangle + \sum_i^N \langle \phi_p \phi_i || \phi_p \phi_i \rangle, \end{aligned} \tag{2.9}$$

which, according to Koopmans' theorem [13], is equal to the frozen orbital estimate of the negative of the ionization potential (IP) for occupied orbitals and similar for the negative of the electron affinity (EA) for unoccupied orbitals

$$IP = {}^{N-1}E_k - {}^{N}E_0 = -\epsilon_k \tag{2.10}$$

$$EA = {}^{N}E_0 - {}^{N+1}E^c = -\epsilon_c. \tag{2.11}$$

${}^{N-1}E_k$ is the expectation value of the Hamiltonian with respect to Φ_0 where an electron in orbital k is removed. ${}^{N+1}E^c$ is the expectation value of the Hamiltonian with respect to Φ_0 where an electron in orbital c is added.

Adding the orbital energies ϵ_i of Eq. 2.9 for all the occupied orbitals, gives

$$\sum_i^N \epsilon_i = \sum_i^N \langle \phi_i | h | \phi_i \rangle + \sum_{ij}^N \langle \phi_i \phi_j || \phi_i \phi_j \rangle. \tag{2.12}$$

Comparing Eq. 2.4 with Eq. 2.12, it is apparent that the total Hartree-Fock energy is not the sum of the orbital energies. The sum of orbital energies counts the electron-electron interaction twice, and has to be corrected by a factor of $\frac{1}{2}$ to yield the correct total energy.

For molecules with an even number of electrons, it is found that the spin orbitals are essentially pairwise degenerate. Restricted Hartree-Fock theory takes that fact

explicitly into account. A restricted set of spin orbitals has the form

$$\phi_p(x) = \begin{cases} \varphi_p(r)\alpha(\omega) \\ \varphi_p(r)\beta(\omega) \end{cases}, \tag{2.13}$$

where the $\varphi_p(r)$ are spatial orbitals dependent on the spatial coordinates r. $\alpha(\omega)$ and $\beta(\omega)$ are spin eigenfunctions dependent on the spin coordinate ω, fulfilling $\langle\alpha|\alpha\rangle = \langle\beta|\beta\rangle = 1$ and $\langle\alpha|\beta\rangle = \langle\beta|\alpha\rangle = 0$.

To convert the Hartree-Fock equations into restricted Hartree-Fock equations, the spin integration is carried out, leading to

$$f|\varphi_i\rangle = \epsilon_i|\varphi_i\rangle, \tag{2.14}$$

with

$$f(r_1) = h(r_1) + \sum_j^{\frac{N}{2}} \int \varphi_j^*(r_2) r_{12}^{-1}(2 - \mathcal{P}_{12})\varphi_j(r_2) dr_2. \tag{2.15}$$

The closed-shell orbital energies are

$$\epsilon_p = \langle\varphi_p|h|\varphi_p\rangle + \sum_i^{\frac{N}{2}} (2\langle\varphi_p\varphi_i|\varphi_p\varphi_i\rangle - \langle\varphi_p\varphi_i|\varphi_i\varphi_p\rangle), \tag{2.16}$$

for which Koopmans' theorem applies as well. The total energy is given by

$$E_0 = 2\sum_i^{\frac{N}{2}} \langle\varphi_i|h|\varphi_i\rangle + \sum_{ij}^{\frac{N}{2}} (2\langle\varphi_j\varphi_i|\varphi_j\varphi_i\rangle - \langle\varphi_j\varphi_i|\varphi_i\varphi_j\rangle). \tag{2.17}$$

2.2 Hohenberg-Kohn-Gilbert Theorem

The Hohenberg-Kohn-Gilbert theorem [25] is the foundation of recent developments in density matrix functional theory. Hohenberg and Kohn [1] proved the existence of a universal energy functional of the external potential and the particle density that is a minimum for the true particle density. The proof was given for a local external potential $v(x, x') = \delta(x - x')v(x)$. Gilbert [25] extended the theorem to a nonlocal external potential. He showed that the universal energy functional of

the nonlocal external potential depends on the one-particle density matrix instead of the density.

2.2.1 Energy Functional of the Density Matrix

The von Neumann N-particle statistical density kernel is given by

$$D^N(x_1 \dots x_N, x'_1 \dots x'_N) = \sum_i w_i \Psi_i(x_1 \dots x_N) \Psi_i^*(x'_1 \dots x'_N), \tag{2.18}$$

where the Ψ_i are a complete set of orthonormal N-particle wave-functions, the w_i are positive numbers normalized to

$$\sum_i w_i = 1. \tag{2.19}$$

The ensemble N-representable one-particle density kernel can be obtained from an N-particle kernel by contraction

$$D^1(x, x') = N \int D^N(x, x_2 \dots x_N; x', x_2 \dots x_N) dx_2 \dots dx_N. \tag{2.20}$$

Similarly, the ensemble N-representable two-particle density kernel can be defined

$$D^2(x_1 x_2, x'_1 x'_2) = \begin{pmatrix} N \\ 2 \end{pmatrix} \int D^N(x_1, x_2, x_3 \dots x_N; x'_1, x'_2, x_3 \dots x_N) dx_3 \dots dx_N, \tag{2.21}$$

and so on.

Partition the Hamiltonian in the following way

$$H = \sum_i t(i) + \sum_i v(i) + \sum_{i<j} u(i, j), \tag{2.22}$$

t is the kinetic energy operator, v is the external potential, and u is the electron-electron interaction. The energy can be written as a functional of the N-particle density kernel and the external potential (t and u will always be the same; their

functional dependence does not need to be indicated)

$$E\{D^N, v\} \equiv \langle D^N H\rangle = \langle D^1 t\rangle + \langle D^1 v\rangle + \langle D^2 u\rangle. \tag{2.23}$$

The external potential $v(x, x')$ does not have to be local, but is restricted to the class of potentials for which E is real and has a lower bound. The ground state Ψ_0 is assumed to be nondegenerate, so that $D_0^N = \Psi_0 \Psi_0^1$.

From Eq. 2.23 it can be seen that the energy is trivially a function of the two-matrix. In 1951 Coleman [61] attempted to vary the energy with respect to the two-matrix and was surprised to find an energy for the lithium atom that was 20% below the experimental value. The reason for the failure of the variational principle is that the space of two-matrices in which he varied was too large. The condition that must be fulfilled by the two-matrices is that they correspond to a fermion wave-function, and that they can be obtained by integrating the N-particle density matrix over $N-2$ particles. Ensuring this condition is known as the N-representability problem, currently thought to be an unsolved problem (at least practically) for two-matrices. Therefore, it is not particularly useful to write the energy as a functional of the two-matrix.

In Eq. 2.23, the ensemble energy functional $E = \langle D^N H\rangle$ has been used rather than the pure-state energy functional $E = \langle \Psi | H | \Psi \rangle$, because the constraints needed to apply the variational principle are known only for ensembles. Next it is shown that the same stationary values are obtained for ensemble or pure-state energy functionals.

To derive the stationary conditions for ensembles, the constraints $\langle \Psi_i | \Psi_j \rangle \equiv \langle i|j\rangle = \delta_{ij}$ and $\sum w_i = 1$ must be imposed by the method of Lagrangian multipliers. The w_i are set to be $cos^2\theta_i$ to satisfy the constraint $0 \leq w_i \leq 1$. The functional to

be varied with respect to Ψ_i, $\Psi_i^\dagger$ and θ_i is

$$\mathcal{E} = E - \sum_{i,j} \lambda_{ij} \langle i|j\rangle + \lambda(1 - \sum w_i), \tag{2.24}$$

where λ and λ_{ij} are Lagrangian multipliers. The variation leads to the following equations

$$\frac{\delta \mathcal{E}}{\delta \Psi_i^\dagger} = w_i H \Psi_i - \sum_j \Psi_j \lambda_{ij} = 0 \tag{2.25}$$

$$\frac{\delta \mathcal{E}}{\delta \Psi_i} = w_i H \Psi_i^\dagger - \sum_j \Psi_j^\dagger \lambda_{ij} = 0 \tag{2.26}$$

$$\frac{\partial \mathcal{E}}{\partial \theta_i} = \sin 2\theta_i (E_i - \lambda) = 0, \tag{2.27}$$

where $E_i = \langle i|H|i\rangle$. Eq. 2.25 and Eq. 2.26 reduce to the single condition

$$(w_i - w_j)\langle i|H|j\rangle = 0. \tag{2.28}$$

From Eq. 2.27 it can be concluded that one of the following conditions

$$(i)\ w_i = 1 \quad (ii)\ E_i = \lambda \quad (iii)\ w_i = 0$$

must be satisfied. If (i) is true, then all other $w_j = 0$, and since $\langle i|H|j\rangle = 0$ for $i \neq j$, according to Eq. 2.28. Therefore,

$$H\Psi_i = E_i \Psi_i. \tag{2.30}$$

If (ii) is true, then all states for which $w_i \neq 0$ must belong to the same degenerate state, and Eq. 2.30 is still satisfied. In all other cases, $w_i = 0$. This shows that stationary values for the ensemble energy functional are the same as for the pure-state energy functional.

Extending the Hohenberg-Kohn theorem to nonlocal potentials [25] requires only slight modifications of the proof given by Hohenberg and Kohn [1]. v^1 and v^2 are two external potentials that give rise to to two distinct nondegenerate ground

states Ψ_0^1 and Ψ_0^2. The corresponding Schrödinger equations are given by

$$H^1\Psi_0^1 = E_0^1\Psi_0^1 \tag{2.31}$$

$$H^2\Psi_0^2 = E_0^2\Psi_0^2. \tag{2.32}$$

The reduced one-particle density kernels for the two different wave-functions are

$${}^1D_0^1 = N\langle {}^1D_0^N\rangle \quad {}^1D_0^N = \Psi_0^1\Psi_0^{1\dagger} \tag{2.33}$$

$${}^2D_0^1 = N\langle {}^2D_0^N\rangle \quad {}^2D_0^N = \Psi_0^2\Psi_0^{2\dagger}. \tag{2.34}$$

Applying the variational principle leads to

$$E_0^1 = \langle {}^1D_0^N H^1\rangle < E^1 = \langle {}^2D_0^N H^1\rangle \tag{2.35}$$

$$E_0^2 = \langle {}^2D_0^N H^2\rangle < E^2 = \langle {}^1D_0^N H^2\rangle, \tag{2.36}$$

where E_0^1 and E_0^2 are the ground-state energies. E^1 and E^2 are necessarily greater since to calculate E^1 the ground-state density matrix of system 2 (which is different from the ground-state density matrix of system 1) is used. An energy difference can be defined

$$\Delta E \equiv (E^2 - E_0^2) + (E^1 - E_0^1) > 0, \tag{2.37}$$

where Eq. 2.35 and Eq. 2.36 have been used. Rearranging Eq. 2.37 and inserting the definitions Eq. 2.35 and 2.36 leads to

$$\Delta E = (E^2 - E_0^1) + (E^1 - E_0^2) \tag{2.38}$$

$$= \langle {}^1D_0^N(H^2 - H^1)\rangle + \langle {}^2D_0^N(H^1 - H^2)\rangle. \tag{2.39}$$

The difference between the two Hamiltonians is the difference between the two external potentials $\delta v = v^2 - v^1$, which is by definition nonzero. Then

$$\Delta E = \langle {}^1D_0^N \delta v\rangle - \langle {}^2D_0^N \delta v\rangle \tag{2.40}$$

$$= -\langle \delta D_0^1 \delta v\rangle > 0, \tag{2.41}$$

where $\delta D_0^1 = {}^2D_0^1 - {}^1D_0^1$.

For the inequality Eq. 2.41 to hold, δD_0^1 cannot be zero. Therefore if Ψ_0^1 and Ψ_0^2 are distinct, then their one-particle density kernels ${}^1D_0^1$ and ${}^2D_0^1$ must also be distinct, implying that there is a one-to-one correspondence between D_0^N and D_0^1. Hereby, the existence of an energy functional of the one-particle reduced-density kernel and the external potential is established

$$E\{D_0^1, v\} \equiv E\{D_0^N\{D_0^1\}, v\} = \langle D_0^1 v\rangle + F\{D_0^1\}, \tag{2.42}$$

where $F\{D_0^1\}$ is a universal functional of D_0^1 alone.

The domain of $F\{D_0^1\}$ (as defined in Eq. 2.42) consists only of those density kernels that can be constructed from the nondegenerate ground-state wave-function in a local or nonlocal external potential. To extend this domain, define a set $\{D^N\}$ that includes D_0^N and any other N-particle density kernel that is needed for a one-to-one mapping between $\{D^N\}$ and the set of one-particle reduced-density kernels $\{D^1\}$. The set $\{D^N\}$ is not uniquely defined, in particular because a set $\{D^N\}$ can be found for which a many-to-one mapping onto $\{D^1\}$ exists. However, here it is only important that one set can be found, which allows for the one-to-one mapping. Then

$$E\{D^1, v\} \equiv E\{D^N\{D^1\}, v\} = \langle D^1 v\rangle + F\{D^1\}, \tag{2.43}$$

where D^1 is now any density kernel associated with a ground state in an external potential. This allows for the definition of the variational principle

$$E\{D_0^1, v\} < E\{D_0^1 + \delta D^1, v\}. \tag{2.44}$$

The existence of a 1-matrix functional theory was also shown by other authors. Berrondo and Goscinski [62] added a nonlocal external potential to the N-particle Hamiltonian and then obtained a variational principle involving the 1-matrix for a local external potential by eliminating the nonlocal external source. Donnelly and Parr [63] showed that the existence of a universal variational functional of the 1-matrix is implied in the original Hohenberg-Kohn theorem [1].

2.2.2 V-Representability Problem

A limitation of $F\{D^1\}$ is that it is undefined for any D^1 that is not v-representable. A ground-state v-representable D^1 is one that is associated with an antisymmetric ground-state wave-function of some Hamiltonian with a local or nonlocal potential. The v-representability constraint is very severe, since most one-particle density matrices are not v-representable (for instance, no idempotent one-matrix is v-representable). It was shown by Levy [64] with the constrained search formalism that v-representability is not required. The N-representability constraint, where the one-matrix must be derivable from an antisymmetric wave-function, is sufficient. The proof is presented in the following.

Define the universal functional

$$W\{D^1\} = \min\langle\Psi_{D^1}|u|\Psi_{D^1}\rangle. \tag{2.45}$$

$W\{D^1\}$ searches all antisymmetric wave-functions Ψ_{D^1} that yield the fixed trial D^1, where D^1 does not need to be v-representable. $W\{D^1\}$ delivers the minimal expectation value. For $W\{D^1\}$ to be a valid universal variational functional for any N-representable D^1 two theorems need to be proven.

$$\text{Theorem I} \qquad \langle D^1 v\rangle + \langle D^1 t\rangle + W\{D^1\} \;\geq\; E_0 \tag{2.46}$$

$$\text{Theorem II} \qquad \langle D_0^1 v\rangle + \langle D_0^1 t\rangle + W\{D_0^1\} \;=\; E_0 \tag{2.47}$$

Call $\Psi^{\min}_{D^1}$ that wave-function that satisfies the right-hand side of Eq. 2.45

$$W\{D^1\} = \langle \Psi^{\min}_{D^1} | u | \Psi^{\min}_{D^1} \rangle \tag{2.48}$$

and

$$W\{D^1_0\} = \langle \Psi^{\min}_{D^1_0} | u | \Psi^{\min}_{D^1_0} \rangle. \tag{2.49}$$

To prove Theorem I, insert Eq. 2.48 into the left-hand side of Eq. 2.46

$$\langle D^1 v \rangle + \langle D^1 t \rangle + W\{D^1\} = \langle \Psi^{\min}_{D^1} | t + v + u | \Psi^{\min}_{D^1} \rangle. \tag{2.50}$$

But by the variational principle

$$\langle \Psi^{\min}_{D^1} | t + v + u | \Psi^{\min}_{D^1} \rangle \geq E_0. \tag{2.51}$$

Adding the last two equations concludes the proof of Theorem I.

To prove Theorem II, again use the variational principle

$$E_0 \leq \langle \Psi^{\min}_{D^1_0} | t + v + u | \Psi^{\min}_{D^1_0} \rangle \tag{2.52}$$

$$E_0 = \langle \Psi_0 | t + v + u | \Psi_0 \rangle. \tag{2.53}$$

From there it is seen that

$$\langle D^1_0 v \rangle + \langle D^1_0 t \rangle + \langle \Psi_0 | u | \Psi_0 \rangle \leq \langle D^1_0 v \rangle + \langle D^1_0 t \rangle + \langle \Psi^{\min}_{D^1_0} | u | \Psi^{\min}_{D^1_0} \rangle, \tag{2.54}$$

which leads to

$$\langle \Psi_0 | u | \Psi_0 \rangle \leq \langle \Psi^{\min}_{D^1_0} | u | \Psi^{\min}_{D^1_0} \rangle. \tag{2.55}$$

But the definition of $\Psi^{\min}_{D^1_0}$ dictates that

$$\langle \Psi_0 | u | \Psi_0 \rangle \geq \langle \Psi^{\min}_{D^1_0} | u | \Psi^{\min}_{D^1_0} \rangle. \tag{2.56}$$

The last two equations can only hold at the same time if

$$\langle \Psi_0 | u | \Psi_0 \rangle = \langle \Psi^{\min}_{D^1_0} | u | \Psi^{\min}_{D^1_0} \rangle = W\{D^1_0\}. \tag{2.57}$$

The ground-state energy is given by

$$E_0 = \langle \Psi_0 | t + v + u | \Psi_0 \rangle = \langle D_0^1 t \rangle + \langle D_0^1 v \rangle + \langle \Psi_0 | u | \Psi_0 \rangle. \tag{2.58}$$

Substitution of Eq. 2.57 into Eq. 2.58 completes the proof of Theorem II. Notice that $F\{D^1\} = W\{D^1\}$ if D^1 is v-representable.

In addition to the v-representability constraint, the condition that the ground state is nondegenerate is lifted within the constrained search formalism. If Ψ_0 is degenerate, then all of the ground-state wave-functions may be obtained, one at a time, by the foregoing procedure.

2.2.3 Euler Equations

Euler equations that determine the density matrix can now be derived by applying the variational principle. According to Coleman [65], a Hermitian one-electron operator $D^1(x, x')$ will be ensemble N-representable if and only if $\int D^1(x, x) = N$ and all eigenvalues satisfy the inequality $0 \leq n_p \leq 1$,

$$\int D^1(x, x') \phi_p(x') dx' = n_p \phi_p(x). \tag{2.59}$$

The $\{\phi_i\}$ are the natural orbitals [66], the eigenfunctions of the one-particle density kernel. The N-representability conditions on the pure-state one-particle density kernel are not known. However, as already shown above, one obtains the same stationary conditions for unreduced-ensemble or pure-state energy functionals. The problem of ensemble N-representability versus pure-state N-representability was also discussed by different authors [64, 67–69]. They all came to the conclusion that the distinction between pure-state N-representability and ensemble N-representability is not necessary.

Even though the N-representability condition for 1-matrices is known, it is not quite clear what further restrictions must be imposed for a correct Euler equation

to result. Valone [67] gave an example of an unacceptable variation in which the partitioning of the primed and unprimed coordinates was not maintained.

However, an orbital parameterization of the 1-matrix is always possible [25, 63, 68, 70, 71]. $D^1(x,x')$ can be expanded in terms of the natural orbitals

$$D^1(x,x') = \sum_{p=1}^{\infty} n_p \phi_p(x) \phi_p^*(x'). \tag{2.60}$$

This is rather a formal expression because natural spin orbitals are obtained a posteriori. For this reason, some authors [63, 68] expand the 1-matrix in a nondiagonal representation of orthonormal spin orbitals. However, if the Euler equations obtained with that more general ansatz are cast into canonical form, the same Euler equations are recovered as for the diagonal representation [63].

The N-representability conditions for 1-matrices in their natural orbital representation [72] can conveniently be introduced with the method of Lagrange multipliers. If $n_p = \cos^2\theta_p$, the following constraints must be applied,

$$\langle \phi_p | \phi_q \rangle = \langle p | q \rangle = \delta_{pq}, \qquad \sum_{p=1}^{\infty} \cos^2\theta_p = N, \qquad 0 \le \theta_p \le \pi. \tag{2.61}$$

It is assumed that the natural orbitals form a complete set. The functional $E\{D^1\}$ is now replaced by

$$\mathcal{E}\{D^1\} = E\{D^1\} - \sum_{pq} \lambda_{pq} \langle q | p \rangle + \lambda (N - \sum_{p=1}^{\infty} n_p), \tag{2.62}$$

where λ_{pq} and λ are Lagrangian multipliers and variations are with respect to ϕ_p^*, ϕ_p and θ_p. Beginning with ϕ_p^* the variation of the last two terms of the right-hand side of Eq. 2.62 is given by

$$\frac{\delta \left(\sum_{rq} \lambda_{rq} \int \phi_r^*(x) \phi_q(x) dx \right)}{\delta \phi_p^*(x)} = \sum_q \lambda_{pq} \phi_q(x) \tag{2.63}$$

$$\frac{\delta \left(\lambda \left(N - \sum_{p=1}^{\infty} n_p \right) \right)}{\delta \phi_p^*(x)} = 0. \tag{2.64}$$

To vary the first term of the right-hand side of Eq. 2.62 the formal identity

$$\frac{\delta E}{\delta \phi_p^*(x)} = \int\int \frac{\delta E}{\delta D^1(x',x'')} \frac{\delta D^1(x',x'')}{\delta \phi_p^*(x)} dx' dx'' \tag{2.65}$$

can be made. It should be mentioned at this point that the existence of $\frac{\delta E}{\delta D^1} \delta D^1(x,x')$ is not proven. However its existence is a reasonable assumption [25].

The variation of the 1-matrix with respect to ϕ_p^* is given by

$$\begin{aligned} \frac{\delta D^1(x',x'')}{\delta \phi_p^*(x)} &= \frac{\delta \left(\sum_q \phi_q(x') n_q \phi_q^*(x'') \right)}{\delta \phi_p^*(x)} && (2.66) \\ &= n_p \phi_p(x') \delta(x''-x). && (2.67) \end{aligned}$$

Substituting Eq. 2.67 into Eq. 2.65 leads to

$$\begin{aligned} \frac{\delta E}{\delta \phi_p^*(x)} &= \int\int \frac{\delta E}{\delta D^1(x',x'')} n_p \phi_p(x') \delta(x''-x) dx' dx'' && (2.68) \\ &= n_p \int \frac{\delta E}{\delta D^1(x',x)} \phi_p(x') dx' && (2.69) \\ &= n_p \int h(x,x') \phi_p(x') dx', && (2.70) \end{aligned}$$

with

$$h(x,x') = \frac{\delta E}{\delta D^1(x',x)}. \tag{2.71}$$

The variation of the functional 2.62 with respect to ϕ_p^* is obtained by combining Eq. 2.70, Eq. 2.63 and Eq. 2.64

$$\frac{\delta \mathcal{E}}{\delta \phi_p^*} = n_p h \phi_p - \sum_q \lambda_{pq} \phi_q = 0. \tag{2.72}$$

Similarly, the foregoing procedure can be repeated for the variation with respect to ϕ_p, leading to

$$\frac{\delta \mathcal{E}}{\delta \phi_p} = n_p \phi_p^* h - \sum_q \lambda_{pq} \phi_q^* = 0. \tag{2.73}$$

The two equations 2.72 and 2.73 can be reduced to a single condition

$$(n_p - n_q) \langle p|h|q \rangle = 0. \tag{2.74}$$

Since the energy is written in terms of the 1-matrix, the orbitals in h occur in pairs of ϕ_p^* and ϕ_p. Therefore, the operator h is invariant under unitary transformation of the orbitals, and the orbitals can always be chosen to be the solutions to the eigenvalue equation

$$h\phi_p = \epsilon_p \phi_p, \tag{2.75}$$

where $\epsilon_p = \langle p|h|p\rangle$.

Finally the functional 2.62 has to be varied with respect to θ_p. The variation of the last two terms of the right-hand side of Eq. 2.62 is given by

$$\frac{\delta\left(\sum_{pq}\lambda_{pq}\int\phi_p^*(x)\phi_q(x)dx\right)}{\delta\theta_p} = 0 \tag{2.76}$$

$$\frac{\delta\left(\lambda\left(N-\sum_{r=1}^{\infty}\cos^2\theta_r\right)\right)}{\delta\theta_p} = \lambda 2\sin\theta_p\cos\theta_p \tag{2.77}$$

$$= \lambda\sin 2\theta_p. \tag{2.78}$$

Again the formal identity

$$\frac{\delta E}{\delta\theta_p} = \int\int\frac{\delta E}{\delta D^1(x',x)}\frac{\delta D^1(x',x)}{\delta\theta_p}dx'dx \tag{2.79}$$

can be used, where the variation of the density matrix with respect to θ_p is given by

$$\frac{\delta D^1(x',x)}{\delta\theta_p} = \frac{\delta\left(\sum_q\phi_q(x')\cos^2\theta_q\phi_q^*(x)\right)}{\delta\theta_p} \tag{2.80}$$

$$= -\sin 2\theta_p\phi_p(x')\phi_p^*(x). \tag{2.81}$$

Substitution of Eq. 2.81 in Eq. 2.79 leads to

$$\frac{\delta E}{\delta\theta_p} = -\sin 2\theta_p\int\int\frac{\delta E}{\delta D^1(x',x)}\phi_p(x')\phi_p^*(x)dx'dx \tag{2.82}$$

$$= -\sin 2\theta_p\epsilon_p, \tag{2.83}$$

with

$$\epsilon_p = \int\int\phi_p^*(x)\frac{\delta E}{\delta D^1(x',x)}\phi_p(x')dx'dx. \tag{2.84}$$

Combining Eq. 2.83, Eq. 2.76, and Eq. 2.78 the variation of the functional 2.62 with respect to θ_p is obtained

$$\frac{\delta \mathcal{E}}{\delta \theta_p} = \sin 2\theta_p(\epsilon_p - \lambda) = 0. \tag{2.85}$$

From Eq. 2.85 it can be deduced that one of the following conditions has to be satisfied

$$\text{(i) } n_p = 1 \quad \text{(ii) } \epsilon_p = \lambda \quad \text{(iii) } n_p = 0, \tag{2.86}$$

implying that all partially filled natural orbitals must belong to the same degenerate eigenvalue. There is a many-to-one mapping between the eigenvalues of D^1 and the eigenvalues of h for partially filled orbitals. These results have been verified by Donelly and Parr [63] and Zumbach and Maschke [70]. If one attempts to obtain the exact density matrix that is built from partially occupied natural orbitals, the operator h must be quite different from the one-electron operators employed in Hartree-Fock, and similar theories and the equations must be of radically different mathematical structure [73]. The problem disappears in the Hartree-Fock approximation for a closed-shell system, because all orbitals are then either fully occupied or empty. Even if general one-matrices are allowed, the solution of the Hartree-Fock equations at stationarity is an idempotent density matrix [74].

2.2.4 Hartree-Fock Theory: a Special Case

Assuming that the correlation energy is zero, the expression for the operator h in Eq. 2.75 can be explicitly found [71]. The eigenvalue equation was given in Eq. 2.75

$$h\phi_p = \epsilon_p \phi_p, \tag{2.87}$$

with

$$h(x, x') = \frac{\delta E}{\delta D^1(x', x)}. \tag{2.88}$$

In an orthonormal basis $\{\varphi_p\}$ (which could for instance be the basis of atomic orbitals, orthogonalized with Löwdin's procedure $\varphi_p = \sum_r S_{pr}^{-\frac{1}{2}} \chi_r$, S_{pr} being an element of the overlap matrix) the matrix representation of the 1-matrix is given by

$$D^1(x, x') = \sum_p \sum_q P_{pq} \varphi_p(x) \varphi_q^*(x'), \tag{2.89}$$

with P_{pq} being the elements of a Hermitian matrix $P_{pq} = \langle p|D^1|q\rangle$. Once the basis has been introduced, the 1-matrix is fully specified by the matrix $\mathbf{P}$, and the energy functional $E\{D^1\}$ is converted to a function of $\mathbf{P}$. Then, the functional derivative of $E\{D^1\}$ with respect to D^1 can be written as the partial derivative of the energy with respect to the elements of $\mathbf{P}$

$$h(x, x') = \sum_p \sum_q H_{pq} \varphi_p(x) \varphi_q^*(x'), \tag{2.90}$$

with

$$H_{pq} = \langle p|h|q\rangle, \qquad \langle p|h|q\rangle \equiv \left(\frac{\partial E}{\partial P_{pq}}\right). \tag{2.91}$$

If the correlation energy is zero, the energy functional of the density matrix can be written as

$$\begin{aligned} E &= -\frac{1}{2}\int \nabla^2 D^1(x_1, x_1')|_{x_1=x_1'} dx_1 + \int v(x_1) D^1(x_1, x_1) dx_1 \\ &\quad + \frac{1}{2}\left(\int\int \frac{1}{r_{12}} D^1(x_1, x_1) D^1(x_2, x_2) dx_1 dx_2 \right. \\ &\quad \left. - \int\int \frac{1}{r_{12}} D^1(x_1, x_2) D^1(x_2, x_1) dx_1 dx_2\right). \end{aligned} \tag{2.92}$$

In matrix representation the energy is given by

$$E = \sum_{rs} P_{rs} \left(\langle r| - \frac{1}{2}\nabla^2 + v(x)|s\rangle + \frac{1}{2}\sum_{pq} P_{pq} \langle rp||sq\rangle \right). \tag{2.93}$$

The matrix elements of the matrix $\mathbf{H}$ can be found by taking the derivative of the energy with respect to P_{tu}

$$\begin{aligned} H_{tu} = \left(\frac{\partial E}{\partial P_{tu}}\right) &= \frac{\partial \sum_{rs} P_{rs}}{\partial P_{tu}} \left(\langle r| - \frac{1}{2}\nabla^2 + v(x)|s\rangle + \frac{1}{2}\sum_{pq} P_{pq}\langle rp||sq\rangle \right) \\ &+ \sum_{rs} P_{rs} \frac{\partial \left(\langle r| - \frac{1}{2}\nabla^2 + v(x)|s\rangle + \frac{1}{2}\sum_{pq} P_{pq}\langle rp||sq\rangle \right)}{\partial P_{tu}} \\ &= \langle t| - \frac{1}{2}\nabla^2 + v(x)|u\rangle + \sum_{pq} P_{pq}\langle tp||uq\rangle. \end{aligned} \tag{2.94}$$

The matrix $\mathbf{H}$ represents the nonlocal Fock operator, defined in Eq. 2.7.

2.3 Correlated Independent Particle Model

The previous section establishes the foundation of density matrix functional theory in the sense that it is possible to find an expression for the energy in terms of the one-matrix only, and that the variational principle can be applied. However, if the one-matrix is expressed in terms of natural orbitals, the resulting Euler equations reveal that all eigenvalues of D^1 that lie between 0 and 1, must be mapped into a single eigenvalue of the one-electron operator $h(x, x')$. To avoid the degeneracy problem, the density matrix within the CIP model is restricted to be idempotent. The operator $h(x, x')$ includes a correlation potential $v_c\{D^1\} = \frac{\delta E_C\{D^1\}}{\delta D^1(x,x')}$, so that the orbitals and the eigenvalues of the CIP model include correlation. The density matrix cannot be expected to be exact. However, the question of how good the density matrix obtained from a single determinant can be will be addressed in a later chapter.

If the correlation energy E_c is zero, the energy functional $E\{D^1\}$ is given by the Hartree-Fock energy functional. If the correlation energy is nonzero, and the density matrix restricted to be idempotent, the operator $h(x, x')$ can be expressed as the sum of the Fock operator $f(x, x')$ and an operator $v_c(x, x')$, the correlation potential

$$h(x, x') = f(x, x') + v_c(x, x'). \tag{2.95}$$

If the correlation potential is derived from a partitioned equation-of-motion approach, as described in the next chapter, the correlation potential is energy-dependent. The resultant orbitals are nonorthogonal, and the density matrix is therefore not idempotent. Strictly speaking, the model is not an independent particle model, if an energy-dependent correlation potential is used, and the density matrix could, in principle, be obtained exactly. The disadvantage of an energy-dependent correlation potential is that a different eigenvalue problem has to be solved for each orbital separately with corresponding eigenvalue. Our efforts therefore aim towards an energy-independent correlation potential, which can be constructed using the Fock space coupled-cluster method.

Our goal is to express the correlation potential v_c in a basis (i.e., a matrix representation), symbolized by

$$\mathbf{V_c} = \mathbf{H} - \mathbf{F}. \tag{2.96}$$

Since the eigenvalues of $\mathbf{F}$ are Koopmans' values for ionization potentials (IP's) and electron affinities (EA's), a reasonable assumption would be that the eigenvalues of $\mathbf{H}$ are the exact IP's and EA's. The condition of exactness of the IP's and EA's as the eigenvalues of $\mathbf{H}$ could then be used to derive the correlation potentials for the CIP model.

The extended Koopmans' theorem employs one-particle operators whose eigenvalues are IP's and EA's while using the exact wave-function. Since the extended Koopmans' theorem (EKT) inspired and supported our choice of the condition we want to impose on the correlation potential of the CIP model, the EKT is described next.

2.4 Extended Koopmans' Theorem

Within the Hartree-Fock theory, Koopmans' theorem Eq. 2.10 and Eq. 2.11 provides a simple one-electron model for ionization and electron attachment. A

similar model using the exact wave-function or a correlated wave-function for the unionized/unattached system is given by the extended Koopmans' theorem, which was independently developed by Day, Smith and Garrod [52, 59, 75, 76] for single ionization and attachment processes and a generalization of it for ionization, which includes double and higher ionization by Morrell, Parr and Levy [53].

The EKT method folds the information of the 2-matrix into two distinct one-particle potentials. One has eigenvalues that represent ionization energies and eigenfunctions, which represent the orbitals from which the electron is removed. The other has eigenvalues that represent electron affinities and eigenfunctions, which represent the orbitals for the addition of an electron.

The basic assumption of the EKT method is that ionization and electron capture can be described by the creation or annihilation of a single spin orbital. Ionization is viewed as elimination of a variationally determined orbital from a fixed correlated reference wave-function of the N-electron system, electron attachment as addition of a variationally determined orbital to a fixed correlated reference wave-function. The model accounts for correlation and relaxation effects.

The wave-function of the $N+1$ system, where an electron in orbital ψ_r was added to the wave-function of the N electron system Ψ^N, can be expressed as

$$\Psi_r^{N+1} = (N+1)^{-\frac{1}{2}} \mathcal{A}\psi_r(x_1)\Psi^N(x_2 \ldots x_{N+1}) = \mathcal{O}_r^\dagger \Psi^N, \tag{2.97}$$

where r is the particular state of the negative ion. The wave-function of the $N-1$ system, where an electron in orbital ψ_s was deleted from the wave-function of the N electron system, is given by

$$\Psi_s^{N-1} = N^{\frac{1}{2}} \int \psi_s^*(x_1)\Psi^N(x_1, x_2 \ldots x_N)dx_1 = \mathcal{O}_s^\dagger \Psi^N, \tag{2.98}$$

where s is the particular state of the positive ion and $\mathcal{A}$ is the antisymmetrizer. The operators $\mathcal{O}^\dagger$ and the optimized one-electron function are defined as

$$\mathcal{O}_r^\dagger = \sum_p p^\dagger c_{pr}^+ \qquad \mathcal{O}_s^\dagger = \sum_p p(c_{ps}^-)^* \tag{2.99}$$

$$\psi_r = \sum_p \phi_p c_{pr}^+ \qquad \psi_s = \sum_p \phi_p c_{ps}^-, \tag{2.100}$$

where $p^\dagger$ is the creation operator and p is the annihilation operator for the basis spin orbital ϕ_p, and the c_{ps}^- and the c_{pr}^+ are the coefficients, which are to be determined variationally. The creation and annihilation operators satisfy the following anticommutation relations

$$\begin{aligned} 0 &= sr + rs \\ 0 &= s^\dagger r^\dagger + r^\dagger s^\dagger \\ \delta_{rs} &= sr^\dagger + r^\dagger s. \end{aligned} \tag{2.101}$$

If Ψ^N is normalized, and ω is r or s, then the energy difference ϵ_ω between the ionic and the parent species is defined by

$$\epsilon_\omega = \frac{\langle \mathcal{O}_\omega^\dagger \Psi^N | H | \mathcal{O}_\omega^\dagger \Psi^N \rangle}{\langle \mathcal{O}_\omega^\dagger \Psi^N | \mathcal{O}_\omega^\dagger \Psi^N \rangle} - \langle \Psi^N | H | \Psi^N \rangle. \tag{2.102}$$

ϵ_ω is an orbital-energy-like quantity, because if Ψ^N is frozen and ψ_ω is varied, the right-hand side of Eq. 2.102 depends only on the parameters in the orbital ψ_ω. Eq. 2.102 takes a simple form, if Ψ^N is an eigenfunction of the Hamiltonian H, because then the second term on the right-hand side of Eq. 2.102 can be written as

$$\begin{aligned} \langle \Psi^N | H | \Psi^N \rangle &= \frac{\langle \Psi^N | \mathcal{O}_\omega \mathcal{O}_\omega^\dagger | \Psi^N \rangle \langle \Psi^N | H | \Psi^N \rangle}{\langle \Psi^N | \mathcal{O}_\omega \mathcal{O}_\omega^\dagger | \Psi^N \rangle} \\ &= \frac{\langle \Psi^N | \mathcal{O}_\omega \mathcal{O}_\omega^\dagger | \Psi^N \rangle \langle \Psi^N | \Psi^N \rangle E}{\langle \mathcal{O}_\omega^\dagger \Psi^N | \mathcal{O}_\omega^\dagger | \Psi^N \rangle} \\ &= \frac{\langle \Psi^N | \mathcal{O}_\omega \mathcal{O}_\omega^\dagger H | \Psi^N \rangle}{\langle \mathcal{O}_\omega^\dagger \Psi^N | \mathcal{O}_\omega^\dagger | \Psi^N \rangle}, \end{aligned} \tag{2.103}$$

and Eq. 2.102 becomes

$$\epsilon_\omega = \frac{\langle \Psi^N | \mathcal{O}_\omega [H, \mathcal{O}_\omega^\dagger] | \Psi^N \rangle}{\langle \Psi^N | \mathcal{O}_\omega \mathcal{O}_\omega^\dagger | \Psi^N \rangle}. \tag{2.104}$$

In case of an electron removal, $\mathcal{O}_\omega^\dagger = \mathcal{O}_s^\dagger$, given by Eq. 2.99. Insertion into Eq. 2.104 leads to

$$\sum_{pq} c_{ps}^- (c_{qs}^-)^* \langle \Psi^N | p^\dagger q | \Psi^N \rangle \epsilon_s = \sum_{pq} c_{ps}^- (c_{qs}^-)^* \langle \Psi^N | p^\dagger [H, q] | \Psi^N \rangle, \tag{2.105}$$

which can be written in matrix form

$$(\mathbf{c}^-)^\dagger (\mathbf{V}^- - \epsilon^- \mathbf{S}^-) \mathbf{c}^- = 0, \tag{2.106}$$

with the matrices $\mathbf{V}^-$ and $\mathbf{S}^-$ defined as

$$V_{qp}^- = -\langle \Psi^N | p^\dagger [H, q] | \Psi^N \rangle \tag{2.107}$$

$$S_{qp}^- = \langle \Psi^N | p^\dagger q | \Psi^N \rangle. \tag{2.108}$$

$\mathbf{V}^-$ is the effective one-body potential in which the electron to be ionized moves. The variationally stable orbitals $\mathbf{c}^-$ are the eigenvectors of $\mathbf{V}^-$ with respect to the metric $\mathbf{S}^-$. The eigenvectors and eigenenergies are solutions to the equation

$$\mathbf{V}^- \mathbf{c}^- = \mathbf{S}^- \mathbf{c}^- \epsilon^-. \tag{2.109}$$

The matrix $\mathbf{S}^-$ can be identified with the first-order reduced-density matrix written in second quantization. With the metric $\mathbf{S}^-$ the domain of the operator $\mathbf{V}^-$ is limited to the region of the one-particle space spanned by the eigenfunctions of the 1-matrix, having nonzero eigenvalues.

If the reference function is not an exact eigenfunction of the Hamiltonian, $\mathbf{V}^-$ will not, in general, be Hermitian. The right-hand side of Eq. 2.107 should then be

replaced by its Hermitian component

$$V_{qp}^{-} = -\frac{1}{2}\langle\Psi^N|p^\dagger[H,q] + [p^\dagger, H]q|\Psi^N\rangle. \tag{2.110}$$

The metric remains unaltered.

To derive an explicit expression for $\mathbf{V}^-$, the Hamiltonian in second quantization, given by

$$\begin{aligned} H &= \sum_{rs} h_{rs} r^\dagger s + \frac{1}{2}\sum_{rstu}\langle rs|ut\rangle r^\dagger s^\dagger tu \\ &= \sum_{rs} h_{rs} r^\dagger s + \frac{1}{4}\sum_{rstu}\langle rs||ut\rangle r^\dagger s^\dagger tu, \end{aligned} \tag{2.111}$$

is inserted in Eq. 2.107. Using the anticommutation relations 2.101, the one-electron part of V_{qp}^- can be written as

$$\begin{aligned} \left(V_{qp}^1\right)^- &= -\langle\Psi^N|p^\dagger[\sum_{rs} h_{rs} r^\dagger s, q]|\Psi^N\rangle \\ &= -\sum_{rs} h_{rs}\langle\Psi^N|p^\dagger r^\dagger sq|\Psi^N\rangle + \sum_{rs} h_{rs}\langle\Psi^N|p^\dagger qr^\dagger s|\Psi^N\rangle \\ &= \sum_{rs} h_{rs}\langle\Psi^N|p^\dagger r^\dagger qs|\Psi^N\rangle + \sum_{rs} h_{rs}\langle\Psi^N|p^\dagger s|\Psi^N\rangle\delta_{qr} \\ &\quad -\sum_{rs} h_{rs}\langle\Psi^N|p^\dagger r^\dagger qs|\Psi^N\rangle = \sum_{s} h_{qs} D_{ps}^1. \end{aligned} \tag{2.112}$$

Similar steps can be done for the two-electron part

$$\begin{aligned} \left(V_{qp}^2\right)^- &= -\frac{1}{2}\sum_{rstu}\langle rs|ut\rangle\langle\Psi^N|p^\dagger[r^\dagger s^\dagger tu, q]|\Psi^N\rangle \\ &= -\frac{1}{2}\sum_{rstu}\langle rs|ut\rangle\langle\Psi^N|p^\dagger r^\dagger s^\dagger tuq|\Psi^N\rangle + \frac{1}{2}\sum_{rstu}\langle rs|ut\rangle\langle\Psi^N|p^\dagger qr^\dagger s^\dagger tu|\Psi^N\rangle \\ &= -\frac{1}{2}\sum_{rstu}\langle rs|ut\rangle\langle\Psi^N|p^\dagger r^\dagger s^\dagger qtu|\Psi^N\rangle + \frac{1}{2}\sum_{rstu}\langle rs|ut\rangle\langle\Psi^N|p^\dagger s^\dagger tu|\Psi^N\rangle\delta_{qr} \\ &\quad -\frac{1}{2}\sum_{rstu}\langle rs|ut\rangle\langle\Psi^N|p^\dagger r^\dagger tu|\Psi^N\rangle\delta_{qs} + \frac{1}{2}\sum_{rstu}\langle rs|ut\rangle\langle\Psi^N|p^\dagger r^\dagger s^\dagger qtu|\Psi^N\rangle \\ &= \frac{1}{2}\sum_{rtu}\langle rq||ut\rangle\langle\Psi^N|p^\dagger r^\dagger tu|\Psi^N\rangle = 2\sum_{rtu}\langle rq||ut\rangle D_{prtu}^2, \end{aligned} \tag{2.113}$$

where D^2_{prtu} is the symmetric part of the second-order reduced-density matrix

$$\frac{1}{2}\langle\Psi^N|p^\dagger r^\dagger tu|\Psi^N\rangle \equiv D^2_{prtu} - D^2_{prut}. \tag{2.114}$$

Adding Eq. 2.112 and Eq. 2.113 leads to

$$V^-_{qp} = \sum_s h_{qs} D^1_{ps} + 2\sum_{rtu}\langle rq||ut\rangle D^2_{prtu}. \tag{2.115}$$

For exact 2-matrices $D^2_{prtu} = -D^2_{prut}$ holds, for approximated wave-functions that might be an approximation. The matrix $\mathbf{V}$ is also known as the generalized Fock matrix [66].

The coordinate representation of the nonlocal potential Eq. 2.115 is given by

$$V^-(x,x') = h(x)D^1(x,x') + 2\int u(x,x'')D^2(x''x,x''x')dx''. \tag{2.116}$$

Eigenfunctions and eigenenergies to that operator are solutions to

$$\int V^-(x,x')\psi_s(x')dx' = \epsilon_s \int D^1(x,x')\psi_s(x'). \tag{2.117}$$

The one-particle functions ψ_s are some linear combination of natural orbitals having nonzero occupancy in the reference function Ψ^N.

Similarly, for the attachment of an electron the one-electron potential is defined by

$$\begin{aligned} V^+_{qp} &= \langle\Psi^N|q[H,p^\dagger]|\Psi^N\rangle & (2.118)\\ &= h_{qp} + \sum_{tu}\langle pt||qu\rangle D^1_{ut} - V^-_{qp}. & (2.119)\end{aligned}$$

The potential is defined with respect to the metric

$$\begin{aligned} S^+_{qp} &= \langle\Psi^N|qp^\dagger|\Psi^N\rangle & (2.120)\\ &= \delta_{qp} - D^1_{qp} & (2.121)\end{aligned}$$

The corresponding nonlocal operator to Eq. 2.119 in coordinate representation is given by

$$V^+(x,x') = \delta(x-x')h(x) + \delta(x-x')\int u(x,x'')D^1(x'',x''')dx'' - u(x,x')D^1(x,x') - h(x)D^1(x,x') - 2\int u(x,x'')D^2(x''x,x'''x')dx''. \quad (2.122)$$

The metric in coordinate representation can be written as

$$S^+(x,x') = \delta(x-x') - D^1(x,x'). \quad (2.123)$$

The potential is defined with respect to the orbital basis spanned by natural orbitals, having nonunity occupation numbers. If the 2-matrix is not derived from an exact eigenfunction of the Hamiltonian, the Hermitian component is used as before.

Defining a new potential by combining the first three terms of the right-hand side of Eq. 2.122

$$V(x,x') = \delta(x-x')h(x) + \delta(x-x')\int u(x,x'')D^1(x'',x''')dx'' - u(x,x')D^1(x,x'), \quad (2.124)$$

the one-particle potential $V^+(x,x')$ can be written as

$$V^+(x,x') = V(x,x') - V^-(x,x'). \quad (2.125)$$

V corresponds directly to the Hartree-Fock potential with the Hartree-Fock density matrix replaced by a correlated 1-matrix.

The variationally stable orbitals ψ_r, to which an electron is added, and the eigenenergies are obtained as solutions of

$$\int V^+(x,x')\psi_r(x')dx' = \epsilon_r \int S^+(x,x')\psi_r(x'), \quad (2.126)$$

which in matrix representation is given by

$$\mathbf{V}^+\mathbf{c}^+ = \mathbf{S}^+\mathbf{c}^+\epsilon^+. \quad (2.127)$$

Orthogonalization of the eigenvectors by substituting $\mathbf{c}^{\pm} = \mathbf{S}^{\pm\frac{1}{2}}(\mathbf{c}')^{\pm}$ into Eq. 2.109 and Eq. 2.127, and symbolizing ionization or attachment by $\pm$, leads to

$$\mathbf{F}^{\pm}_{EKT}(\mathbf{c}')^{\pm} = (\mathbf{c}')^{\pm}\epsilon^{\pm} \tag{2.128}$$

with

$$\mathbf{F}^{\pm}_{EKT} = \mathbf{S}^{\pm\frac{1}{2}}\mathbf{V}^{\pm}\mathbf{S}^{\pm\frac{1}{2}}. \tag{2.129}$$

$\mathbf{F}^{\pm}_{EKT}$ the nonlocal extended Koopmans' theorem Fock operator in matrix form. $\mathbf{F}^{\pm}_{EKT}$ is nonhermitian for approximate wave-functions that include correlation. However, its eigenvalues are real and equal to the variationally optimized energy differences between the ionic and parent species: the IP's and the negative of the EA's.

The question whether or not the EKT method is exact has been discussed by several authors. Morrell et al. [53] suggested that the lowest ionization potential is correct. Katriel and Davidson [54] showed that if the N-electron wave-function is exact, at least the smallest ionization energy and the corresponding orbital are exact, meaning that the partner to the eigenfunction of the one-particle operator is an exact eigenfunction of the $(N-1)$-particle Hamiltonian. Based on a second-order perturbation analysis Pickup and Snijders [77] concluded that except for a two-electron system none of the EKT eigenvalues is exact. Numerical support for the exactness of the lowest ionization potential was given by Morrison and Sundholm and Olsen [56–58]. Olsen and Sundholm [55] also argued that for the lowest IP and a complete basis set, the second and higher-order correction, obtained from the EKT method, are correct. Recently Pernal and Cioslowski [78] published a theorem that provides a sufficient condition for the validity of the extended Koopmans' theorem.

The EKT defines one-particle operators, whose eigenvalues are IP's and the negative of EA's, of which at least the highest IP is exact, if the exact wave-function is used. That supports our choice of the condition on the correlation potential to reproduce the exact IP's and EA's as eigenvalues of $h(x_1, x_1')$.

If the wave-function is a single Slater determinant, the 2-matrix can be written as

$$D^2(x_1x_2, x_1'x_2') = \frac{1}{2}\left[D^1(x_1, x_1')D^1(x_2, x_2') - D^1(x_1, x_2')D^1(x_2, x_1')\right]. \quad (2.130)$$

The one-particle potentials reduce to

$$V^-(x, x') = \int V(x, x'')D^1(x'', x')dx'' \quad (2.131)$$

$$V^+(x, x') = \int V(x, x'')\left(\delta(x'' - x') - D^1(x'', x')\right)dx'' \quad (2.132)$$

These are representations of the Hartree-Fock potential, projected onto the disjoint spaces spanned by $\mathbf{D^1}$ and $\mathbf{1 - D^1}$. Orthonormalization of the eigenvectors gives the Fock operator in its common form. The eigenenergies of the two potentials are Koopmans' values for IP's and EA's.

2.5 Alternative Models Based on the Hohenberg-Kohn-Gilbert Theorem

Within the last six years, density matrix functional theory based on the Hohenberg-Kohn-Gilbert theorem has received new interest. Most of the proposed density matrix functionals are written in terms of natural orbitals, and are usually referred to as natural orbital functionals.

The total energy can be expressed in terms of the natural orbitals ϕ_p, and the diagonal elements of the second-order reduced-density matrix $\sigma(x_1, x_2)$

$$\sigma(x_1, x_2) = D^2(x_1x_2, x_1x_2). \quad (2.133)$$

The energy is given by

$$E = -\frac{1}{2}\sum_p n_p \int \phi_p(x_1)\nabla^2\phi_p(x_1)dx_1 + \int v(x_1)D^1(x_1, x_1)dx_1 + \int\int \frac{\sigma(x_1, x_2)}{r_{12}}dx_1dx_2. \quad (2.134)$$

In order to formulate a functional that depends on natural orbitals, the two-particle density σ has to be approximated, since the exact dependence of the 2-matrix on the 1-matrix is not known. The different natural orbital functionals differ in the approximation scheme used for the two-particle density.

Csányi and Arias [26] introduced the terminology of corrected Hartree and corrected Hartree-Fock functionals, in which most of the natural orbital functionals can be divided. They considered tensor product approximations to the 2-matrix to provide estimates of the 2-matrix in terms of the 1-matrix. The 2-matrix, which depends on four variables, is expanded in terms of one-body operators g_p and h_p, which depend on two variables,

$$D^2 = \sum_p g_p \otimes h_p. \tag{2.135}$$

The tensor product denotes one of the three possible choices for separating four variables

$$I: \qquad g \otimes h = g(x_1, x_1')h(x_2, x_2') \tag{2.136}$$

$$II: \qquad g \otimes h = g(x_1, x_2)h(x_1', x_2') \tag{2.137}$$

$$III: \qquad g \otimes h = g(x_1, x_2')h(x_2, x_1'). \tag{2.138}$$

If the 2-matrix is approximated by a single tensor product of type I, the familiar Hartree approximation is recovered, and a corrected Hartree scheme can be defined by

$$D^2_{CH} = \frac{1}{2}\left(D^1 \otimes_I D^1\right) + D^2_{xc}. \tag{2.139}$$

The factor $\frac{1}{2}$ is needed to maintain normalization. D^2_{xc} represents exchange and correlation effects, and can be expanded according to Eq. 2.135.

Alternatively antisymmetry might be ensured explicitly, which leads to the corrected Hartree-Fock scheme

$$D^2_{CHF} = \frac{1}{2}\left(D^1 \otimes_I D^1 - D^1 \otimes_{III} D^1\right) + D^2_c. \tag{2.140}$$

The unknown D^2_c, representing the correlation effects, can again be expanded as in Eq. 2.135.

Terms of type II violate the condition that $D^2 \to 0$ as the insertion $x'_1 x'_2$ and removal $x_1 x_2$ locations are placed further apart. Such terms are therefore not included in an expansion of D^2.

If one wants to expand D^2 beyond the Hartree-Fock approximation, antisymmetry requires representing D^2 as a pair of terms, so that in its simplest form

$$D^2 = \frac{1}{2}\left(D^1 \otimes_I D^1 - D^1 \otimes_{III} D^1 + g \otimes_I g - g \otimes_{III} g\right). \tag{2.141}$$

The sum rule requires $g = \sqrt{\pm D^1(1 - D^1)}$. However, the structure of the energy functional Eq. 2.134 is such, that for this choice the resulting energy functional of D^1 is equal to that, generated by representing D^2_c as a single type III product.

The two simplest representations of the 2-matrix to explore are the corrected Hartree approximation

$$D^2_{CH} = \frac{1}{2}\left(D^1 \otimes_I D^1 - \sqrt{D^1} \otimes_{III} \sqrt{D^1}\right) \tag{2.142}$$

and the corrected Hartree-Fock approximation

$$D^2_{CHF} = \frac{1}{2}\left(D^1 \otimes_I D^1 - D^1 \otimes_{III} D^1 - \sqrt{D^1(1 - D^1)} \otimes_{III} \sqrt{D^1(1 - D^1)}\right). \tag{2.143}$$

Expressing the density matrix in terms of natural orbitals, leads to the different natural orbital functionals.

However, there are different choices for the expansion of the 2-matrix possible, if more terms are included in the expansion Eq. 2.135. Holas [79] also suggested

expanding the 2-matrix as a linear combination of products of type I and III, which leads to the corrected Hartree and corrected Hartree-Fock approaches as special cases of such an expansion.

Gödecker and Umrigar [28] employed a corrected Hartree type expression for the 2-matrix. For a spin-independent Hamiltonian each natural orbital can be chosen to be either spin up or spin down, and be labeled by an orbital index p and a spin index s_p. The approximate σ in Eq. 2.134 takes the following form

$$\sigma[\{n\},\{\phi\}] = \sum_{pq}{}' \frac{n_p n_q}{2}\phi_p^2(r_1)\phi_q^2(r_2) - \sum_{pq}{}' \frac{\sqrt{n_p n_q}}{2}\delta_{s_p s_q}\phi_p(r_1)\phi_q(r_1)\phi_p(r_2)\phi_q(r_2). \tag{2.144}$$

The n_p are the occupation numbers. The primes indicate that the $p = q$ terms are omitted. Omitting the terms $p = q$ in the sums in Eq. 2.144, introduces a correction for electron self-interaction, but it also causes the sum rule not to be fulfilled.

The ground state can be found by substituting the definition of σ, Eq. 2.144, into Eq. 2.134 and minimizing the energy with respect to the natural orbitals and the occupation numbers under the constraint that the natural orbitals be orthogonal. The functional derivatives are

$$\begin{aligned}\frac{\partial E}{\partial \phi_p(r_1)} &= -\frac{n_p}{2}\nabla^2\phi_p(r_1) + n_p v(r_1)\phi_p(r_1) + \sum_q{}' n_p n_q \phi_p(r_1)\int \frac{\phi_q^2(r_2)}{r_{12}}dr_2 \\ &\quad - \sum_q{}' \sqrt{n_p n_q}\delta_{s_p s_q}\phi_q(r_1)\int \frac{\phi_p(r_2)\phi_q(r_2)}{r_{12}}dr_2 \qquad (2.145) \\ \frac{\partial E}{\partial n_p} &= -\frac{1}{2}\int \phi_p(r_1)\nabla^2\phi_p(r_1)dr_1 + \int v(r_1)\phi_p^2(r_1)dr_1 \\ &\quad + \sum_q{}' n_q \int\int \frac{\phi_q^2(r_2)\phi_p^2(r_1)}{r_{12}}dr_1 dr_2 \\ &\quad - \frac{1}{2}\sum_q{}' \sqrt{\frac{n_q}{n_p}}\delta_{s_p s_q}\int\int \frac{\phi_p(r_2)\phi_q(r_2)\phi_p(r_1)\phi_q(r_1)}{r_{12}}dr_1 dr_2. \qquad (2.146)\end{aligned}$$

Note that the resulting functional coincides with the Hartree-Fock functional, if the occupation numbers are constrained to be 0 or 1.

Buijse and Bärends [27, 80] independently derived an expression for the two-particle density that is equivalent to Eq. 2.144, but where the sums run over all indices i and j, and is, therefore, not electron self-interaction corrected. Eq. 2.144 was derived by approximating the full exchange and coulomb correlation hole in a way that is analogous to the Fermi hole in the Hartree-Fock model.

Despite their simplicity, the corrected Hartree (CH) and corrected Hartree-Fock (CHF) functionals predict reasonably accurate correlation energies for atoms [28, 81]. On the other hand, the reconstructed 2-matrices fulfill only a few necessary conditions for N-representability [32, 33, 79], and fail to describe the homogeneous electron gas properly[29–31]. It was reported that the CH, CHF, and hybrids [32] potential energy curves for diatomics have almost no minimum, because of severe overcorrelation at large R [32, 82], whereas the Gödecker and Umrigar functional gave plausible molecular dissociation curves [32].

An alternative idea to construct the correlation energy functional was presented by Yasuda [34]. He used the density equation [83, 84], whose basic variable is the reduced-density matrix instead of the wave-function. The density equation is equivalent to the Schrödinger equation. Approximation of the correlation energy functional is introduced as the decoupling of the higher-order reduced-density matrices. Yasuda proposed a two-step procedure. In the first step the first-order density equation is used to reconstruct the one-body operator of the Hamiltonian. Once the Hamiltonian is obtained, the connected piece of the second-order reduced-density matrix Δ^2 is calculated by the second-order density equation, although it could be obtained by any other *ab initio* method. The two steps are repeated until convergence of Δ^2 is reached. The correlation energy can then be calculated from the converged Δ^2.

The first-order reduced-density equation is given by

$$\begin{aligned} 0 &= \{h(x_1) - E\}\, D^1(x_1', x_1) + 2\int \{h(x_2) + u(x_1, x_2)\}\, D^2(x_1' x_2, x_1 x_2) dx_2 \\ &+ 3\int u(x_2, x_3) D^3(x_1' x_2 x_3, x_1 x_2 x_3) dx_2 dx_3. \end{aligned} \tag{2.147}$$

The reduced-density matrices of the exact eigenstate of H satisfy this equation. The second- and third-order reduced-density matrices can symbolically be expressed as

$$D^2 = D^1 \wedge D^1 + \Delta^2 \tag{2.148}$$

$$D^3 = D^1 \wedge D^1 \wedge D^1 + 3D^1 \wedge \Delta^2 + \Delta^3. \tag{2.149}$$

The wedge product $\wedge$ generates the normalized antisymmetrized product. Δ^3 is the connected piece of the third-order reduced-density matrix. In Yasuda's approach the third-order reduced-density matrix is approximated in terms of D^1 and Δ^2 alone, when substituted in Eq. 2.147.

If the natural spin orbitals are used as the one-particle basis, the diagonal elements of the generalized Fock operator are given by

$$\epsilon_p = \frac{2\alpha(2n_p - 1)}{n_p(1 - n_p)} \sum_{qrs} \langle pq||rs\rangle \Delta^2_{pqrs}, \tag{2.150}$$

with n_i being the natural occupation numbers. The rescaling factor α is introduced to compensate for the effect of the higher-order terms.

Eq. 2.147 and Eq. 2.150 determine the one-body operator or the generalized Fock operator in terms of the 1-matrix and a trial 2-matrix. With the reconstructed Hamiltonian, the 2-matrix can be determined and the calculation of the one-body operator is repeated until convergence. The correlation energy is given by

$$\begin{aligned} E_c &= \int u(x_1, x_2) \Delta^2(x_1 x_2, x_1 x_2) dx_1 dx_2 \\ &= \sum_p \frac{n_p(1 - n_p)\epsilon_p}{2\alpha(2n_p - 1)}. \end{aligned} \tag{2.151}$$

If the second-order density equation is used to determine the 2-matrix, then, in principle, the exact correlation functional could be obtained, if one were to use the exact reconstruction formulas of the third- and fourth-order reduced-density matrices.

The Yasuda functional reproduces the correlation energy of selected atoms and molecules accurately [34], satisfies the homogeneous scaling relation [85], and the particle-hole symmetry [34]. It also performs well for the homogeneous electron gas [86]. However, if the approximate reconstruction formulas for the higher-order density matrices are used, the N-representability condition on the 2-matrix is not fulfilled [34], and the energy functional becomes unbounded from below [87]. Yasuda also presented a local approximation to the correlation energy functional [36], which is very similar in appearance to the local density approximation [3, 88] in DFT.

Mazziotti also suggested an iterative scheme in which the first-order density equation is employed to construct an energy functional of the 1-matrix [35]. He proposed the use of an antisymmetrized geminal power ansatz [61] to reconstruct the reduced-density matrices of different order.

Alternatively, Cioslowski and Lopez-Boada [38, 39] presented a scheme that applies the hypervirial theorem, yielding a functional of the 1-matrix. The functional is parameterized by a single screening function, retrieved from the correlation energy of the homogeneous electron gas.

CHAPTER 3
CORRELATION POTENTIALS YIELDING EXACT IONIZATION POTENTIALS AND ELECTRON AFFINITIES

In the last chapter the correlated independent particle (CIP) model, which can be viewed as a generalization to the Hartree-Fock model, or an approximation to density matrix functional theory, was discussed. Within the CIP model the exchange energy and the kinetic energy can be expressed exactly in terms of the density matrix. The remaining unknown is the functional of the correlation energy in terms of the density matrix. A model was proposed in which the energy functional is decomposed into the Hartree-Fock functional, plus a correlation potential. From Koopmans' theorem and the extended Koopmans' theorem it was found reasonable to impose the condition of exactness of the ionization potentials (IP) and electron affinities (EA) as the negative of the orbital energies, in order to obtain a correlation potential.

In this chapter, I will discuss how to obtain a correlation potential, yielding the exact IP's and EA's. First the equation-of-motion coupled-cluster (EOM-CC) approach is reformulated to extract an energy-dependent correlation potential. Then the equivalence to the propagator approach will be shown. Finally the Fock space coupled-cluster (FSCC) method is exploited to obtain an energy-independent correlation potential that is universal for all orbitals.

3.1 Correlation Potential Derived from the Equation-of-Motion Coupled-Cluster Method

The EOM-CC method gives the exact IP's and EA's, if no truncation is employed. In order to find a correlation potential for the CIP model, so that the negative of the independent particle eigenvalues are the exact IP's and EA's, the

EOM-CC method is reformulated in this section. An effective Hamiltonian is obtained, from which a correlation potential can be extracted. First the coupled-cluster (CC) method is introduced, followed by the EOM-CC method. The partitioning technique, which yields the effective Hamiltonian, from which an energy-dependent correlation potential is obtained, is discussed, and finally the connection to the propagator method is shown.

3.1.1 Coupled-Cluster Method

Before outlining the CC method, the concept of normal ordering, which is conveniently used later, is introduced. A product of creation and annihilation operators is said to be in normal order relative to the Fermi vacuum Φ_0, if all particle creation operators $a^\dagger, b^\dagger, \ldots$ and all hole annihilation operators $i, j, \ldots$ are to the left of all particle annihilation operators $a, b, \ldots$ and of all hole creation operators $i^\dagger, j^\dagger, \ldots$. The Fermi vacuum expectation value of a normal-ordered product of such operators vanishes.

The Hamiltonian in second quantization was given in Eq. 2.111. The Hamiltonian is rewritten in normal order with respect to the Fermi vacuum by applying Wick's theorem (for a detailed proof [89]), which states, that the normal-ordered result of the product of two normal-ordered operator strings $\{A\}$ and $\{B\}$, equals the sum of the normal product $\{AB\}$ and all the possible contractions between operators from A and operators from B. The contraction of two fermion construction operators is defined as their anticommutator, if they are not in normal order and zero otherwise. The fermion construction operators fulfill the anticommutation relations, Eq. 2.101.

A contraction is denoted by a bullet following the operator, if necessary a double bullet is used to distinguish between two different contractions. The one-electron

part of the Hamiltonian then reads

$$\sum_{rs} h_{rs} r^\dagger s = \sum_{rs} h_{rs} \{r^\dagger s\} + \sum_{rs} h_{rs} r^{\dagger\bullet} s^\bullet = \sum_{rs} h_{rs} \{r^\dagger s\} + \sum_{i} h_{ii}. \tag{3.1}$$

The two-electron part can be rewritten as

$$\begin{aligned}
\frac{1}{2}\sum_{rstu} \langle rs|ut\rangle r^\dagger s^\dagger tu &= \frac{1}{2}\sum_{rstu} \langle rs|ut\rangle \{r^\dagger s^\dagger tu\} + \frac{1}{2}\sum_{rstu} \langle rs|ut\rangle \left(r^{\dagger\bullet} s^\dagger t^\bullet u \right. \\
&+ r^{\dagger\bullet} s^\dagger tu^\bullet + r^\dagger s^{\dagger\bullet} t^\bullet u + r^\dagger s^{\dagger\bullet} tu^\bullet + r^{\dagger\bullet} s^{\dagger\bullet} t^\bullet u^{\bullet\bullet} \\
&+ \left. r^{\dagger\bullet} s^{\dagger\bullet} t^{\bullet\bullet} u^\bullet \right) \\
&= \frac{1}{2}\sum_{rstu} \langle rs|ut\rangle \{r^\dagger s^\dagger tu\} + \sum_{rsi} \left(\langle ir|is\rangle - \langle ir|si\rangle \right) \{r^\dagger s\} \\
&+ \frac{1}{2}\sum_{ij} \left(\langle ij|ij\rangle - \langle ij|ji\rangle \right).
\end{aligned} \tag{3.2}$$

The energy of the Hartree-Fock reference state is defined as

$$E_0 = \langle \Phi_0 | H | \Phi_0 \rangle = \sum_i h_{ii} + \frac{1}{2}\sum_{ij} \left(\langle ij|ij\rangle - \langle ij|ji\rangle \right), \tag{3.3}$$

and the matrix elements of the Fock matrix corresponding to Φ_0 are given by

$$f_{rs} = h_{rs} + \sum_i \left(\langle ir|is\rangle - \langle ir|si\rangle \right). \tag{3.4}$$

Combining Eq. 3.1, Eq. 3.2, Eq. 3.3, and Eq. 3.4, the Hamiltonian is rewritten as

$$\begin{aligned}
H &= E_0 + \sum_{rs} f_{rs} \{r^\dagger s\} + \frac{1}{2}\sum_{rstu} \langle rs|ut\rangle \{r^\dagger s^\dagger tu\} \\
&= E_0 + \sum_{rs} f_{rs} \{r^\dagger s\} + \frac{1}{4}\sum_{rstu} \langle rs||ut\rangle \{r^\dagger s^\dagger tu\},
\end{aligned} \tag{3.5}$$

The normal-ordered Hamiltonian H_N can now be defined as

$$H_N = H - E_0 = \sum_{rs} f_{rs} \{r^\dagger s\} + \frac{1}{4}\sum_{rstu} \langle rs||ut\rangle \{r^\dagger s^\dagger tu\}. \tag{3.6}$$

Having the necessary conventions established, the coupled-cluster ansatz can be discussed. The coupled-cluster wave-function [90, 91] is parameterized by an

exponential ansatz

$$\Psi = e^T \Phi_0, \tag{3.7}$$

where T is an excitation operator. The exponential ansatz ensures extensivity, and exhibits better convergence to the full configuration interaction (CI) limit than a linear expansion.

The operator T consists of one-body (T_1), two-body (T_2), etc. cluster operators

$$T = T_1 + T_2 + T_3 \ldots. \tag{3.8}$$

Each cluster operator is a sum of creation and annihilation operators, which fulfill Eq. 2.101, multiplied by an appropriate coefficient, called the amplitudes

$$\begin{aligned} T_1 &= \sum_{ia} t_i^a \{a^\dagger i\} \\ T_2 &= \frac{1}{4} \sum_{ijab} t_{ij}^{ab} \{a^\dagger i b^\dagger j\} \\ T_3 &= \frac{1}{36} \sum_{ijkabc} t_{ijk}^{abc} \{a^\dagger i b^\dagger j c^\dagger k\} \ldots. \end{aligned} \tag{3.9}$$

The braces $\{\}$ indicate normal ordering. In general the cluster operator is given by

$$T_m = \frac{1}{(m!)^2} \sum_{\substack{ij\ldots \\ ab\ldots}} t_{ij\ldots}^{ab\ldots} \{a^\dagger i b^\dagger j \ldots\}, \tag{3.10}$$

where $m \leq N$, the number of electrons. The factor $\frac{1}{(m!)^2}$ accounts for the fact, that permutations among the hole indices or the particle indices do not create distinct contributions. For example

$$\begin{aligned} t_{ij}^{ab} &= -t_{ji}^{ab} = -t_{ij}^{ba} = t_{ji}^{ba} \\ a^\dagger i b^\dagger j &= -a^\dagger j b^\dagger i = -b^\dagger i a^\dagger j = b^\dagger j a^\dagger i \end{aligned} \tag{3.11}$$

contribute 4 equal terms.

If the operator T is not truncated, the expansion Eq. 3.7 is the exact wave-function. However, to make the calculation feasible, the operator T usually has to be truncated. A common approximation is the CCSD method, in which only T_1 and T_2 are kept in Eq. 3.7. If the exponential is expanded in a Taylor series

$$e^T = 1 + T + \frac{1}{2}T^2 + \frac{1}{3!}T^3 + \ldots, \tag{3.12}$$

the CCSD wave-function is given by

$$\begin{aligned} \Psi &= \Phi_0 + T_1\Phi_0 + T_2\Phi_0 + \frac{1}{2}T_1^2\Phi_0 + T_1T_2\Phi_0 + \frac{1}{2}T_2^2\Phi_0 \\ &+ \frac{1}{3!}T_1^3\Phi_0 + \frac{1}{2}T_1^2T_2\Phi_0 + \frac{1}{2}T_1T_2^2\Phi_0 + \frac{1}{3!}T_2^3\Phi_0 + \ldots. \end{aligned} \tag{3.13}$$

Terms in Ψ, which contain only a single cluster operator, are called connected-cluster contributions. Terms, which contain products of cluster operators, are called disconnected contributions, which are the reason for the extensivity of the coupled-cluster method.

The coupled-cluster equations can be derived with the help of Wick's theorem. The general idea holds for any truncation level, however, the following material will concentrate on the CCSD approximation. Inserting the coupled-cluster wave-function, Eq. 3.7, into the Schrödinger equation gives

$$H\Psi_{CCSD} = E_{CCSD}\Psi_{CCSD}. \tag{3.14}$$

If the reference energy E_0 is subtracted on both sides, the Schrödinger equation can alternatively be written as

$$H_N\Psi_{CCSD} = \Delta E_{CCSD}\Psi_{CCSD}, \tag{3.15}$$

where the normal-ordered Hamiltonian, Eq. 3.6, is used. $\Delta E_{CCSD} = E_{CCSD} - E_0$ is the correlation energy in the CCSD model, which can be obtained by projecting

from the left by the reference function Φ_0

$$\Delta E_{CCSD} = \langle \Phi_0 | H_N | \Psi_{CCSD} \rangle. \tag{3.16}$$

The intermediate normalization $\langle \Phi_0 | \Psi_{CCSD} \rangle = 1$ is chosen. Expanding the coupled-cluster wave-function leads to

$$\Delta E_{CCSD} = \langle \Phi_0 | H_N (1 + T_1 + T_2 + \frac{1}{2} T_1^2) | \Phi_0 \rangle. \tag{3.17}$$

Notice that the exponential series is self terminating because of the two-particle character of the Hamiltonian. Recalling that the vacuum expectation value of a normal-product operator is zero, the energy is given by

$$\begin{aligned} \Delta E_{CCSD} &= \langle \Phi_0 | H_N T_1 | \Phi_0 \rangle + \langle \Phi_0 | H_N T_2 | \Phi_0 \rangle + \frac{1}{2} \langle \Phi_0 | H_N T_1^2 | \Phi_0 \rangle \\ &= L_1 + L_2 + L_3. \end{aligned} \tag{3.18}$$

As an example the term L_2 is analyzed. If the definitions of the normal-ordered Hamiltonian, Eq. 3.6, and the T_2 cluster operator, Eq. 3.9, are inserted, L_2 is given by

$$L_2 = \frac{1}{4} \sum_{ijab} \langle \Phi_0 | \left[\sum_{rs} f_{rs} \{ r^\dagger s \} + \frac{1}{4} \sum_{rstu} \langle rs || ut \rangle \{ r^\dagger s^\dagger tu \} \right] \{ a^\dagger i b^\dagger j \} | \Phi_0 \rangle t_{ij}^{ab}. \tag{3.19}$$

The contribution of the one-electron part of H_N vanishes, since it is not possible to contract all the operators in this term without using an internal contraction in one of the normal-ordered products. That leaves

$$L_2 = \frac{1}{16} \sum_{ijab} \sum_{rstu} \langle rs || ut \rangle \langle \Phi_0 | \{ r^\dagger s^\dagger tu \} \{ a^\dagger i b^\dagger j \} | \Phi_0 \rangle t_{ij}^{ab}. \tag{3.20}$$

There are four ways to contract all the operators between the normal products

$$\begin{aligned} L_2 &= \frac{1}{16}\sum_{ijab}\sum_{rstu}\langle rs||ut\rangle\langle\Phi_0|\{r^{\dagger\bullet}s^{\dagger\bullet\bullet}t^{\circ}u^{\circ\circ}\}\{a^{\dagger\circ}i^{\bullet\bullet}b^{\dagger\circ\circ}j^{\bullet}\} \\ &+ \{r^{\dagger\bullet}s^{\dagger\bullet\bullet}t^{\circ}u^{\circ\circ}\}\{a^{\dagger\circ}i^{\bullet}b^{\dagger\circ\circ}j^{\bullet\bullet}\} + \{r^{\dagger\bullet}s^{\dagger\bullet\bullet}t^{\circ}u^{\circ\circ}\}\{a^{\dagger\circ\circ}i^{\bullet\bullet}b^{\dagger\circ}j^{\bullet}\} \\ &+ \{r^{\dagger\bullet}s^{\dagger\bullet\bullet}t^{\circ}u^{\circ\circ}\}\{a^{\dagger\circ\circ}i^{\bullet}b^{\dagger\circ}j^{\bullet\bullet}\}|\Phi_0\rangle t_{ij}^{ab} \\ &= \frac{1}{16}\sum_{ijab}\sum_{rstu}\langle rs||ut\rangle\left(\delta_{ta}\delta_{ub}\delta_{si}\delta_{rj} - \delta_{ta}\delta_{ub}\delta_{sj}\delta_{ri} - \delta_{tb}\delta_{ua}\delta_{si}\delta_{rj}\right. \\ &+ \left.\delta_{tb}\delta_{ua}\delta_{sj}\delta_{ri}\right)t_{ij}^{ab}. \end{aligned} \tag{3.21}$$

In addition to the bullets, circles are used to indicate a certain contraction. Adding the four terms, leads to

$$L_2 = \frac{1}{4}\sum_{ijab}\langle ij||ab\rangle t_{ij}^{ab}. \tag{3.22}$$

Similar manipulations can be done for the L_1 and L_3 terms, which gives for the CCSD energy

$$\Delta E_{CCSD} = \sum_{ia} f_{ia}t_i^a + \frac{1}{4}\sum_{ijab}\langle ij||ab\rangle t_{ij}^{ab} + \frac{1}{2}\sum_{ijab}\langle ij||ab\rangle t_i^a t_j^b. \tag{3.23}$$

The coupled-cluster energy depends on the amplitudes. Equations for the amplitudes are obtained by projecting Eq. 3.15 onto all excited determinants, in particular onto all singly and doubly excited determinants in the CCSD model. The number of resulting equations is exactly the same as the number of amplitudes to be determined. The amplitude equations for the CCSD model are

$$\begin{aligned} \Delta E_{CCSD}t_i^a &= \langle\Phi_i^a|H_N\left(1 + T_1 + T_2 + \frac{1}{2}T_1^2 + T_1T_2 + \frac{1}{3!}T_1^3\right)|\Phi_0\rangle \\ \Delta E_{CCSD}t_{ij}^{ab} &= \langle\Phi_{ij}^{ab}|H_N\left(1 + T_1 + T_2 + \frac{1}{2}T_1^2 + T_1T_2 + \frac{1}{2}T_2^2\right. \\ &+ \left.\frac{1}{3!}T_1^3 + \frac{1}{2}T_1^2T_2 + \frac{1}{4!}T_1^4\right)|\Phi_0\rangle. \end{aligned} \tag{3.24}$$

An important feature of the amplitude equations is that the energy-dependent terms on the left-hand side of Eq. 3.24 cancel with disconnected contributions on the

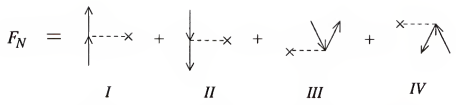

Figure 3–1. One-electron part of the normal-ordered Hamiltonian

right-hand side (linked-diagram theorem [92, 93]). The amplitude equations can be rewritten as

$$\begin{aligned} 0 &= \langle \Phi_i^a | H_N \left(1 + T_1 + T_2 + \frac{1}{2} T_1^2 + T_1 T_2 + \frac{1}{3!} T_1^3 \right) | \Phi_0 \rangle_c \\ 0 &= \langle \Phi_{ij}^{ab} | H_N \left(1 + T_1 + T_2 + \frac{1}{2} T_1^2 + T_1 T_2 + \frac{1}{2} T_2^2 \right. \\ &+ \left. \frac{1}{3!} T_1^3 + \frac{1}{2} T_1^2 T_2 + \frac{1}{4!} T_1^4 \right) | \Phi_0 \rangle_c, \end{aligned} \tag{3.25}$$

where c stands for connected contributions only.

It is possible to derive the amplitude equations using Wick's thereom, as demonstrated above in the example of the L_2 term in the energy expression. However, Eq. 3.21 shows that those manipulations can become tedious. For that reason the diagrammatic formalism is introduced next.

The diagrammatic derivation of the coupled-cluster equations is a pictorial way of applying Wick's theorem. The normal-ordered Hamiltonian and the cluster operators in diagrammatic form are used and the pieces are connected appropriately, which represents a particular class of contractions. The normal-ordered Hamiltonian is divided into a one-electron and a two-electron part

$$H_N = F_N + W_N. \tag{3.26}$$

The diagrammatic representation of F_N is given in Fig. 3–1, and its algebraic interpretation in Table 3–1. Down going lines represent holes, up going lines represent particles. Notice that in the Hartree-Fock case the last two contributions in

Table 3–1. Algebraic interpretation of F_N

diagram	I	II	III	IV
	$f_{ab}\{a^\dagger b\}$	$f_{ij}\{i^\dagger j\}$	$f_{ai}\{a^\dagger i\}$	$f_{ia}\{i^\dagger a\}$

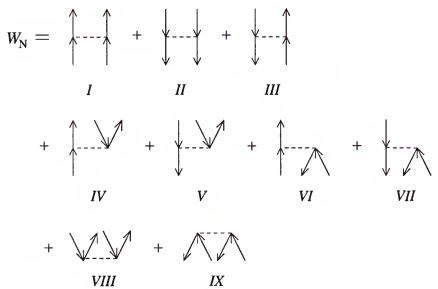

Figure 3–2. Two-electron part of the normal-ordered Hamiltonian

Fig. 3–1 vanish because of the block-diagonal nature of the Fock operator. The diagrammatic representation of W_N can be found in Fig. 3–2, and its algebraic interpretation in Table 3–2.

The last fragments, needed to formulate the CCSD equations diagrammatically, are the amplitudes, given in Fig. 3–3 and in Table 3–3. In order to obtain the coupled-cluster equations, the different fragments have to be connected in all possible ways that produce a particular excitation level. The excitation level for energy diagrams is zero, for T_1 amplitudes one, and for T_2 amplitudes two.

The CCSD energy was given in Eq. 3.18. To represent the first term in Eq. 3.18, one has to find all possible ways to connect a T_1 amplitude with the Hamiltonian that create diagrams with zero excitation level (i.e. closed diagrams, where all lines

Table 3–2. Algebraic interpretation of W

diagram	I	II	III		
	$\langle ab\|\|cd\rangle\{a^\dagger b^\dagger dc\}$	$\langle ij\|\|kl\rangle\{i^\dagger j^\dagger lk\}$	$\langle ai\|\|bj\rangle\{a^\dagger i^\dagger jb\}$		
diagram	IV	V	VI		VII
	$\langle ab\|\|ci\rangle\{a^\dagger b^\dagger ic\}$	$\langle ia\|\|jk\rangle\{i^\dagger a^\dagger kj\}$	$\langle ai\|\|bc\rangle\{a^\dagger i^\dagger cb\}$		$\langle ij\|\|ka\rangle\{i^\dagger j^\dagger ak\}$
diagram	VIII	IX			
	$\langle ab\|\|ij\rangle\{a^\dagger b^\dagger ji\}$	$\langle ij\|\|ab\rangle\{i^\dagger j^\dagger ba\}$			

T_1 T_2

Figure 3–3. Amplitudes

lead into a vertex). A vertex is the Hamiltonian or an amplitude. There is only one possibility to achieve that. The second term has to be represented by closed diagrams, for which the Hamiltonian is connected to a T_2 amplitude. Again there is only one way to do that. The last term involves closed diagrams, in which two T_1 amplitudes are connected to the Hamiltonian. Fig. 3–4 shows the CCSD energy (algebraically given Eq. 3.23) represented in diagrammatic form.

There are few rules to follow, when evaluating the coupled-cluster (antisymmetric) diagrams. As can be seen in Fig. 3–1, Fig. 3–2, and Table 3–1, Table 3–2, each one-particle Hamiltonian vertex is associated with $f_{\text{out,in}}$, and each two-particle Hamiltonian vertex is associated with $\langle \text{left} - \text{out right} - \text{out}||\text{left} - \text{in right} - \text{in}\rangle$. The creation and annihilation operators are implicitly considered by connecting the different diagram fragments according to the net excitation level of the diagram. Internal lines are summed over, those are lines that end on both sides in a vertex. With every pair of equivalent internal lines there is a factor of $\frac{1}{2}$ associated. A pair

Table 3–3. Algebraic interpretation of the amplitudes

diagram	T_1	T_2
	$t_i^a\{a^\dagger i\}$	$t_{ij}^{ab}\{a^\dagger i b^\dagger j\}$

of internal lines is equivalent, if they connect the same vertices and go in the same direction. There is also a factor of $\frac{1}{2}$ associated with every pair of equivalent T vertices. T vertices are considered equivalent if they are connected with the same number of lines equivalently connected to the Hamiltonian. All distinct permutations P of inequivalent external lines have to be summed over, with the exception of lines that would become equivalent if they were connected by a vertex. External lines are lines that are not connected on both sides to a vertex. With each permutation a factor of $(-1)^{\sigma(P)}$, where $\sigma(P)$ is the number of necessary exchanges of creation and annihilation operators to obtain the particular permutation, is associated. The sign of a diagram is determined by $-1^{(h-l)}$, where h is the number of internal hole lines and l is the number of loops.

To better follow which diagram belongs to which term in the amplitude equations, Eq. 3.25 is divided in different groups

$$\begin{aligned}
0 &= \langle\Phi_i^a|H_N\left(1+T_1+T_2+\frac{1}{2}T_1^2+T_1T_2+\frac{1}{3!}T_1^3\right)|\Phi_0\rangle_c \\
&= S_1+S_2+S_3+S_4+S_5+S_6 \\
0 &= \langle\Phi_{ij}^{ab}|H_N\left(1+T_1+T_2+\frac{1}{2}T_1^2+T_1T_2+\frac{1}{2}T_2^2\right. \\
&+ \left.\frac{1}{3!}T_1^3+\frac{1}{2}T_1^2T_2+\frac{1}{4!}T_1^4\right)|\Phi_0\rangle_c \\
&= D_1+D_2+D_3+D_4+D_5+D_6+D_7+D_8+D_9. \qquad (3.27)
\end{aligned}$$

Notice that the connected amplitude equations are used, where disconnected diagrams were already canceled by energy-dependent terms. To find the diagrams

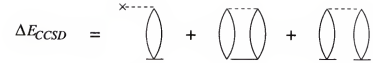

Figure 3–4. CCSD energy

contributing to the equation determining the T_1 amplitudes (all S terms), the amplitude vertices have to be connected in all possible ways to the Hamiltonian to give a net single excitation, where a hole line and a particle line is not connected to a vertex from the top. The T_2 amplitude equations can be obtained by finding all possible ways to connect the amplitudes with the Hamiltonian to give a net double excitation, where two hole lines and two particle lines are not connected to a vertex from the top. In Fig. 3–5 all the single excitation (S) terms can be found. The diagrams for the T_2 amplitudes are split, in Fig. 3–6 diagrams D_1 to D_4 are given, in Fig. 3–7 diagrams D_5, and in Fig. 3–8 diagrams D_6 to D_9. The diagrams can be interpreted with the rules given above. Notice that if Hartree-Fock orbitals are used diagrams S_1, the first S_3, the last S_4, and the first two D_5 are zero.

3.1.2 The EOM-CC Method

Quantum chemical treatment of electron correlation within the coupled-cluster approximation [90, 91] traditionally has been based on a single Slater determinant. That usually limits its applicability to the lowest electronic states of a particular symmetry and multiplicity. An efficient tool to access electronically excited states is the equation-of-motion coupled-cluster (EOM-CC) method [94–96]. The excited-state wave-function is generated from the coupled-cluster wave-function by the action of a wave operator. The wave operator is not restricted to conserve the number of particles. If the excited state is chosen to be a state, where an electron has been removed, the IP-EOM-CC method [97] emerges. If an electron is added, while forming the excited state, the approach is referred to as EA-EOM-CC method

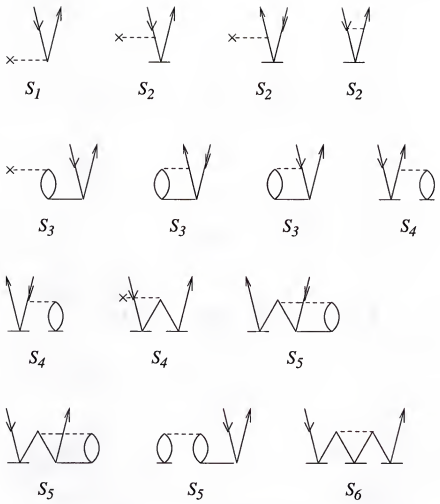

Figure 3–5. Single-excitation CCSD equations

[98]. Here, the focus is on the IP-EOM-CC and the EA-EOM-CC methods, since those are reformulated to obtain a correlation potential for the CIP model.

The equation of motion is given by

$$[H_N, \Omega_k]\,\Psi_0 = \omega_k \Omega_k \Psi_0. \tag{3.28}$$

Ψ_0 is the reference wave-function and H_N is the normal-ordered operator, introduced before in Eq. 3.6. The operator Ω_k consist of a constant and a string of creation and annihilation operators. If it preserves the number of particles, ω_k is an excitation

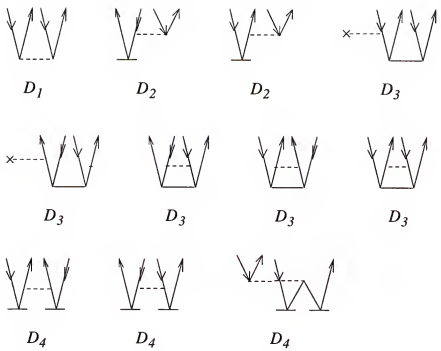

Figure 3–6. Double-excitation CCSD equations, terms D_1 through D_4

energy $E_k - E_0 = \Delta E_k - \Delta E_0 = \omega_k$. However, Ω_k may as well change the number of particles, making different sectors of the Fock space accessible.

The $(N-1)$-particle eigenstates may be obtained by using

$$\Omega_k = \sum_i c_i \{\hat{i}\} + \sum_{i<j,b} c_{ij}^b \{\hat{b}^\dagger \hat{j}\hat{i}\} + \dots . \tag{3.29}$$

In this case ω_k is an ionization energy. The $(N+1)$-particle eigenstates can be accessed by using

$$\Omega_k = \sum_a c^a \{\hat{a}^\dagger\} + \sum_{i,a<b} c_i^{ab} \{\hat{b}^\dagger \hat{a}^\dagger \hat{i}\} + \dots . \tag{3.30}$$

Choosing the wave operator as in Eq. 3.30, causes ω_k to be the negative of an electron affinity. The braces refer to normal ordering. The parameters c_λ are the amplitudes to be determined for the linear expansion of the eigenstates.

In the EOM-CC approach the reference function is chosen to be the coupled-cluster wave-function, Eq. 3.7, specifically, in the EOM-CCSD model, the CCSD

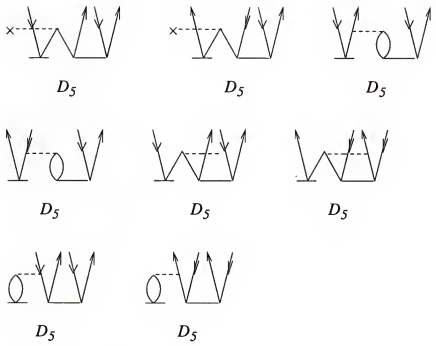

Figure 3–7. Double-excitation CCSD equations, terms D_5

wave-function 3.13 is used. Usually a balanced description for the reference function and the linear expansion of eigenstates is employed, which means that in the IP-EOM-CCSD and the EA-EOM-CCSD model at most a single excitation in addition to an ionization or attachment process are considered (i.e., the dots in Eq. 3.29 and Eq. 3.30 disappear).

Inserting ansatz 3.7 in Eq. 3.28, the equation-of-motion becomes

$$[H_N, \Omega_k]\, e^T \Phi_0 = \omega_k \Omega_k e^T \Phi_0. \tag{3.31}$$

Multiplying on the left with e^{-T}, and and using the fact that $[\Omega, T] = 0$, leads to

$$\left[\bar{H}_N, \Omega_k\right] \Phi_0 = \omega_k \Omega_k \Phi_0, \tag{3.32}$$

where $\bar{H}_N$ is the transformed Hamiltonian, consisting only of the connected part of the operator product

$$\bar{H}_N = e^{-T} H_N e^T = (H_N e^T)_c. \tag{3.33}$$

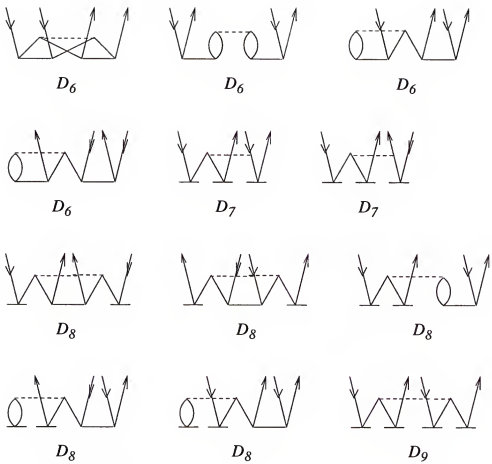

Figure 3–8. Double-excitation CCSD equations, terms D_6 through D_9

$\bar{H}_N$ contains all the ground-state CC information.

Eq. 3.32 can be rewritten into an eigenvalue problem by considering the following

$$\begin{aligned}\left[\bar{H}_N, \Omega_k\right]\Phi_0 &= \bar{H}_N\Omega_k\Phi_0 - \Omega_k\bar{H}_N\Phi_0 \\ &= \Delta E_k\Omega_k\Phi_0 - \Omega_k\Delta E_{CC}\Phi_0 \\ &= (\Delta E_k - \Delta E_{CC})\Omega_k\Phi_0 \\ &= (\bar{H}_N - \Delta E_{CC})\Omega_k\Phi_0. \end{aligned} \tag{3.34}$$

Since ΔE_{CC} represents a closed diagram, Eq. 3.34 can also be written as

$$\left[\bar{H}_N, \Omega_k\right]\Phi_0 = \left(\bar{H}_N\Omega_k\right)_c\Phi_0. \tag{3.35}$$

Therefore, Eq. 3.32 can be formulated as a nonhermitian CI-like eigenvalue problem for each eigenvalue ω_k.

Because of the nonhermiticity of $\bar{H}_N$, there is a right and a left eigenvalue problem, where the left and right eigenvectors correspond to the same eigenvalues. In matrix form Eq. 3.32 is given by

$$\left(\bar{\mathbf{H}}_N \mathbf{C}_k\right)_c = \mathbf{C}_k \omega_k, \qquad \tilde{\mathbf{C}}_k^\dagger \bar{\mathbf{H}}_N = \tilde{\mathbf{C}}_k^\dagger \omega_k. \tag{3.36}$$

The eigenvectors $\mathbf{C_k}$ contain the amplitudes c_λ from Eq. 3.29 or Eq. 3.30, depending on whether $\bar{\mathbf{H}}_N$ is expressed in the basis of hole determinants, corresponding to the $(N-1)$-particle states, or in the basis of particle determinants, corresponding to the $(N+1)$-particle states. The eigenvalues ω_k are the exact ionization potentials or the negative of the exact electron affinities respectively, if no truncation is applied.

If the excitation space is chosen according to the IP-EOM-CCSD model or the EA-EOM-CCSD model, the ionization potentials or electron affinities are in general well approximated. $\bar{\mathbf{H}}_N$ in Eq. 3.36 then takes the form

$$\bar{\mathbf{H}}_N = \begin{pmatrix} \langle S|\bar{H}_N|S\rangle & \langle S|\bar{H}_N|D\rangle \\ \langle D|\bar{H}_N|S\rangle & \langle D|\bar{H}_N|D\rangle \end{pmatrix}, \tag{3.37}$$

where S stands for determinants with a single ionization or attachment process, and D for determinants with an additional excitation.

The left and right eigenvectors of a nonhermitian matrix form a biorthogonal set, which can be chosen to be biorthonormal, so that

$$\tilde{\mathbf{C}}^{(\lambda)} \cdot \mathbf{C}^{(\mu)} = \sum_\nu \tilde{c}_\nu^{(\lambda)} \cdot c_\nu^{(\mu)} = \delta_{\lambda\mu}. \tag{3.38}$$

For simplicity the subscript k, discriminating between the different choices of Ω is omitted.

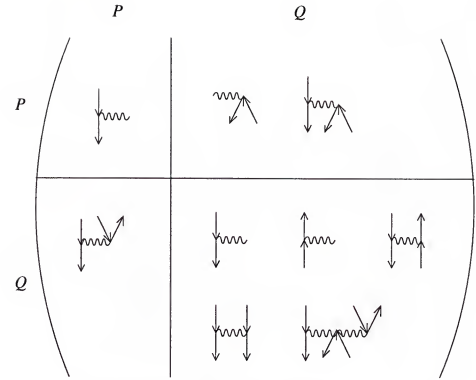

Figure 3–9. $\bar{\mathbf{H}}^{IP}$ for ionization potentials

Since the wave-function is explicitly known in the EOM-CC method

$$\langle\tilde{\Psi}_\lambda| = \sum_\nu \tilde{c}_\nu^{(\lambda)}\langle\Phi_\nu| \qquad |\Psi_\mu\rangle = \sum_\kappa |\Phi_\kappa\rangle c_\kappa^{(\mu)}, \tag{3.39}$$

properties can be calculated as a generalized expectation value

$$\theta = \mathrm{Tr}(D^N\Theta), \tag{3.40}$$

where Θ is an arbitrary linear operator. The N-particle reduced-density matrix is defined as

$$D^N_{pq\ldots rs} = \langle\tilde{\Psi}_\lambda|p^\dagger q^\dagger \ldots sr|\Psi_\lambda\rangle. \tag{3.41}$$

However, the N-particle reduced-density matrix is not size consistent [99], and as a result, properties calculated as expectation values depend on the physical extent of the system. Properties should preferentially be defined as energy derivatives.

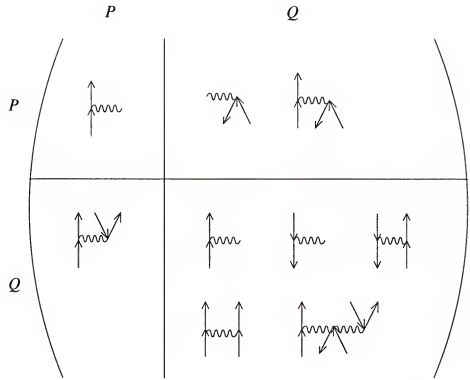

Figure 3–10. $\bar{\mathbf{H}}^{EA}$ for electron attachment

The particular realization of $\bar{\mathbf{H}}$ for the IP-EOM-CCSD model is diagrammatically shown in Fig. 3–9, and for the EA-EOM-CCSD model in Fig. 3–10. The space is conveniently partitioned into the P space, which includes in the case of IP-EOM-CCSD all determinants resulting from a single excitation of an electron into the continuum, also called 1-hole space, and in the case EA-EOM-CCSD all determinants, resulting from the attachment of one electron, also called 1-particle space. In the IP-EOM-CCSD model the Q space consists of all determinants, resulting from an ionization in addition to a single excitation, the 2-hole 1-particle space. In the case of EA-EOM-CCSD the Q space is composed out of all determinants, obtained by an attachment in addition to a single excitation, the 2-particle 1-hole space. Wiggling lines in Fig. 3–9 and Fig. 3–10 refer to $\bar{H}$ interactions. Their interpretation can be found in Fig. 3–11. Diagonalization of $\bar{\mathbf{H}}^{IP}$ delivers the normal IP's in the PP block, and the shake-up IP's in the QQ block. Diagonalization of

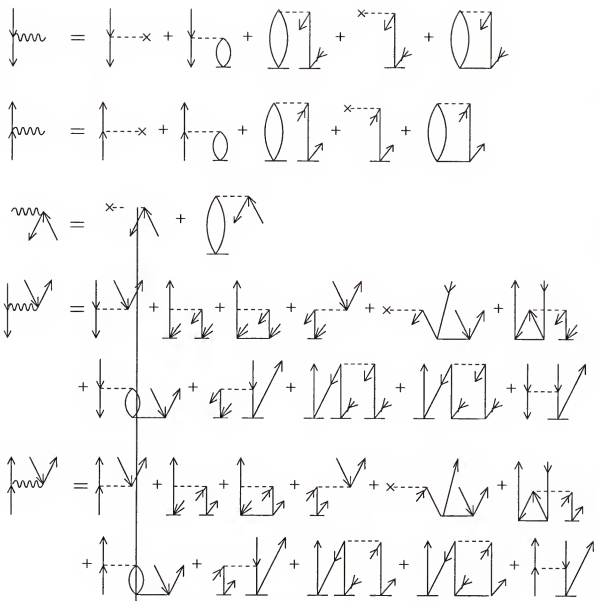

Figure 3–11. Interpretation of $\bar{\mathbf{H}}$ interactions

$\bar{\mathbf{H}}^{EA}$ yields the negative of the normal EA's in the PP block, and the negative of the shake-up EA's in the QQ block.

3.1.3 Partitioned EOM-CC Approach

In this section a correlation potential that yields the exact IP's and the exact EA's as the negative of the orbital energies is discussed. The EOM-CC method is exploited, since it gives the exact IP's and EA's if not truncated.

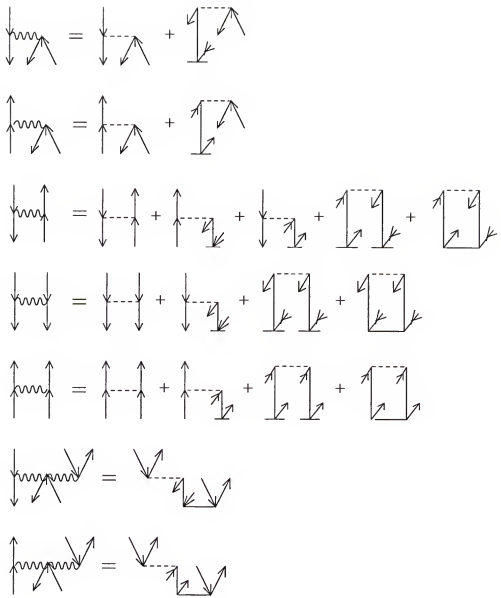

Figure 3–11. Continued

$\bar{\mathbf{H}}^{IP}$ and $\bar{\mathbf{H}}^{EA}$ as given in Fig. 3–9 and Fig. 3.10 cannot directly be used to extract a correlation potential, since the operators act in their P+Q spaces. To obtain a correlation potential for an independent particle model according to Eq. 2.96, the operators have to act only in their P spaces. Matrix partitioning [100] can be applied to formulate an effective Hamiltonian with reduced dimension. This

$$\mathbf{V_C} = \left\langle \begin{array}{c|c} \mathbf{V_C^{IP}} & \mathbf{0} \\ \hline \mathbf{0} & \mathbf{V_C^{EA}} \end{array} \right\rangle$$

Figure 3–12. Illustration of $\mathbf{V}_c$

well-known technique has been used to simplify excited state calculations [101, 102], and calculations of NMR coupling constants [103].

The partitioning of $\bar{\mathbf{H}}^{IP}$ and $\bar{\mathbf{H}}^{EA}$ in P and Q space was introduced in Fig. 3–9 and Fig. 3–10. The eigenvectors in Eq. 3.36 can be partitioned accordingly, leading to the partitioned equation of motion. However, since the IP-EOM-CC method yields IP's, but the orbital energies of the CIP model are sought to be the negative of the IP's, the partitioned equation is multiplied by minus one. The negative of the IP is denoted by ε. The partitioned IP-EOM-CC equation is then given by

$$\begin{pmatrix} -\bar{\mathbf{H}}_{PP}^{IP} & -\bar{\mathbf{H}}_{PQ}^{IP} \\ -\bar{\mathbf{H}}_{QP}^{IP} & -\bar{\mathbf{H}}_{QQ}^{IP} \end{pmatrix} \begin{pmatrix} \mathbf{C}_P \\ \mathbf{C}_Q \end{pmatrix} = \varepsilon \begin{pmatrix} \mathbf{C}_P \\ \mathbf{C}_Q \end{pmatrix}. \tag{3.42}$$

Eq. 3.42 can be divided into two equations

$$-\bar{\mathbf{H}}_{PP}^{IP}\mathbf{C}_P - \bar{\mathbf{H}}_{PQ}^{IP}\mathbf{C}_Q = \varepsilon\mathbf{C}_P \tag{3.43}$$

$$-\bar{\mathbf{H}}_{QP}^{IP}\mathbf{C}_P - \bar{\mathbf{H}}_{QQ}^{IP}\mathbf{C}_Q = \varepsilon\mathbf{C}_Q. \tag{3.44}$$

Solving Eq. 3.44 for $\mathbf{C}_Q$ leads to

$$-\left(\varepsilon\mathbf{1} + \bar{\mathbf{H}}_{QQ}^{IP}\right)^{-1}\bar{\mathbf{H}}_{QP}^{IP}\mathbf{C}_P = \mathbf{C}_Q. \tag{3.45}$$

Substituting Eq. 3.45 into Eq. 3.43 gives

$$\left[-\bar{\mathbf{H}}_{PP}^{IP} + \bar{\mathbf{H}}_{PQ}^{IP}\left(\varepsilon\mathbf{1} + \bar{\mathbf{H}}_{QQ}^{IP}\right)^{-1}\bar{\mathbf{H}}_{QP}^{IP}\right]\mathbf{C}_P = \varepsilon\mathbf{C}_P. \tag{3.46}$$

An effective Hamiltonian $\bar{\mathbf{H}}^{IP}_{eff}$ can now be defined

$$\bar{\mathbf{H}}^{IP}_{eff}(\varepsilon) = -\bar{\mathbf{H}}^{IP}_{PP} + \bar{\mathbf{H}}^{IP}_{PQ}\left(\varepsilon\mathbf{1} + \bar{\mathbf{H}}^{IP}_{QQ}\right)^{-1}\bar{\mathbf{H}}^{IP}_{QP}, \tag{3.47}$$

which yields the negative of the principal IP's upon diagonalization. A new eigenvalue equation is obtained, which is solved only in the P space, where the effects of the Q space are included through the effective Hamiltonian

$$\bar{\mathbf{H}}^{IP}_{eff}(\varepsilon)\mathbf{C}_P = \varepsilon\mathbf{C}_P. \tag{3.48}$$

Partitioning $\bar{\mathbf{H}}^{EA}$, Fig. 3–10, in the basis of net particle determinants leads to the effective Hamiltonian that yields the negative of the principal EA's upon diagonalization

$$\bar{\mathbf{H}}^{EA}_{eff}(\varepsilon) = \bar{\mathbf{H}}^{EA}_{PP} + \bar{\mathbf{H}}^{EA}_{PQ}\left(\varepsilon\mathbf{1} - \bar{\mathbf{H}}^{EA}_{QQ}\right)^{-1}\bar{\mathbf{H}}^{EA}_{QP}. \tag{3.49}$$

There is no need to multiply by minus, like for the IP-EOM model. The effective eigenvalue problem solved in the 1-particle space, is given by

$$\bar{\mathbf{H}}^{EA}_{eff}(\varepsilon)\mathbf{C}_P = \varepsilon\mathbf{C}_P. \tag{3.50}$$

Notice that the Q spaces are not restricted to the 2-hole 1-particle space or the 2-particle 1-hole space respectively, but can consist of any number of particle and hole combinations that amounts to a net hole determinant or a net particle determinant. If no restrictions to the Q space are applied, the eigenvalues of the effective Hamiltonians are the negative of the formally exact principal IP's or the negative of the formally exact principal EA's.

If the effective Hamiltonians are expressed in canonical Hartree-Fock orbitals, then the diagonal elements contain the Hartree-Fock orbital energies. This can be seen by expanding the diagrams in the PP blocks according to Fig. 3–11. The leading contribution to $[\bar{\mathbf{H}}^{IP}_{eff}]_{ij}$ is $f_{ij} = \epsilon_{ij}\delta_{ij}$ in canonical Hartree-Fock orbitals. The

leading contribution to $[\bar{\mathbf{H}}^{EA}_{eff}]_{ab}$ is $f_{ab} = \epsilon_{ab}\delta_{ab}$ in canonical Hartree-Fock orbitals. The diagonal elements of the effective Hamiltonians contain a correlation correction as well, the off-diagonal elements contribute only to correlation. Eq. 3.48 and Eq. 3.50 can be written as

$$\bar{\mathbf{H}}^{IP}_{eff}(\varepsilon)\mathbf{C}^{IP}_{P} = (\boldsymbol{\epsilon}^{IP} + \mathbf{V}^{IP}_{c}(\varepsilon))\mathbf{C}^{IP}_{P} = \varepsilon\mathbf{C}^{IP}_{P} \tag{3.51}$$

$$\bar{\mathbf{H}}^{EA}_{eff}(\varepsilon)\mathbf{C}^{EA}_{P} = (\boldsymbol{\epsilon}^{EA} + \mathbf{V}^{EA}_{c}(\varepsilon))\mathbf{C}^{EA}_{P} = \varepsilon\mathbf{C}^{EA}_{P}, \tag{3.52}$$

with

$$\mathbf{V}^{IP}_{c}(\varepsilon) = -(\bar{\mathbf{H}}^{IP}_{PP})_{corr} + \bar{\mathbf{H}}^{IP}_{PQ}\left(\varepsilon\mathbf{1} + \bar{\mathbf{H}}^{IP}_{QQ}\right)^{-1}\bar{\mathbf{H}}^{IP}_{QP} \tag{3.53}$$

$$\mathbf{V}^{EA}_{c}(\varepsilon) = (\bar{\mathbf{H}}^{EA}_{PP})_{corr} + \bar{\mathbf{H}}^{EA}_{PQ}\left(\varepsilon\mathbf{1} - \bar{\mathbf{H}}^{EA}_{QQ}\right)^{-1}\bar{\mathbf{H}}^{EA}_{QP}. \tag{3.54}$$

Eq. 3.53 and Eq. 3.54 define a correlation potential in the 1-hole and the 1-particle space. To obtain a correlation potential in the unified P spaces, $\mathbf{V}^{IP}_{c}(\varepsilon)$ and $\mathbf{V}^{EA}_{c}(\varepsilon)$ are added as shown in Fig. 3–12. The eigenvalue equation in the CIP model, derived from the partitioned EOM-CC method, is given by

$$\bar{\mathbf{H}}_{eff}(\varepsilon)\mathbf{C}(\varepsilon) = (\boldsymbol{\epsilon} + \mathbf{V}_{c}(\varepsilon))\mathbf{C}(\varepsilon) = \varepsilon\mathbf{C}(\varepsilon). \tag{3.55}$$

Notice, even though Eq. 3.55 yields the negative of the exact IP's and EA's if no truncation is introduced, there is a certain arbitrariness if one is interested in the eigenvectors. Since the IP-EOM-CC and the EA-EOM-CC methods are completely independent, the off-diagonal blocks of the correlation potential are not defined and set to zero. However, if one of the off-diagonal blocks were not equal to zero, the same IP's and EA's would be obtained, but the eigenvectors would be different. That point is discussed further in Section 3.3.

Notice also, in Eq. 3.55 ε appears not only as the eigenvalue, but $\mathbf{V}_{c}(\varepsilon)$ also depends on ε, which in turn causes the eigenvectors to depend on ε. That means that for each IP or EA a new eigenvalue problem has to be solved.

The effective Hamiltonians in Eq. 3.51 and Eq. 3.52 act in the space of N-electron Hartree-Fock determinants, from which an electron has been removed, if the IP sector is considered, or to which an electron is added, if the EA sector is considered. However, each element of $\bar{\mathbf{H}}_{eff}^{IP}$ is defined by

$$[\bar{\mathbf{H}}_{eff}^{IP}]_{ij} = \langle \Phi_0 | j^\dagger \bar{H}_{eff}^{IP} i | \Phi_0 \rangle = \langle \phi_i | \bar{H}_{eff}^{IP} | \phi_j \rangle, \tag{3.56}$$

where the $|\phi_i\rangle$ are one-electron functions, represented by $\mathbf{C}_{PP}$, solved for the IP sector. Equivalently, each element of $\bar{\mathbf{H}}_{eff}^{EA}$ is defined by

$$[\bar{\mathbf{H}}_{eff}^{EA}]_{ab} = \langle \Phi_0 | a \bar{H}_{eff}^{EA} b^\dagger | \Phi_0 \rangle = \langle \phi_a | \bar{H}_{eff}^{EA} | \phi_b \rangle. \tag{3.57}$$

Again, the $|\phi_a\rangle$ are one-electron functions, represented by $\mathbf{C}_{PP}$, solved for the EA sector.

$\bar{\mathbf{H}}_{eff} = \boldsymbol{\epsilon} + \mathbf{V}_c$ can equivalently be regarded as an effective one-particle operator in an orbital space, where the orbitals are solutions to the eigenvalue equation

$$\bar{H}_{eff}(\varepsilon)|\phi_m\rangle = (f + v_c(\varepsilon_m))|\phi_m\rangle = \varepsilon_m|\phi_m\rangle. \tag{3.58}$$

f is the Fock operator, and v_c is the correlation potential given in matrix form in Fig. 3–12.

The effective Hamiltonian for the EOM-CCSD model was implemented. Eq. 3.55 can be solved iteratively, starting with Koopmans' IP's and EA's as a guess. The procedure was tested on various small molecules, and convergence to the IP-EOM-CCSD and the EA-EOM-CCSD values was easily achieved in most cases.

The possibility of approximating the effective Hamiltonians is also considered. The simplest approximation is $\bar{\mathbf{H}}_{eff}^{IP} = \bar{\mathbf{H}}_{PP}^{IP}$ and $\bar{\mathbf{H}}_{eff}^{EA} = \bar{\mathbf{H}}_{PP}^{EA}$ respectively. Test calculations on simple systems showed, that in most cases this approximation is not even an improvement over Hartree-Fock. As one would expect, the influence of the Q space in the effective Hamiltonian is of great importance and cannot be neglected.

Table 3–4. Comparison of different approximation schemes for IP's and EA's for H_2, He_2 and HF, IP's and EA's are given in Hartree

	HF	I	II	III	IV
H_2 IP (DZP)	0.59299	0.62792	0.60167	0.60157	0.60137
H_2 EA (DZP)	-0.26004	-0.26912	-0.24775	-0.24872	-0.24885
	-0.83599	-0.84292	-0.81684	-0.81452	-0.81595
	-1.17694	-1.18550	-1.10297	-1.02271	-1.09046
He_2 IP (DZ)	0.91595	0.93153	0.88355	0.87738	0.87845
	0.91231	0.92805	0.87986	0.87354	0.87462
He_2 EA (DZ)	-1.37551	-1.39015	-1.35772	-1.35060	-1.35118
	-1.42489	-1.43918	-1.40595	-1.39845	-1.39910
HF IP (DZ)	0.64285	0.68434	0.53925	0.55274	0.55843
	0.75240	0.80442	0.68949	0.70360	0.70596
HF EA (DZ)	-0.21248	-0.22614	-0.20102	-0.20265	-0.20278
	-1.05750	-1.07967	-1.01360	-1.02724	-1.02838
	-1.12680	-1.14724	-1.03460	-1.03070	-1.04402

Some illustrative results are summarized in Table 3–4. The column denoted by I contains results of the approximate scheme just mentioned, the Hartree-Fock results are included for comparison in the column denoted by HF, and the last column, denoted by IV, shows results of the fully iterated Eq. 3.55, which coincide with the EOM-CCSD results for IP's and EA's.

Since the Q space is of much higher dimension than the P space, it would be useful to be able to simplify $\bar{\mathbf{H}}^{IP}_{QQ}$ and $\bar{\mathbf{H}}^{EA}_{QQ}$. Since the diagonal elements of $\bar{\mathbf{H}}^{IP}_{QQ}$ and $\bar{\mathbf{H}}^{EA}_{QQ}$ are larger than the off-diagonal elements, the approximation of $\bar{\mathbf{H}}^{IP}_{QQ}$ and $\bar{\mathbf{H}}^{EA}_{QQ}$ by only its diagonal elements was tested. Results for the test examples are included in Table 3–4 in the column denoted by II. The results are good.

It was also tested if the iteration of Eq. 3.55 is necessary, or if good results can be achieved by using Koopman's IP's and EA's in Eq. 3.53 and Eq. 3.54 for ε without iterating. Results of this approximation are included in Table 3–4 in column III. The test calculations showed that the approximations II and III for $\bar{\mathbf{H}}^{IP}_{QQ}$ and

$\bar{\mathbf{H}}^{EA}_{QQ}$ are quite reasonable and can be considered as possible candidates to extract correlation potentials from them.

With the exception of the simplest approximation, which is not recommended, the above schemes all have in common that the correlation potential, resulting from them, depends on ε. That means that for each orbital a different correlation potential would have to be used, and that each IP and EA has to be calculated separately. It also implies that the orbitals are not orthogonal. For those reasons the energy dependence of the correlation potential is viewed as a disadvantage, and in a later section an energy-independent correlation potential, which is universal for all orbitals, is discussed.

3.2 Electron-Propagator Method

An alternative, formally exact one-electron theory, can be derived from the electron-propagator [18]. In contrast to the EOM-CC methods, the 1 hole and the 1 particle sectors are not decoupled, but simultaneously described. The self-energy plays the role of the correlation potential, which incorporates all the many-body effects. The self-energy is generally energy dependent, which causes the orbitals to be energy-dependent as well. They are therefore linearly dependent.

In the treatment of electron propagators, it is common to use the so-called Heisenberg picture [89]. To distinguish the wave-function and the operators from the usual Schrödinger picture, the superscript S is used for the Schrödinger representation, and H for the Heisenberg representation. The time-dependent Schrödinger equation becomes

$$i\hbar\frac{\partial}{\partial t}|\Psi^S(t)\rangle = H^S|\Psi^S(t)\rangle, \tag{3.59}$$

where H^S is assumed to have no explicit time dependence. Since Eq. 3.59 is a first-order differential equation, the initial state t_0 determines the subsequent behavior.

A formal solution to Eq. 3.59 is given by

$$|\Psi^S(t)\rangle = e^{\frac{-iH^S(t-t_0)}{\hbar}}|\Psi^S(t_0)\rangle. \tag{3.60}$$

Since H is hermitian, the exponential represents a unitary operator

$$U(t) = e^{\frac{-iH^S(t-t_0)}{\hbar}}, \tag{3.61}$$

called the evolution operator, which satisfies

$$U^\dagger(t)U(t) = U(t)U^\dagger(t) = 1. \tag{3.62}$$

The evolution operator carries the initial state $|\Psi^S(t_0)\rangle$ into the final state $|\Psi^S(t)\rangle$. If $|\Psi^S(t_0)\rangle$ is a time-independent eigenfunction of H^S, the exponential in Eq. 3.60 becomes the factor $e^{\frac{-iEt}{\hbar}}$ for a stationary state of energy E.

To obtain the wave-function and operators in the Heisenberg picture, a unitary transformation is applied according to

$$|\Psi^H\rangle = U^\dagger(t)|\Psi^S(t)\rangle \qquad A^H(t) = U^\dagger(t)A^S(t)U(t). \tag{3.63}$$

The wave-function in the Heisenberg representation is time independent, since

$$|\Psi^H\rangle = U^\dagger(t)U(t)|\Psi^S(t_0)\rangle = |\Psi^S(t_0)\rangle. \tag{3.64}$$

Operators in general acquire a time dependence. Substituting the definition of the evolution operator into Eq. 3.63, a general Heisenberg operator is given by

$$A^H(t) = e^{\frac{iH^S(t-t_0)}{\hbar}}A^S(t)e^{\frac{-iH^S(t-t_0)}{\hbar}}. \tag{3.65}$$

If A^S is time independent, the time derivative of Eq. 3.65 yields

$$i\hbar\frac{\partial}{\partial t} = e^{\frac{iH(t-t_0)}{\hbar}}[A^S, H]e^{\frac{-iH(t-t_0)}{\hbar}} = [A^H(t), H], \tag{3.66}$$

where the superscript in the Hamiltonian is omitted, since H means the usual time-independent Hamiltonian. Eq. 3.66 establishes the equation-of-motion of an operator in the Heisenberg picture. In particular, if A^S commutes with H, the right-hand side vanishes, and A^H is a constant of the motion.

The Green's function, also called propagator, is an expectation value of field operators. The N-particle many-body Green's function is defined in the Heisenberg representation as

$$G_{pq\ldots sr}(t_p, t_q \ldots t_s, t_r) = (-i)^N \langle \Psi_0^H | T[p^H(t_p) r^{\dagger H}(t_r) q^H(t_q) s^{\dagger H}(t_s) \ldots] | \Psi_0^H \rangle, \quad (3.67)$$

where the operators $p^H(t_p)$ and $r^{\dagger H}(t_r)$ are the annihilation and creation operators in the Heisenberg picture, with the time dependence given by

$$\begin{aligned} p^H(t_p) &= e^{\frac{iH(t-t_0)}{\hbar}} p\, e^{\frac{-iH(t-t_0)}{\hbar}} \\ r^{\dagger H}(t_r) &= e^{\frac{iH(t-t_0)}{\hbar}} r^\dagger e^{\frac{-iH(t-t_0)}{\hbar}}. \end{aligned} \quad (3.68)$$

$|\Psi_0^H\rangle$ is the Heisenberg ground state of the interacting system, which is assumed to be normalized $\langle \Psi_0^H | \Psi_0^H \rangle = 1$. The T product of several operators orders them from right to left in ascending time order and adds a factor of $(-1)^P$, where P is the number of interchanges of fermion operators from the original given order. The N-particle Green's function contains N pairs of creation and annihilation operators, each having a unique time argument.

The single particle Green's function contains only one pair of creation and annihilation operators

$$iG_{pq}(t_p, t_q) = \langle \Psi_0^H | T[p^H(t_p) q^{\dagger H}(t_q)] | \Psi_0^H \rangle. \quad (3.69)$$

Taking the T ordering explicitly into account, Eq. 3.69 can be written as

$$iG_{pq}(t_p,t_q) = \begin{cases} \langle\Psi_0^H|p^H(t_p)q^{\dagger H}(t_q)|\Psi_0^H\rangle & t_p > t_q \\ \langle\Psi_0^H|q^{\dagger H}(t_q)p^H(t_p)|\Psi_0^H\rangle & t_q > t_p \end{cases}. \tag{3.70}$$

Eq. 3.70 can be conveniently expressed by using the Heaviside step function θ

$$\begin{aligned} G_{pq}(t_p,t_q) &= -i\theta(t_p-t_q)\langle\Psi_0^H|p^H(t_p)q^{\dagger H}(t_q)|\Psi_0^H\rangle \\ &+ i\theta(t_q-t_p)\langle\Psi_0^H|q^{\dagger H}(t_q)p^H(t_p)|\Psi_0^H\rangle. \end{aligned} \tag{3.71}$$

A complete set of Heisenberg states is inserted between the field operators. These states are eigenstates of the Hamiltonian and include all possible numbers of particles

$$\begin{aligned} G_{pq}(t_p,t_q) &= \sum_n \left[-i\theta(t_p-t_q)\langle\Psi_0^H|p^H(t_p)|\Psi_n^H\rangle\langle\Psi_n^H|q^{\dagger H}(t_q)|\Psi_0^H\rangle\right. \\ &+ \left. i\theta(t_q-t_p)\langle\Psi_0^H|q^{\dagger H}(t_q)|\Psi_n^H\rangle\langle\Psi_n^H|p^H(t_p)|\Psi_0^H\rangle\right]. \end{aligned} \tag{3.72}$$

Substituting Eq. 3.68 into 3.72 gives

$$\begin{aligned} G_{pq}(t_p,t_q) &= \sum_n \left[-i\theta(t_p-t_q)e^{\frac{-i(E_n-E_0)(t_p-t_q)}{\hbar}}\langle\Psi_0|p|\Psi_n\rangle\langle\Psi_n|q^\dagger|\Psi_0\rangle\right. \\ &+ \left. i\theta(t_q-t_p)e^{\frac{-i(E_0-E_n)(t_p-t_q)}{\hbar}}\langle\Psi_0|q^\dagger|\Psi_n\rangle\langle\Psi_n|p|\Psi_0\rangle\right]. \end{aligned} \tag{3.73}$$

The superscript H is omitted, since the stationary solutions to the Schrödinger equation satisfy the time-independent form of the Schrödinger equation. The integrals in Eq. 3.73 can only be nonzero if the states $|\Psi_n\rangle$ contain $N\pm1$ particles, while the state $|\Psi_0\rangle$ contains N particles.

The Green's functions are often studied in terms of their Fourier transforms

$$G(E) = \int_{-\infty}^{\infty} G(t,t')e^{iE(t-t')}d(t-t'), \tag{3.74}$$

with the inverse relation

$$G(t,t') = \frac{1}{2\pi}\int_{-\infty}^{\infty} G(E)e^{-iE(t-t')}dE. \tag{3.75}$$

Using the identities

$$\lim_{\eta\to 0}\frac{1}{2\pi}\int_{-\infty}^{\infty}\frac{e^{-iE(t-t')}}{E-(E_0-E_n)-i\eta}dE = \begin{cases} 0 & t>t' \\ ie^{-i(E_0-E_n)(t-t')} & t<t' \end{cases} \tag{3.76}$$

and

$$\lim_{\eta\to 0}\frac{1}{2\pi}\int_{-\infty}^{\infty}\frac{e^{-iE(t-t')}}{E-(E_n-E_0)+i\eta}dE = \begin{cases} -ie^{-i(E_n-E_0)(t-t')} & t>t' \\ 0 & t<t' \end{cases} \tag{3.77}$$

The Fourier transform can be written as

$$G_{pq}(E) = \lim_{\eta\to 0}\sum_n\left[\frac{\langle\Psi_0|p|\Psi_n\rangle\langle\Psi_n|q^\dagger|\Psi_0\rangle}{E-E_n+E_0+i\eta} + \frac{\langle\Psi_0|q^\dagger|\Psi_n\rangle\langle\Psi_n|p|\Psi_0\rangle}{E-E_0+E_n-i\eta}\right]. \tag{3.78}$$

This is the so called spectral or Lehmann representation of the propagator. A common notation for $G_{pq}(E)$ is also $\langle\langle p;q^\dagger\rangle\rangle_E$. The electron-propagator in its spectral representation is energy dependent, and poles occur when the energy E is equal to the negative of an electron affinity $-(E_0(N)-E_n(N+1))$ or the negative of an ionization potential $-(E_n(N-1)-E_0(N))$.

The starting point for most approximation schemes is the equation-of-motion, which can be solved directly, without the need to seek a variational approximation to the many-electron wave-function. Using the identity

$$E(E-a)^{-1} = 1 + a(E-a)^{-1}, \tag{3.79}$$

and the relations

$$\begin{aligned} \langle\Psi_0|p|\Psi_n\rangle(E_n-E_0) &= \langle\Psi_0|[p,H]|\Psi_n\rangle \\ \langle\Psi_n|q^\dagger|\Psi_0\rangle(E_n-E_0) &= \langle\Psi_n|[H,q^\dagger]|\Psi_0\rangle, \end{aligned} \tag{3.80}$$

two equivalent forms of the equation-of-motion can be derived from Eq. 3.78

$$\begin{aligned} E\langle\langle p;q^\dagger\rangle\rangle_E &= \langle\Psi_0|[p,q^\dagger]_+|\Psi_0\rangle + \langle\langle [p,H];q^\dagger\rangle\rangle_E \\ &= \langle\Psi_0|[p,q^\dagger]_+|\Psi_0\rangle + \langle\langle p;[H,q^\dagger]\rangle\rangle_E. \end{aligned} \tag{3.81}$$

The so called moment expansion can be obtained by iterating the equation-of-motion. Iterating the second of Eq. 3.81 gives

$$\begin{aligned} \langle\langle p;q^\dagger\rangle\rangle_E &= E^{-1}\langle\Psi_0|[p,q^\dagger]_+|\Psi_0\rangle + E^{-2}\langle\Psi_0|[p,[H,q^\dagger]]_+|\Psi_0\rangle \\ &+ E^{-3}\langle\Psi_0|[p,[H,[H,q^\dagger]]]_+|\Psi_0\rangle + \ldots. \end{aligned} \tag{3.82}$$

To represent the propagator compactly, and to use standard matrix and vector space techniques, superoperators can be employed [104, 105]. A linear space is introduced, whose elements are linear combinations of field operator products

$$\{i,a\} \cup \left\{a^\dagger ij, i^\dagger ab\right\} \cup \ldots. \tag{3.83}$$

Superoperators act on this space, and the superoperator Hamiltonian and the superoperator identity are defined by

$$\begin{aligned} \hat{H}X &= [X,H] \\ \hat{I}X &= X, \end{aligned} \tag{3.84}$$

where X is a general element of the linear space. The scalar product $(X|Y)$, where Y is another element of the linear space, is defined as

$$(X|Y) = \langle\Psi_0|[Y,X^\dagger]_+|\Psi_0\rangle. \tag{3.85}$$

The moment expansion, Eq. 3.82, can then be expressed as

$$\langle\langle p;q^\dagger\rangle\rangle_E = E^{-1}(q|p) + E^{-2}(q|\hat{H}p) + E^{-3}(q|\hat{H}^2p) + \ldots. \tag{3.86}$$

A formal summation is performed to obtain

$$\langle\langle p; q^\dagger \rangle\rangle_E = (q|(E\hat{I} - \hat{H})^{-1}p), \tag{3.87}$$

where $(E\hat{I} - \hat{H})^{-1}$ is the superoperator resolvent. Introducing vector arrays of simple field operators $\mathbf{a}$, the electron-propagator, Eq. 3.87, can be written in matrix form

$$\mathbf{G}(E) = (\mathbf{a}|(E\hat{I} - \hat{H})^{-1}\mathbf{a}). \tag{3.88}$$

The superoperator resolvent $(E\hat{I} - \hat{H})^{-1}$ can be reformulated as a matrix inverse by inner projection [106]. With an orthonormal truncated basis $\mathbf{e}$, there is a projection operator ρ associated

$$\rho = \sum_i |e_i\rangle\langle e_i| = \mathbf{e}\mathbf{e}^\dagger. \tag{3.89}$$

If the basis is not orthonormal, the metric matrix $\mathbf{S} = \mathbf{e}^\dagger\mathbf{e}$ must be included. Using instead of $\mathbf{e}$ the Löwdin basis $\bar{\mathbf{e}} = \mathbf{e}\mathbf{S}^{\frac{1}{2}}$, it follows

$$\rho = \sum_{ij} |e_i\rangle(S^{-1})_{ij}\langle e_j| = \mathbf{e}\mathbf{S}^{-1}\mathbf{e}^\dagger. \tag{3.90}$$

For a complete space, ρ becomes the unit operator. When a truncated basis is used in operator space, there are two kinds of useful projections, the outer and the inner projection

$$A' = \rho A \rho \qquad A'' = A^{\frac{1}{2}}\rho A^{\frac{1}{2}}. \tag{3.91}$$

The inner projection is particularly useful in propagator theory. Neither projection preserves the relationship $AB = C$. Nevertheless, the projected forms may be regarded as approximations, which become increasingly precise, as the basis is extended.

Inserting Eq. 3.90 in the inner projection form of Eq. 3.91, leads to

$$A'' = A^{\frac{1}{2}}\mathbf{e}\mathbf{S}^{-1}\mathbf{e}^\dagger A^{\frac{1}{2}}. \tag{3.92}$$

A is assumed to be Hermitian and positive definite. Introducing the transformed basis $\mathbf{u}$

$$A^{\frac{1}{2}}\mathbf{e} = (A^{\frac{1}{2}}e_1\, A^{\frac{1}{2}}e_2\, \ldots) = \mathbf{u}, \tag{3.93}$$

the metric becomes

$$\mathbf{S} = \mathbf{e}^\dagger\mathbf{e} = (A^{-\frac{1}{2}}\mathbf{u})^\dagger(A^{-\frac{1}{2}}\mathbf{u}) = \mathbf{u}^\dagger A^{-1}\mathbf{u}. \tag{3.94}$$

Using Eq. 3.93 and Eq. 3.94, the inner projection Eq. 3.92 can be written as

$$A'' = \mathbf{u}(\mathbf{u}^\dagger A^{-1}\mathbf{u})^{-1}\mathbf{u}^\dagger. \tag{3.95}$$

Since A is an arbitrary operator, it may be replaced by A^{-1}. Defining $\mathbf{u}^\dagger A\mathbf{u} = \mathbf{A}$, with $A_{ij} = \langle u_i|A|u_j\rangle$, the inverse of the operator A can be approximated in terms of a matrix inverse

$$(A^{-1})'' = \mathbf{u}(\mathbf{u}^\dagger A\mathbf{u})^{-1}\mathbf{u}^\dagger = \mathbf{u}\mathbf{A}^{-1}\mathbf{u}^\dagger. \tag{3.96}$$

If A is taken to be the superoperator resolvent $(E\hat{I} - \hat{H})^{-1}$, and $\mathbf{u}$ is a vector of all electron field operators, Eq. 3.88 can be rewritten as

$$\mathbf{G}(E) = (\mathbf{a}|\mathbf{u})(\mathbf{u}|(E\hat{I} - \hat{H})\mathbf{u})^{-1}(\mathbf{u}|\mathbf{a}), \tag{3.97}$$

where the inverse of a matrix instead of the resolvent operator is employed. If the manifold $\mathbf{u}$ spans the entire space, no approximation is made.

$\mathbf{u}$ can be partitioned into the primary space of simple field operators $\mathbf{a}$ and the orthogonal complement $\mathbf{f}$. Eq. 3.97 then becomes

$$\mathbf{G}(E) = \begin{pmatrix} 1 & 0 \end{pmatrix} \begin{pmatrix} E\mathbf{1} - (\mathbf{a}|\hat{H}\mathbf{a}) & -(\mathbf{a}|\hat{H}\mathbf{f}) \\ -(\mathbf{f}|\hat{H}\mathbf{a}) & E\mathbf{1} - (\mathbf{f}|\hat{H}\mathbf{f}) \end{pmatrix}^{-1} \begin{pmatrix} \mathbf{1} \\ \mathbf{0} \end{pmatrix}, \tag{3.98}$$

where, because of the orthogonality condition $(\mathbf{a}|\mathbf{f}) = 0$, only the upper left corner of the inverse matrix contributes.

The manipulations to obtain the inverse of Eq. 3.98 are done symbolically for simplicity. Upper case letters are used for the elements of the matrix in Eq. 3.98, and lower case letters are used for the inverse. The condition a matrix and its inverse have to fulfill is

$$\begin{pmatrix} A & B \\ C & D \end{pmatrix} \begin{pmatrix} a & b \\ c & d \end{pmatrix} = \begin{pmatrix} 1 & 0 \\ 0 & 1 \end{pmatrix}. \tag{3.99}$$

From Eq. 3.99 the following equations can be obtained

$$Aa + Bc = 1 \tag{3.100}$$

$$Ca + Dc = 0. \tag{3.101}$$

Solving Eq. 3.101 for c leads to

$$-D^{-1}Ca = c, \tag{3.102}$$

which is substituted in Eq. 3.100 and solved for a

$$a = \left(A - BD^{-1}C\right)^{-1}. \tag{3.103}$$

Substituting the appropriate terms from Eq. 3.98 into Eq. 3.103, yields the partitioned form of the inverse propagator matrix

$$\mathbf{G}^{-1}(E) = (\mathbf{a}|(E\hat{I} - \hat{H})\mathbf{a}) - (\mathbf{a}|\hat{H}\mathbf{f})(\mathbf{f}|(E\hat{I} - \hat{H})\mathbf{f})^{-1}(\mathbf{f}|\hat{H}\mathbf{a}). \tag{3.104}$$

Various approximate schemes can be introduced by truncating the manifold $\mathbf{f}$ and by different choices of the approximate ground state $|\Psi_0\rangle$, which defines the scalar product, Eq. 3.85. $\hat{H}$ is commonly chosen to be separated in the unperturbed superoperator $\hat{H}_0$ and the perturbation superoperator $\hat{V}$

$$\hat{H} = \hat{H}_0 + \hat{V}, \qquad H_0 = \sum_p \epsilon_p \{p^\dagger p\}. \tag{3.105}$$

With the definition

$$\mathbf{G}_0^{-1}(E) = (\mathbf{a}|(E\hat{I} - \hat{H}_0)\mathbf{a}), \tag{3.106}$$

the Dyson equation can be written as

$$\mathbf{G}^{-1}(E) = \mathbf{G}_0^{-1}(E) - \mathbf{\Sigma}(E). \tag{3.107}$$

The self-energy $\mathbf{\Sigma}(E)$ is that part of $\mathbf{G}^{-1}(E)$ that contains dynamical relaxation and correlation effects

$$\mathbf{\Sigma}(E) = (\mathbf{a}|\hat{V}\mathbf{a}) + (\mathbf{a}|\hat{H}\mathbf{f})[E\mathbf{1} - (\mathbf{f}|\hat{H}\mathbf{f})]^{-1}(\mathbf{f}|\hat{H}\mathbf{a}). \tag{3.108}$$

As already mentioned, IP's and EA's are given by the negative of the poles of $\mathbf{G}(E)$. When $\det\mathbf{G}(E) \to \infty$, or equivalently, when $\det\mathbf{G}^{-1}(E) \to 0$, E is a pole. It is equivalent to requiring $\mathbf{G}^{-1}(E)$ to have a vanishing eigenvalue at the pole energy

$$\mathbf{G}^{-1}(E)\mathbf{C}(E) = 0\ \mathbf{C}(E). \tag{3.109}$$

If $|\Psi_0\rangle$ is defined to be the Hartree-Fock determinant $|\Phi_0\rangle$ in a canonical molecular orbital basis, the negative of the poles of $\mathbf{G}_0(E)$ are Koopmans' values for IP's and EA's, which is shown in the following. The superoperator algebra defined in Eq. 3.84 and Eq. 3.85 is used. The elements of the zeroth order inverse propagator matrix are given by

$$\begin{aligned}
\left[\mathbf{G}_0^{-1}\right]_{sr} &= (s|(E\hat{I} - \hat{H}_0)r) \\
&= E(s|\hat{I}r) - (s|\hat{H}_0 r) = E(s|r) - (s|[r, H_0]) \\
&= E\langle\Phi_0|[r, s^\dagger]_+|\Phi_0\rangle - \langle\Phi_0|[rH_0, s^\dagger]_+|\Phi_0\rangle + \langle\Phi_0|[H_0 r, s^\dagger]_+|\Phi_0\rangle \\
&= E\langle\Phi_0|rs^\dagger|\Phi_0\rangle + E\langle\Phi_0|s^\dagger r|\Phi_0\rangle - \sum_p \epsilon_p\langle\Phi_0|rp^\dagger ps^\dagger|\Phi_0\rangle \\
&\quad - \sum_p \epsilon_p\langle\Phi_0|s^\dagger rp^\dagger p|\Phi_0\rangle + \sum_p \epsilon_p\langle\Phi_0|p^\dagger prs^\dagger|\Phi_0\rangle + \sum_p \epsilon_p\langle\Phi_0|s^\dagger p^\dagger pr|\Phi_0\rangle \\
&= \delta_{rs}(E - \epsilon_r).
\end{aligned} \tag{3.110}$$

The fourth and the fifth term do not contribute in the line before last in Eq. 3.110. If r and s are occupied orbitals, the first and the third term do not contribute. If r and s are virtual orbitals, the second and the sixth term do not contribute.

Substituting Eq. 3.106 and Eq. 3.107 into Eq. 3.109 gives

$$\begin{aligned} 0\,\mathbf{C}(E) &= (\mathbf{G}_0^{-1}(E) - \mathbf{\Sigma}(E))\mathbf{C}(E) \\ &= [(\mathbf{a}|(E\hat{I} - \hat{H}_0)\mathbf{a}) - \mathbf{\Sigma}(E)]\mathbf{C}(E), \end{aligned} \tag{3.111}$$

and

$$[(\mathbf{a}|\hat{H}_0\mathbf{a}) + \mathbf{\Sigma}(E)]\mathbf{C}(E) = E\mathbf{C}(E), \tag{3.112}$$

which, considering Eq. 3.110, leads to

$$[\boldsymbol{\epsilon} + \mathbf{\Sigma}(E)]\mathbf{C}(E) = E\mathbf{C}(E), \tag{3.113}$$

where $\boldsymbol{\epsilon}$ is a diagonal matrix that contains the Hartree-Fock orbital energies.

From the matrix expression Eq. 3.113, one may abstract one-electron equations from the Fock operator f and the self-energy operator $\Sigma(E)$ [20]

$$[f + \Sigma(E)]\varphi^{Dyson} = E\varphi^{Dyson}. \tag{3.114}$$

The eigenvectors are Dyson orbitals, from which the exact density matrix can be constructed [24]

$$D^1(x, x') = \sum_{p \in IP} g_p \varphi^{*Dyson}(x', E_p)\varphi^{Dyson}(x, E_p), \tag{3.115}$$

where

$$g_p = \left\{ 1 - \left[\frac{dE_p(E)}{dE} \right] \Bigg|_{E=E_p} \right\}^{-1}. \tag{3.116}$$

Since the Dyson orbitals are eigenfunctions of different effective Hamiltonians, they are not orthogonal, and the natural orbitals $\phi_p(x)$ [66] and the occupation numbers

n_p can be obtained by solving the eigenvalue problem

$$\int D^1(x,x')\phi_p(x')dx' = n_p\phi_p(x). \tag{3.117}$$

If the Green's function itself is known, the ground-state density matrix can be obtained using contour integration [89], or equivalently, from sum rules. The contour integration encloses all poles corresponding to ionization potentials

$$\begin{aligned}\frac{1}{2\pi i}\oint_{IP} G_{pq}(E)dE &= \sum_n \langle\Psi_0|q^\dagger|\Psi_n\rangle\langle\Psi_n|p|\Psi_0\rangle \\ &= \langle\Psi_0|q^\dagger p|\Psi_0\rangle = D^1_{pq}.\end{aligned} \tag{3.118}$$

Taking the first moment, leads to

$$\begin{aligned}\frac{1}{2\pi i}\oint_{IP} EG_{pq}(E)dE &= \sum_n (E_0 - E_n)\langle\Psi_0|q^\dagger|\Psi_n\rangle\langle\Psi_n|p|\Psi_0\rangle \\ &= \langle\Psi_0|q^\dagger[p,H]|\Psi_0\rangle \\ &= \sum_s h_{ps}\langle\Psi_0|q^\dagger s|\Psi_0\rangle + \frac{1}{2}\sum_{rst}\langle pr||st\rangle\langle\Psi_0|q^\dagger r^\dagger ts|\Psi_0\rangle \\ &= \sum_s h_{ps}D^1_{sq} + \frac{1}{2}\sum_{rst}\langle pr||st\rangle D^2_{tsrq} = \Delta_{pq},\end{aligned} \tag{3.119}$$

where h is the one-electron part of the Hamiltonian, given in Eq. 2.111. With the knowledge of the 1-matrix and the 2-matrix, the ground-state energy can be calculated

$$E_0 = \sum_{pq} h_{pq}D^1_{qp} + \frac{1}{4}\sum_{rstu}\langle rs||tu\rangle D^2_{utsr} = \frac{1}{2}tr(hD^1 + \Delta). \tag{3.120}$$

Coming back to Eq. 3.108, choosing the Hartree-Fock determinant to be the ground-state wave-function; $\mathbf{a}$ is then the manifold of operators that produces the configurations of the P space for the IP-EOM problem unified with the configurations of the P space for the EA-EOM problem. The $\mathbf{f}$ manifold corresponds to the unified Q spaces of the IP-EOM and the EA-EOM problem. Eq. 3.113 can now be compared to Eq. 3.55. The self-energy and the correlation potential differ by the fact that the

reference state $|\Psi_0\rangle$ in Eq. 3.113 is given by the Hartree-Fock determinant, whereas in Eq. 3.55 it is the coupled-cluster wave-function. In Eq. 3.113 the ionization potential and electron affinity components of the electron-propagator are treated simultaneously, whereas Eq. 3.55 is formulated for IP's, with a similar equation for EA's, which are decoupled and given in Eq. 3.51 and Eq. 3.52.

3.3 Coupled-Cluster Green's Function Method

It was shown by Meissner and Bartlett [107], that the consequence of introducing a coupled-cluster wave-function as the N-electron ground state in the propagator approach, is the vanishing of the $[\mathbf{G}^{-1}(E)]_{ia}$ elements, which decouples the IP and the EA sector for the eigenvalues. The coupled-cluster Greens function approach was also discussed by Nooijen and Snijders [108, 109].

The reference function Ψ_0 in the propagator approach is chosen to be the coupled-cluster wave-function $\Psi_0 = e^T\Phi_0$, with the T operator defined in Eq. 3.8 and Eq. 3.9. Using the fact that strings of creation and annihilation operators commute, a new superoperator $\hat{\bar{H}}$ is defined

$$\hat{\bar{H}} = e^{-T}\hat{H}e^{T} = \hat{H}_0 + \hat{\bar{H}}_{corr}, \tag{3.121}$$

where H_0 is defined as in Eq. 3.105. Analogously to Eq. 3.25, the amplitudes satisfy the equations

$$\begin{aligned} 0 &= \langle\Phi_i^a|\bar{H}|\Phi_0\rangle \\ 0 &= \langle\Phi_{ij}^{ab}|\bar{H}|\Phi_0\rangle \ldots . \end{aligned} \tag{3.122}$$

With the new defined superoperator, Eq. 3.121, the inverse propagator matrix Eq. 3.104 becomes

$$\mathbf{G}^{-1}(E) = (\mathbf{a}|E\hat{I}\mathbf{a}) - (\mathbf{a}|\hat{\bar{H}}\mathbf{a}) - (\mathbf{a}|\hat{\bar{H}}\mathbf{f})(\mathbf{f}|(E\hat{I} - \hat{\bar{H}})\mathbf{f})^{-1}(\mathbf{f}|\hat{\bar{H}}\mathbf{a}). \tag{3.123}$$

Eq. 3.113 defines an effective eigenvalue problem

$$\mathbf{H}_{eff}\mathbf{C}(E) = \mathbf{C}(E)E. \tag{3.124}$$

with

$$\mathbf{H}_{eff} = (\mathbf{a}|\hat{\bar{H}}\mathbf{a}) + (\mathbf{a}|\hat{\bar{H}}\mathbf{f})(\mathbf{f}|(E\hat{I} - \hat{\bar{H}})\mathbf{f})^{-1}(\mathbf{f}|\hat{\bar{H}}\mathbf{a}). \tag{3.125}$$

For convenience, a further classification of the elements of $\mathbf{f}$ is introduced. The two classes of elements $\mathbf{f} = \{\mathbf{X}^\dagger, \mathbf{Y}\}$ are defined as

$$\begin{aligned} f \;&\in\; \mathbf{X}^\dagger \quad \text{if} \quad \langle\Phi_0|f = 0 \\ f \;&\in\; \mathbf{Y} \quad \text{if} \quad f|\Phi_0\rangle = 0. \end{aligned} \tag{3.126}$$

The definition Eq. 3.126 implies, that $\mathbf{X}^\dagger$ includes the two-hole one-particle, three-hole two-particle and so on operators, while $\mathbf{Y}^\dagger$ includes the two-particle one-hole, three-particle two-hole and so on operators.

Considering the $[\mathbf{H}_{eff}]_{ia}$ elements of the first term in Eq. 3.125

$$\begin{aligned} (i|\hat{\bar{H}}a) &= (i|[a, \bar{H}]) \\ &= \langle\Phi_0|[a\bar{H}, i^\dagger]_+|\Phi_0\rangle - \langle\Phi_0|[\bar{H}a, i^\dagger]_+|\Phi_0\rangle \\ &= \langle\Phi_0|a\bar{H}i^\dagger + i^\dagger a\bar{H} - \bar{H}ai^\dagger - i^\dagger\bar{H}a|\Phi_0\rangle = 0. \end{aligned} \tag{3.127}$$

The first, the third, and the fourth term in the last line of Eq. 3.127 are zero because of the properties of the annihilation and creation operators, the second term is zero because of Eq. 3.122.

The first part of the second term of Eq. 3.125 is evaluated for $j^\dagger ab \in \mathbf{Y}$

$$\begin{aligned} (i|\hat{\bar{H}}j^\dagger ab) &= (i|[j^\dagger ab, \bar{H}]) \\ &= \langle\Phi_0|[j^\dagger ab\bar{H}, i^\dagger]_+|\Phi_0\rangle - \langle\Phi_0|[\bar{H}j^\dagger ab, i^\dagger]_+|\Phi_0\rangle \\ &= \langle\Phi_0|j^\dagger ab\bar{H}i^\dagger + i^\dagger j^\dagger ab\bar{H} - \bar{H}j^\dagger abi^\dagger - i^\dagger\bar{H}j^\dagger ab|\Phi_0\rangle = 0. \end{aligned} \tag{3.128}$$

Again, the first, the third, and the fourth term in the last line of Eq. 3.129 are zero because of the properties of the annihilation and creation operators, the second term is zero because of Eq. 3.122. Similarly, the three-particle two-hole or higher excitation operators in $\mathbf{Y}$ give zero contributions.

The last part of the second term with $a^\dagger ij \in \mathbf{X}^\dagger$ is given by

$$\begin{aligned}(a^\dagger ij|\hat{\bar{H}}b) &= (a^\dagger ij|[b,\bar{H}]) \\ &= \langle\Phi_0|[b\bar{H}, j^\dagger i^\dagger a]_+|\Phi_0\rangle - \langle\Phi_0|[\bar{H}b, j^\dagger i^\dagger a]_+|\Phi_0\rangle \\ &= \langle\Phi_0|b\bar{H}j^\dagger i^\dagger a + j^\dagger i^\dagger ab\bar{H} - \bar{H}bj^\dagger i^\dagger a - j^\dagger i^\dagger a\bar{H}b|\Phi_0\rangle = 0. \quad (3.129)\end{aligned}$$

The same argument as above applies, as well as for higher excitation operators in $\mathbf{X}^\dagger$.

The final part, needed to be analyzed to determine the $[\mathbf{H}_{eff}]_{ia}$ elements, is

$$\begin{aligned}(a^\dagger ij|\hat{\bar{H}}k^\dagger cd) &= (a^\dagger ij|[k^\dagger cd,\bar{H}]) \\ &= \langle\Phi_0|[k^\dagger cd\bar{H}, j^\dagger i^\dagger a]_+|\Phi_0\rangle - \langle\Phi_0|[\bar{H}k^\dagger cd, j^\dagger i^\dagger a]_+|\Phi_0\rangle \\ &= \langle\Phi_0|k^\dagger cd\bar{H}j^\dagger i^\dagger a + j^\dagger i^\dagger ak^\dagger cd\bar{H} - \bar{H}k^\dagger cdj^\dagger i^\dagger a \\ &\quad -j^\dagger i^\dagger a\bar{H}k^\dagger cd|\Phi_0\rangle = 0. \quad (3.130)\end{aligned}$$

Again, the only term left in the last line is the second term, which is zero because of Eq. 3.122. Higher excitation operators in $\mathbf{X}^\dagger$ and $\mathbf{Y}$ yield zero as well.

Summarizing the above results:

$$\begin{aligned}(i|\hat{\bar{H}}a) &= 0 \\ (\mathbf{X}^\dagger|\hat{\bar{H}}a) &= \mathbf{0} \\ (i|\hat{\bar{H}}\mathbf{Y}) &= \mathbf{0} \\ (\mathbf{X}^\dagger|\hat{\bar{H}}\mathbf{Y}) &= \mathbf{0}. \quad (3.131)\end{aligned}$$

Eq. 3.131 together with the expansion

$$(\mathbf{f}|(E\hat{I}-\hat{\bar{H}})\mathbf{f})^{-1}=\sum_{k=1}^{\infty}E^{-k}(\mathbf{f}|\hat{\bar{H}}\mathbf{f})^{k-1} \tag{3.132}$$

implies that

$$(i|\hat{\bar{H}}\mathbf{f})(\mathbf{f}|(E\hat{I}-\hat{\bar{H}})\mathbf{f})^{-1}(\mathbf{f}|\hat{\bar{H}}a)=0, \tag{3.133}$$

which shows that

$$[\mathbf{H}_{eff}]_{ia}=0 \quad \forall\, i,a. \tag{3.134}$$

However, if the same analysis for the $[\mathbf{H}_{eff}]_{ai}$ elements is done, it is found that the condition needed for the $[\mathbf{H}_{eff}]_{ai}$ elements to be zero, is that the Hermitian conjugate of Eq. 3.122 is fulfilled. Here only one example is shown

$$\begin{aligned}(a|\hat{\bar{H}}i) &= (a|[i,\bar{H}]) \\ &= \langle\Phi_0|[i\bar{H},a^\dagger]_+|\Phi_0\rangle-\langle\Phi_0|[\bar{H}i,a^\dagger]_+|\Phi_0\rangle \\ &= \langle\Phi_0|i\bar{H}a^\dagger+a^\dagger i\bar{H}-\bar{H}ia^\dagger-a^\dagger\bar{H}i|\Phi_0\rangle.\end{aligned} \tag{3.135}$$

The first, the second, and the fourth term are zero but for the third term to be zero, $\langle\Phi_0|\bar{H}|\Phi_i^a\rangle$ would have to be zero. Since $\bar{H}$ is not Hermitian, $(a|\hat{\bar{H}}i)$ is in general nonzero. The nonhermiticity also results in

$$\begin{aligned}(a|\hat{\bar{H}}\mathbf{X}^\dagger) &\neq \mathbf{0} \\ (\mathbf{Y}|\hat{\bar{H}}i) &\neq \mathbf{0} \\ (\mathbf{Y}|\hat{\bar{H}}\mathbf{X}^\dagger) &\neq \mathbf{0}.\end{aligned} \tag{3.136}$$

It follows that

$$[\mathbf{H}_{eff}]_{ai}\neq 0. \tag{3.137}$$

The $[\mathbf{H}_{eff}]_{ij}$ and the $[\mathbf{H}_{eff}]_{ab}$ elements are in general nonzero. Hence, the general structure of the matrix representation of the effective Hamiltonian in Eq.

3.124 is

$$\mathbf{H}_{eff} = \left(\begin{array}{c|c} [\mathbf{H}_{eff}]_{ij} & \mathbf{0} \\ \hline [\mathbf{H}_{eff}]_{ai} & [\mathbf{H}_{eff}]_{ab} \end{array} \right). \tag{3.138}$$

To obtain the eigenvalues of the effective Hamiltonian, the 1-hole sector can be considered separately from the 1-particle sector.

By introducing correlation effects in the ground state, the calculation of ionization potentials and electron affinities decouples. However, if one is interested in the eigenvectors of Eq. 3.124, the separation is not justified. For a complete decoupling of the IP and EA sector, which also holds for the eigenvectors, the $[\mathbf{H}_{eff}]_{ai}$ and the $[\mathbf{H}_{eff}]_{ia}$ elements have to be zero. In the following the IP and EA sector are regarded as decoupled, keeping in mind, that this is only true for the eigenvalues.

Because of Eq. 3.138, Eq. 3.124 can be rewritten into an eigenvalue equation for the negative of the IP's, and an eigenvalue equation for the negative of the EA's

$$\begin{aligned} [\boldsymbol{\epsilon}^{IP} + \boldsymbol{\Sigma}^{IP}(E)]\mathbf{C}(E) &= \mathbf{C}(E)E \\ [\boldsymbol{\epsilon}^{EA} + \boldsymbol{\Sigma}^{EA}(E)]\mathbf{C}(E) &= \mathbf{C}(E)E. \end{aligned} \tag{3.139}$$

For the calculation of the principal IP's the self-energy expression is simplified because of Eq. 3.131. The manifold $\mathbf{f}$ can be replaced by the manifold $\mathbf{X}^\dagger$

$$\boldsymbol{\Sigma}^{IP}(E) = (\mathbf{h}|\hat{\bar{H}}\mathbf{h})_{corr} + (\mathbf{h}|\hat{\bar{H}}\mathbf{X}^\dagger)(\mathbf{X}^\dagger|(E\hat{I} - \hat{\bar{H}})\mathbf{X}^\dagger)^{-1}(\mathbf{X}^\dagger|\hat{\bar{H}}\mathbf{h}), \tag{3.140}$$

where $\mathbf{h}$ is an array of field operators, annihilating occupied orbitals in the Hartree-Fock determinant. The following shows that Eq. 3.140 is equivalent to Eq. 3.54 for the IP sector.

Starting with the first term in Eq. 3.140

$$\begin{aligned} (k|\hat{\bar{H}}i)_{corr} &= -\langle\Phi_0|\bar{H}ik^\dagger + k^\dagger\bar{H}i - i\bar{H}k^\dagger - k^\dagger i\bar{H}|\Phi_0\rangle_{corr} \\ &= -\langle\Phi_0|k^\dagger\bar{H}i|\Phi_0\rangle_{corr}. \end{aligned} \tag{3.141}$$

Further, assuming the truncation level of the IP-EOM-CCSD model,

$$\begin{aligned}(k|\hat{\bar{H}}a^\dagger ij) &= -\langle\Phi_0|\bar{H}a^\dagger ijk^\dagger + k^\dagger\bar{H}a^\dagger ij - a^\dagger ij\bar{H}k^\dagger - k^\dagger a^\dagger ij\bar{H}|\Phi_0\rangle \\ &= -\langle\Phi_0|k^\dagger\bar{H}a^\dagger ij|\Phi_0\rangle \qquad (3.142)\\ (b^\dagger lk|\hat{\bar{H}}i) &= -\langle\Phi_0|\bar{H}ik^\dagger l^\dagger b + k^\dagger l^\dagger b\bar{H}i - i\bar{H}k^\dagger l^\dagger b - k^\dagger l^\dagger bi\bar{H}|\Phi_0\rangle \\ &= -\langle\Phi_0|k^\dagger l^\dagger b\bar{H}i|\Phi_0\rangle. \qquad (3.143)\end{aligned}$$

Finally,

$$\begin{aligned}(b^\dagger lk|\hat{\bar{H}}a^\dagger ij) &= -\langle\Phi_0|\bar{H}a^\dagger ijk^\dagger l^\dagger b + k^\dagger l^\dagger b\bar{H}a^\dagger ij - a^\dagger ij\bar{H}k^\dagger l^\dagger b - k^\dagger l^\dagger ba^\dagger ij\bar{H}|\Phi_0\rangle \\ &= -\langle\Phi_0|k^\dagger l^\dagger b\bar{H}a^\dagger ij|\Phi_0\rangle. \qquad (3.144)\end{aligned}$$

Using Eq. 3.141 through Eq. 3.144, the ij elements of the self-energy for the IP sector are given by

$$\begin{aligned}[\Sigma^{IP}(E)]_{ij} &= -\langle\Phi_0|i^\dagger\bar{H}j|\Phi_0\rangle_{corr} + \langle\Phi_0|i^\dagger\bar{H}\mathbf{X}^\dagger|\Phi_0\rangle[E\mathbf{1} \\ &\quad +\langle\Phi_0|\mathbf{X}\bar{H}\mathbf{X}^\dagger|\Phi_0\rangle]^{-1}\langle\Phi_0|\mathbf{X}\bar{H}j|\Phi_0\rangle. \qquad (3.145)\end{aligned}$$

Since $\mathbf{X}^\dagger$ includes in general the two-holes one-particle, three-holes two-particles and so on operators, Eq. 3.145 can be written in matrix form with the excited determinants of the Q space of the IP-EOM model as basis. Eq. 3.145 can then be identified with Eq. 3.53 for the IP sector, where E is the negative of the ionization potential ε.

It was shown above, that the $[\mathbf{H}_{eff}]_{ai}$ do not vanish because of the nonhermicity of $\bar{H}$. As a consequence, in particular, because of Eq. 3.136, the equations for electron affinities are more complicated, since certain simplifications for the EA sector do not occur if $\hat{\bar{H}}$ is used. However, the use of $\hat{\bar{H}}^\dagger$ leads to the vanishing of the $[\mathbf{H}'_{eff}]_{ai}$ elements, and again a decoupling of the IP and EA sector, and similar

equations to those for the IP's can be derived for the EA's. $\mathbf{H}'_{eff}$ is given by

$$\mathbf{H}'_{eff} = (\mathbf{a}|\hat{\bar{H}}^{\dagger}\mathbf{a}) + (\mathbf{a}|\hat{\bar{H}}^{\dagger}\mathbf{f})(\mathbf{f}|(E\hat{I} - \hat{\bar{H}}^{\dagger})\mathbf{f})^{-1}(\mathbf{f}|\hat{\bar{H}}^{\dagger}\mathbf{a}). \tag{3.146}$$

Similar to Eq. 3.122, the amplitudes can be determined through the following set of equations

$$\begin{aligned} 0 &= \langle\Phi_0|\bar{H}^{\dagger}|\Phi_i^a\rangle \\ 0 &= \langle\Phi_0|\bar{H}^{\dagger}|\Phi_{ij}^{ab}\rangle \ldots . \end{aligned} \tag{3.147}$$

A similar analysis, as above for the $[\mathbf{H}_{eff}]_{ia}$ elements, can be done for the $[\mathbf{H}'_{eff}]_{ai}$ elements.

As an example, consider

$$\begin{aligned} (a|\hat{\bar{H}}^{\dagger}i) &= (a|[i,\bar{H}]) \\ &= \langle\Phi_0|[i\bar{H}^{\dagger},a^{\dagger}]_+|\Phi_0\rangle - \langle\Phi_0|[\bar{H}^{\dagger}i,a^{\dagger}]_+|\Phi_0\rangle \\ &= \langle\Phi_0|i\bar{H}^{\dagger}a^{\dagger} + a^{\dagger}i\bar{H}^{\dagger} - \bar{H}^{\dagger}ia^{\dagger} - a^{\dagger}\bar{H}^{\dagger}i|\Phi_0\rangle = 0. \end{aligned} \tag{3.148}$$

The first, the second, and the fourth term in the last line of Eq. 3.148 are zero, because of the properties of the annihilation and creation operators, the third term is zero, because of Eq. 3.147.

Proceeding as above will lead to

$$\begin{aligned} (a|\hat{\bar{H}}^{\dagger}\mathbf{X}^{\dagger}) &= \mathbf{0} \\ (\mathbf{Y}|\hat{\bar{H}}^{\dagger}i) &= \mathbf{0} \\ (\mathbf{Y}|\hat{\bar{H}}^{\dagger}\mathbf{X}^{\dagger}) &= \mathbf{0}, \end{aligned} \tag{3.149}$$

from which the conclusion can be drawn that the $[\mathbf{H}'_{eff}]_{ai}$ elements are zero. $\mathbf{H}'_{eff}$ has the following general structure

$$\mathbf{H}'_{eff} = \left(\begin{array}{c|c} [\mathbf{H}'_{eff}]_{ij} & [\mathbf{H}'_{eff}]_{ia} \\ \hline \mathbf{0} & [\mathbf{H}'_{eff}]_{ab} \end{array} \right). \tag{3.150}$$

That shows that the decoupling of the IP and the EA block is also valid if $\hat{\bar{H}}^{\dagger}$ is used. Because of Eq. 3.150, the self-energy expression for the EA sector can be simplified as well

$$\mathbf{\Sigma}^{EA}(E) = (\mathbf{p}|\hat{\bar{H}}^{\dagger}\mathbf{p})_{corr} + (\mathbf{p}|\hat{\bar{H}}^{\dagger}\mathbf{Y})(\mathbf{Y}|(E\hat{I} - \hat{\bar{H}}^{\dagger})\mathbf{Y})^{-1}(\mathbf{Y}|\hat{\bar{H}}^{\dagger}\mathbf{p}), \tag{3.151}$$

where $\mathbf{p}$ is an array of field operators, annihilating virtual orbitals in the Hartree-Fock determinant.

Applying superoperator algebra as above, leads to

$$\begin{aligned} [\mathbf{\Sigma}^{EA}(E)]_{ab} &= \langle\Phi_0|b\bar{H}^{\dagger}a^{\dagger}|\Phi_0\rangle_{corr} + \langle\Phi_0|\mathbf{Y}\bar{H}^{\dagger}a^{\dagger}|\Phi_0\rangle[E\mathbf{1} \\ &\quad -\langle\Phi_0|\mathbf{Y}\bar{H}^{\dagger}\mathbf{Y}^{\dagger}|\Phi_0\rangle]^{-1}\langle\Phi_0|b\bar{H}^{\dagger}\mathbf{Y}^{\dagger}|\Phi_0\rangle. \end{aligned} \tag{3.152}$$

Taking the Hermitian adjoint of Eq. 3.152, gives

$$\begin{aligned} [\mathbf{\Sigma}^{EA}(E)]^{*}_{ba} &= \langle\Phi_0|a\bar{H}b^{\dagger}|\Phi_0\rangle_{corr} + \langle\Phi_0|a\bar{H}\mathbf{Y}^{\dagger}|\Phi_0\rangle[E\mathbf{1} \\ &\quad -\langle\Phi_0|\mathbf{Y}\bar{H}\mathbf{Y}^{\dagger}|\Phi_0\rangle]^{-1}\langle\Phi_0|\mathbf{Y}\bar{H}b^{\dagger}|\Phi_0\rangle. \end{aligned} \tag{3.153}$$

Since $\mathbf{Y}^{\dagger}$ includes the two-particles one-hole, three-particles two-holes and so on operators, Eq. 3.153 can be written in matrix form, with the excited determinants of the Q space of the EA-EOM model as basis. Assuming the correlation potential is real, Eq. 3.153 can then be identified with Eq. 3.54, where E is the negative of the electron affinity ε.

It can be concluded, that if the coupled-cluster wave-function is used to describe the N-electron ground state, the propagator approach is equivalent to the

partitioned equation-of-motion coupled-cluster approach, as far as the eigenvalues are considered.

3.4 Correlation Potential Derived from the Fock Space Coupled-Cluster Method

In the last two sections a correlation potential, Eq. 3.53 and 3.54, was derived that yields the exact ionization potentials and electron affinities as the negative of the orbital energies within the correlated independent particle (CIP) model. Its equivalence to the propagator method was shown if the coupled-cluster wave-function is used as the N-electron ground state and if only the eigenvalues are considered. However, the derived correlation potential is energy-dependent and consequently, a different correlation potential corresponds to each orbital, so that the orbital equations have to be solved for each eigenvalue separately. The eigenvectors are nonorthogonal. In this section a correlation potential, using the Fock space coupled-cluster ansatz, is derived. A potential for the IP sector and a potential for the EA sector are obtained, both are energy-independent and universal for each sector. All IP's and, in an independent calculation, all EA's can be obtained by a single diagonalization of an effective Hamiltonian. The resultant orbitals are biorthogonal, and the eigenvalues are the negative of the exact principal IP's and EA's.

In the following the Fock space coupled-cluster method is introduced, and it is then shown, how a correlation potential can be obtained. Alternatively, a partitioning technique is used to obtain the Fock space coupled-cluster equations and the correlation potential. In the last part of this section the quality of the orbitals is discussed.

3.4.1 Fock Space Coupled-Cluster Method

Fock space methods, for a review [110], just like equation-of-motion methods [95, 96], provide energy differences between electronic states directly. The Fock space coupled-cluster method introduced by Lindgren [92] and Haque and Mukherjee

[111] is a multi-reference method, in which a multiple-cluster expansion ansatz is used to create the different states in Fock space. The Fock space is divided into sectors (m,n), according to how many electrons are added or removed relative to the reference function. We are only interested in the $(0,1)$ sector of single ionization and the $(1,0)$ sector of single electron attachment.

The model space for the $(N-1)$ electron system contains a linear combination of one-hole determinants, and the model space for the $(N+1)$ electron system is a linear combination of one-particle determinants relative to the reference determinant. Since we are interested in all orbital energies, the number of hole determinants is equal to the number of occupied orbitals and the number of particle determinants is equal to the number of virtual orbitals

$$|\Psi_k^{IP}\rangle = \sum_i^{occ} c_{ki}\{\hat{i}\}|\Phi_0\rangle \tag{3.154}$$

$$|\Psi_k^{EA}\rangle = \sum_a^{vir} c_{ka}\{\hat{a}^\dagger\}|\Phi_0\rangle. \tag{3.155}$$

In general, the Fock space CC method is formulated for incomplete model spaces, where only certain hole and particle determinants are selected [110]. The total wave-function for the $(N-1)$ state and the $(N+1)$ state is given by

$$|\Phi_k^{IP}\rangle = \Omega^{IP}|\Psi_k^{IP}\rangle \tag{3.156}$$

$$|\Phi_k^{EA}\rangle = \Omega^{EA}|\Psi_k^{EA}\rangle. \tag{3.157}$$

An exponential ansatz is used for the wave operator Ω

$$\Omega^{IP} = \{e^{T^{(0,0)}+T^{(0,1)}}\} \tag{3.158}$$

$$\Omega^{EA} = \{e^{T^{(0,0)}+T^{(1,0)}}\}. \tag{3.159}$$

$T^{(0,0)}$ is the normal closed-shell coupled-cluster operator from Eq. 3.8. $e^{T^{(0,1)}}$ acts on the model space $|\Psi_k^{IP}\rangle$ to deliver its orthogonal complement of net one-hole excited

determinants, the Q^{IP} space for the IP sector. $e^{T^{(1,0)}}$ acts on the model space $|\Psi_k^{EA}\rangle$ to deliver its orthogonal complement of net one-particle excited determinants, the Q^{EA} space for the EA sector. Since the $(0,0)$ cluster operator commutes with other cluster operators in normal order, the $(0,0)$ calculation can be decoupled from the rest of the Fock space calculation

$$\Omega^{IP} = e^{T^{(0,0)}}\left\{e^{T^{(0,1)}}\right\} = e^{T^{(0,0)}}\tilde{\Omega}^{IP} \tag{3.160}$$

$$\Omega^{EA} = e^{T^{(0,0)}}\left\{e^{T^{(1,0)}}\right\} = e^{T^{(0,0)}}\tilde{\Omega}^{EA}. \tag{3.161}$$

Defining $\bar{H}_N = \bar{H} - E_{CC}$, the Schroedinger equation can be written in terms of the model spaces. Using the model space projectors P^{IP} and P^{EA}, the Schroedinger equation is given by

$$\bar{H}_N\tilde{\Omega}^{IP}P^{IP} = \tilde{\Omega}^{IP}\omega^{IP}P^{IP} \tag{3.162}$$

$$\bar{H}_N\tilde{\Omega}^{EA}P^{EA} = \tilde{\Omega}^{EA}\omega^{EA}P^{EA}, \tag{3.163}$$

where ω^{IP} are the principal IP's, and ω^{EA} are the negative principal EA's. The effective Hamiltonians $\bar{H}_{eff}^{IP}$ and $\bar{H}_{eff}^{EA}$ can be defined by projecting Eq. 3.162 and Eq. 3.163 on the left with $P^{IP}\tilde{\Omega}^{IP^{-1}}$ and with $P^{EA}\tilde{\Omega}^{EA^{-1}}$

$$\begin{aligned} P^{IP}\tilde{\Omega}^{IP^{-1}}\bar{H}_N\tilde{\Omega}^{IP}P^{IP} &= P^{IP}(\bar{H}_N\tilde{\Omega}^{IP})_c P^{IP} \\ &= P^{IP}\tilde{\Omega}^{IP^{-1}}\tilde{\Omega}^{IP}\omega^{IP}P^{IP} = P^{IP}\omega^{IP}P^{IP} \\ \bar{H}_{eff}^{IP} &= P^{IP}(\bar{H}_N\tilde{\Omega}^{IP})_c P^{IP} \end{aligned} \tag{3.164}$$

$$\begin{aligned} P^{EA}\tilde{\Omega}^{EA^{-1}}\bar{H}_N\tilde{\Omega}^{EA}P^{EA} &= P^{EA}(\bar{H}_N\tilde{\Omega}^{EA})_c P^{EA} \\ &= P^{EA}\tilde{\Omega}^{EA^{-1}}\tilde{\Omega}^{EA}\omega^{EA}P^{EA} = P^{EA}\omega^{EA}P^{EA} \\ \bar{H}_{eff}^{EA} &= P^{EA}(\bar{H}_N\tilde{\Omega}^{EA})_c P^{EA}. \end{aligned} \tag{3.165}$$

To determine the expansion coefficients of $\tilde{\Omega}^{IP}$ and $\tilde{\Omega}^{EA}$, Eq. 3.162 and Eq. 3.163 are projected onto the left by Q^{IP} and Q^{EA}, followed by insertion of Eq. 3.164 and

Eq. 3.165, giving

$$Q^{IP}\bar{H}_N\tilde{\Omega}^{IP}P^{IP} - Q^{IP}\tilde{\Omega}^{IP}P^{IP}\bar{H}^{IP}_{eff}P^{IP} = 0 \tag{3.166}$$

$$Q^{EA}\bar{H}_N\tilde{\Omega}^{EA}P^{EA} - Q^{EA}\tilde{\Omega}^{EA}P^{EA}\bar{H}^{EA}_{eff}P^{EA} = 0, \tag{3.167}$$

the Bloch equations. Expanding the operators in Eq. 3.166 and Eq. 3.167, yields the equations for the amplitudes for the $(0,1)$ and for the $(1,0)$ sector. Both sectors can be solved with amplitudes for the $(0,0)$ sector alone. In Fig. 3–13 and Fig. 3–14 the equations for the effective Hamiltonians in the IP and in the EA sector and the amplitude equations are given diagrammatically. The interpretation of the $\bar{H}$ interaction vertices was given in Fig. 3–11. The equations are written for the general case of incomplete model spaces, where only selected orbitals are active, others remain inactive. The number of active orbitals is equal to the number of IP's and EA's that can be obtained. The closed arrows represent inactive orbitals, the double arrows represent active orbitals. Notice that if all orbitals are chosen to be active, the contribution from the simple hole and particle amplitudes is zero. Since it is necessary for all orbitals to be active to derive the correlation potential, further consideration will involve only simple arrows, where it is assumed that all orbitals are active.

If the effective Hamiltonians are expressed in canonical Hartree-Fock orbitals, the leading contribution to the diagonal elements of $-\tilde{\mathbf{H}}^{IP}_{eff}$ and $\tilde{\mathbf{H}}^{EA}_{eff}$ are the Hartree-Fock orbital energies. That can be understood by expanding the $\bar{H}$ interaction lines in Fig. 3–13 and Fig. 3–14 according to Fig. 3–11, see the discussion in Section 3.1.3. The correlation potential can be found by subtracting the Hartree-Fock orbital energies from the diagonal elements of the effective Hamiltonians

$$-\bar{\mathbf{H}}^{IP}_{eff}\mathbf{C}_{PP} = (\boldsymbol{\epsilon}^{IP} + \mathbf{V}^{IP}_c)\mathbf{C}_{PP} = \mathbf{C}_{PP}\boldsymbol{\varepsilon}^{IP}_P \tag{3.168}$$

$$\bar{\mathbf{H}}^{EA}_{eff}\mathbf{C}_{PP} = (\boldsymbol{\epsilon}^{EA} + \mathbf{V}^{EA}_c)\mathbf{C}_{PP} = \mathbf{C}_{PP}\boldsymbol{\varepsilon}^{EA}_P, \tag{3.169}$$

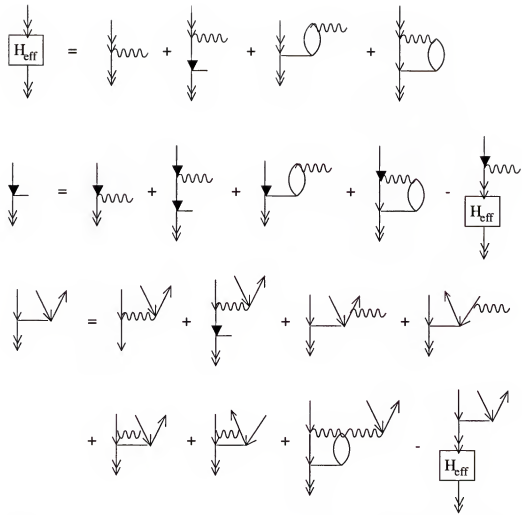

Figure 3–13. Equations for the effective Hamiltonian and the amplitudes in the IP sector for the FS-CCSD method

where ε^{IP} and ε^{EA} contain again the negative of the IP's and the negative of the EA's. The correlation potential for the IP sector is given in Fig. 3–15, and the correlation potential for the EA sector is given in Fig. 3–16.

The amplitude equations in Fig. 3–13 and Fig. 3–14 can be solved iteratively. However, unlike for the EOM method, convergence breaks down in most cases due to intruder states. Intruder states are eigenstates that lie outside the model space but can become quasi-degenerate with a reference space determinant, causing the amplitudes connecting the reference function with the intruder state to become

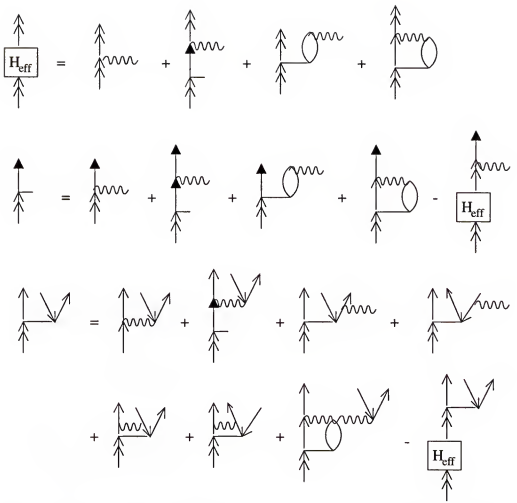

Figure 3–14. Equations for the effective Hamiltonian and the amplitudes in the EA sector for the FS-CCSD method

large. The intruder state problem can be partially avoided for incomplete model spaces [112]. Since it is desired to obtain a correlation potential for all orbitals, the incomplete model space approach, which delivers only a few IP's or EA's respectively, is of limited use for us.

3.4.2 Fock Space Coupled-Cluster Derived from a Partitioning Scheme

If the coupled-cluster amplitudes, the $T^{(0,1)}$, and the $T^{(1,0)}$ amplitudes are given, or somehow approximated, Fig. 3–15 and Fig. 3–16 defines the correlation potential. To avoid convergence problems introduced by intruder states, the Fock space coupled-cluster equations can be cast into a different form.

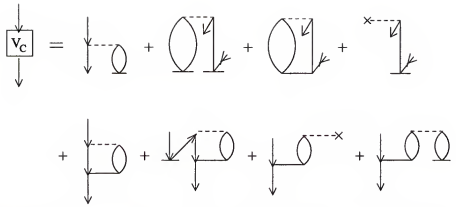

Figure 3–15. Correlation potential in the IP sector for the FS-CCSD method

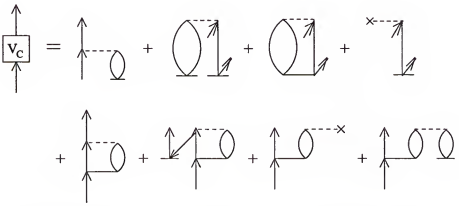

Figure 3–16. Correlation potential in the EA sector for the FS-CCSD method

Substitution of the wave operators by $\tilde{\Omega}^{IP} = e^{T^{(0,1)}} = 1 + S^{IP}$ and $\tilde{\Omega}^{EA} = e^{T^{(1,0)}} = 1 + S^{EA}$ in Eq. 3.164-3.167, leads to

$$\bar{H}^{IP}_{eff} = P^{IP}\bar{H}(1+S^{IP})P^{IP} \tag{3.170}$$

$$0 = Q^{IP}\bar{H}(1+S^{IP})P^{IP} - Q^{IP}S^{IP}\bar{H}^{IP}_{eff} \tag{3.171}$$

$$\bar{H}^{EA}_{eff} = P^{EA}\bar{H}(1+S^{EA})P^{EA} \tag{3.172}$$

$$0 = Q^{EA}\bar{H}(1+S^{EA})P^{EA} - Q^{EA}S^{EA}\bar{H}^{EA}_{eff}, \tag{3.173}$$

where the fact was used that $Q^{IP}P^{IP} = Q^{EA}P^{EA} = 0$. To simplify the notation, the subscript N in $\bar{H}_N$ is omitted. The matrix form of Eq. 3.170-Eq. 3.173 is given by

$$\bar{\mathbf{H}}^{IP}_{eff} = \bar{\mathbf{H}}^{IP}_{PP} + \bar{\mathbf{H}}^{IP}_{PQ}\mathbf{S}^{IP} \tag{3.174}$$

$$0 = \bar{\mathbf{H}}^{IP}_{QP} + \bar{\mathbf{H}}^{IP}_{QQ}\mathbf{S}^{IP} - \mathbf{S}^{IP}(\bar{\mathbf{H}}^{IP}_{PP} + \bar{\mathbf{H}}^{IP}_{PQ}\mathbf{S}^{IP}) \tag{3.175}$$

$$\bar{\mathbf{H}}^{EA}_{eff} = \bar{\mathbf{H}}^{EA}_{PP} + \bar{\mathbf{H}}^{EA}_{PQ}\mathbf{S}^{EA} \tag{3.176}$$

$$0 = \bar{\mathbf{H}}^{EA}_{QP} + \bar{\mathbf{H}}^{EA}_{QQ}\mathbf{S}^{EA} - \mathbf{S}^{EA}(\bar{\mathbf{H}}^{EA}_{PP} + \bar{\mathbf{H}}^{EA}_{PQ}\mathbf{S}^{EA}), \tag{3.177}$$

where the definition of the effective Hamiltonian is substituted into Eq. 3.175 and Eq. 3.177. If $\mathbf{S}^{IP}$ is known, diagonalization of $\bar{\mathbf{H}}^{IP}_{eff}$ gives all IP's, and if $\mathbf{S}^{EA}$ is known, diagonalization of $\bar{\mathbf{H}}^{EA}_{eff}$ gives all EA's. One could attempt to solve Eq. 3.175 and Eq. 3.177 iteratively by taking as starting guesses

$$\mathbf{S}^{IP} = -\bar{\mathbf{H}}^{IP^{-1}}_{QQ}\bar{\mathbf{H}}^{IP}_{QP} \tag{3.178}$$

$$\mathbf{S}^{EA} = -\bar{\mathbf{H}}^{EA^{-1}}_{QQ}\bar{\mathbf{H}}^{EA}_{QP}. \tag{3.179}$$

Unfortunately these guesses are not sufficient, and convergence cannot be achieved according to my experience.

However, it is possible to reformulate the partitioned equation-of-motion eigenvalue problem to find an expression for $\mathbf{S}$. It was shown by diagrammatic arguments [113] and otherwise [97] that the IP-EOM-CCSD and the EA-EOM-CCSD approaches are equivalent to the FS-CCSD method for the principal IP's or EA's, solved in the $(0,1)$ and the $(1,0)$ sector, respectively. In those cases the exponential ansatz for the wave operator Ω reduces to a linear ansatz. Therefore, S contains only linear terms, and the FS-CC methods for IP's and EA's can be regarded as an eigenvalue problem for the transformed Hamiltonian $\bar{H}$, described by Eq. 3.36.

The partitioned eigenvalue equation for the (0,1) sector is once again used, but slightly differently,

$$\begin{pmatrix} -\bar{\mathbf{H}}^{IP}_{PP} & -\bar{\mathbf{H}}^{IP}_{PQ} \\ -\bar{\mathbf{H}}^{IP}_{QP} & -\bar{\mathbf{H}}^{IP}_{QQ} \end{pmatrix} \begin{pmatrix} \mathbf{C}_{PP} & \mathbf{C}_{PQ} \\ \mathbf{C}_{QP} & \mathbf{C}_{QQ} \end{pmatrix} = \begin{pmatrix} \mathbf{C}_{PP} & \mathbf{C}_{PQ} \\ \mathbf{C}_{QP} & \mathbf{C}_{QQ} \end{pmatrix} \begin{pmatrix} \boldsymbol{\varepsilon}_P & \mathbf{0} \\ \mathbf{0} & \boldsymbol{\varepsilon}_Q \end{pmatrix}, \quad (3.180)$$

where the equation was multiplied by minus one to obtain the negative of the IP, ε. The two equations are selected that depend upon ε_P,

$$-\bar{\mathbf{H}}^{IP}_{PP}\mathbf{C}_{PP} - \bar{\mathbf{H}}^{IP}_{PQ}\mathbf{C}_{QP} = \mathbf{C}_{PP}\boldsymbol{\varepsilon}_P \quad (3.181)$$

$$-\bar{\mathbf{H}}^{IP}_{QP}\mathbf{C}_{PP} - \bar{\mathbf{H}}^{IP}_{QQ}\mathbf{C}_{QP} = \mathbf{C}_{QP}\boldsymbol{\varepsilon}_P. \quad (3.182)$$

Multiplication of Eq. 3.181 and Eq. 3.182 with $\mathbf{C}^{-1}_{\mathbf{PP}}$ on the right, leads to the equivalent of Eq. 3.174 and Eq. 3.175, where the effective Hamiltonian yields the negative of the principal IP's upon diagonalization

$$\bar{\mathbf{H}}^{IP}_{eff} = -\bar{\mathbf{H}}^{IP}_{PP} - \bar{\mathbf{H}}^{IP}_{PQ}\mathbf{S}^{IP} \quad (3.183)$$

$$0 = -\bar{\mathbf{H}}^{IP}_{QP} - \bar{\mathbf{H}}^{IP}_{QQ}\mathbf{S}^{IP} + \mathbf{S}^{IP}(\bar{\mathbf{H}}^{IP}_{PP} + \bar{\mathbf{H}}^{IP}_{PQ}\mathbf{S}^{IP}), \quad (3.184)$$

with the definitions

$$\mathbf{S}^{IP} = \mathbf{C}_{QP}\mathbf{C}^{-1}_{PP} \quad (3.185)$$

$$\bar{\mathbf{H}}^{IP}_{eff} = \mathbf{C}_{PP}\boldsymbol{\varepsilon}_P\mathbf{C}^{-1}_{PP}. \quad (3.186)$$

$\mathbf{C_{QP}}$ and $\mathbf{C_{PP}}^{-1}$ can be obtained from a diagonalization of the transformed Hamiltonian in the entire P and Q space for the IP sector. This bypasses any explicit energy dependence. Also, for a diagonalization in the entire space, intruder state problems do not occur, and the effective Hamiltonian defined in Eq. 3.183 can now be easily built.

The partitioned eigenvalue equation for the (1,0) sector is given similarly to Eq. 3.180, where the negative of the EA is denoted by ε

$$\begin{pmatrix} \bar{\mathbf{H}}_{PP}^{EA} & \bar{\mathbf{H}}_{PQ}^{EA} \\ \bar{\mathbf{H}}_{QP}^{EA} & \bar{\mathbf{H}}_{QQ}^{EA} \end{pmatrix} \begin{pmatrix} \mathbf{C}_{PP} & \mathbf{C}_{PQ} \\ \mathbf{C}_{QP} & \mathbf{C}_{QQ} \end{pmatrix} = \begin{pmatrix} \mathbf{C}_{PP} & \mathbf{C}_{PQ} \\ \mathbf{C}_{QP} & \mathbf{C}_{QQ} \end{pmatrix} \begin{pmatrix} \boldsymbol{\varepsilon}_P & \mathbf{0} \\ \mathbf{0} & \boldsymbol{\varepsilon}_Q \end{pmatrix}. \quad (3.187)$$

Notice, multiplication by minus one is not necessary. Selecting the two equations that depend upon ε_P and multiplying by $\mathbf{C_{PP}^{-1}}$ on the right, leads to

$$\bar{\mathbf{H}}_{eff}^{EA} = \bar{\mathbf{H}}_{PP}^{EA} + \bar{\mathbf{H}}_{PQ}^{EA}\mathbf{S}^{EA} \quad (3.188)$$

$$0 = \bar{\mathbf{H}}_{QP}^{EA} + \bar{\mathbf{H}}_{QQ}^{EA}\mathbf{S}^{EA} - \mathbf{S}^{EA}(\bar{\mathbf{H}}_{PP}^{EA} + \bar{\mathbf{H}}_{PQ}^{EA}\mathbf{S}^{EA}), \quad (3.189)$$

with the definitions

$$\mathbf{S}^{EA} = \mathbf{C}_{QP}\mathbf{C}_{PP}^{-1} \quad (3.190)$$

$$\bar{\mathbf{H}}_{eff}^{EA} = \mathbf{C}_{PP}\boldsymbol{\varepsilon}_P\mathbf{C}_{PP}^{-1}. \quad (3.191)$$

Again the $\mathbf{C_{QP}}$ and $\mathbf{C_{PP}}^{-1}$ can be obtained by diagonalization of the transformed Hamiltonian in the entire P and Q space for the EA sector. Diagonalization of $\bar{\mathbf{H}}_{eff}^{EA}$ yields the principal EA's.

From the effective Hamiltonians defined in Eq. 3.183 and Eq. 3.188, the correlation potentials can be obtained by subtracting Koopman's values as before, leading to Eq. 3.168 and Eq. 3.169, where the effective Hamiltonians are now built by using the eigenvectors of the transformed Hamiltonian in the P and Q spaces, avoiding the difficulty of converging the iterative amplitude equations, when all orbitals are chosen to be active.

Eq. 3.168 and Eq. 3.169 define a correlation potential for all occupied orbitals and a correlation potential for all unoccupied orbitals. Simply adding the two contributions together, as schematically shown in Fig. 3–12, results in an energy-independent correlation potential for the CIP model, which is the same for all orbital

energies. With $\mathbf{V}_c$ given in Fig. 3–12, the eigenvalue problem is now given by

$$\bar{\mathbf{H}}_{eff}\mathbf{C} = (\boldsymbol{\epsilon} + \mathbf{V}_c)\mathbf{C} = \mathbf{C}\boldsymbol{\varepsilon}. \tag{3.192}$$

The matrix $\boldsymbol{\varepsilon}$ contains the principal IP's and EA's of the IP-EOM-CC and the EA-EOM-CC model, or equivalently, the principal IP's and EA's of the FS-CC method, which are exact if no truncation is introduced.

As pointed out before, the effective Hamiltonians in Eq. 3.51 and Eq. 3.52, which were derived from the partitioned equation-of-motion approach, act in the space of N-electron Hartree-Fock determinants, from which an electron has been removed, if the IP sector is considered, or to which an electron is added, if the EA sector is considered. The effective Hamiltonians in Eq. 3.168 and Eq. 3.169 also act in the space of N-particle determinants. However, as before, each element of $\bar{\mathbf{H}}^{IP}_{eff}$ and $\bar{\mathbf{H}}^{EA}_{eff}$ is defined by

$$[\bar{\mathbf{H}}^{IP}_{eff}]_{ij} = \langle\Phi_0|j^\dagger \tilde{H}^{IP}_{eff} i|\Phi_0\rangle = \langle\phi_i|\tilde{H}^{IP}_{eff}|\phi_j\rangle \tag{3.193}$$

$$[\bar{\mathbf{H}}^{EA}_{eff}]_{ab} = \langle\Phi_0|a\tilde{H}^{EA}_{eff} b^\dagger|\Phi_0\rangle = \langle\phi_a|\tilde{H}^{EA}_{eff}|\phi_b\rangle. \tag{3.194}$$

where the $|\phi_i\rangle$ are one-electron functions, represented by $\mathbf{C}_{PP}$, solved for the IP sector, and the $|\phi_a\rangle$ are one-electron functions, represented by $\mathbf{C}_{PP}$, solved for the EA sector. Again, Eq. 3.192 can equivalently be regarded as an effective one-particle equation in an orbital space, where the orbitals are solutions to the biorthogonal eigenvalue equation

$$\tilde{H}_{eff}|\phi_m\rangle = (f + v_c)|\phi_m\rangle = \varepsilon_m|\phi_m\rangle. \tag{3.195}$$

f is the Fock operator and v_c is the correlation potential, given in matrix form in Fig. 3–12. Since the effective Hamiltonian is nonhermitian, diagonalization yields the right eigenvectors $|\phi_m\rangle$ as well as the left eigenvectors $\langle\tilde{\phi}_m|$, corresponding to the same eigenvalue ε_m. The eigenfunctions can be chosen to be biorthonormal

$\langle\tilde{\phi}_m|\phi_n\rangle = \delta_{mn}$. The orbital energies $\langle\tilde{\phi}_m|\bar{H}_{eff}|\phi_m\rangle = \varepsilon_m$ are the negative of the principal IP's and EA's.

Since the Fock space coupled-cluster method for IP's and EA's is equivalent to the IP-EOM-CC and the EA-EOM-CC method respectively, solving the eigenvalue equation, Eq. 3.192, is therefore equivalent to solving Eq. 3.55 for each ε. The energy dependence of $\mathbf{V}_c(\varepsilon)$ in Eq. 3.55 is removed by virtue of the Rayleigh-Schrödinger expansion, which is implicit in the Fock space ansatz, or by using the eigenvectors of the full transformed Hamiltonian (in P and Q space) to build the effective Hamiltonian. In Section 3.3 we have also identified $\mathbf{V}_c(\varepsilon)$ in Eq. 3.55 with the self-energy, employed in propagator methods if one is only concerned with the eigenvalues. That means, that the correlation potential in Eq. 3.192 is equivalent to the self-energy, giving, if no truncation is employed, the exact IP's and EA's. Since the energy dependence is removed, all IP's and EA's can be obtained by a single diagonalization, whereas the IP's and EA's in propagator methods have to each be calculated separately.

3.4.3 Orbitals and Properties Obtained within the CIP Model

In this section a correlation potential for the CIP model was derived, which is energy-independent, leading to a biorthogonal eigenvalue equation, given by Eq. 3.192

$$\bar{\mathbf{H}}_{eff}\mathbf{C} = (\boldsymbol{\epsilon} + \mathbf{V}_c)\mathbf{C} = \mathbf{C}\boldsymbol{\varepsilon}. \tag{3.196}$$

The left and the right eigenvectors of the nonhermitian matrix $\bar{\mathbf{H}}_{eff}$ form a biorthogonal set, chosen to be orthonormal

$$\tilde{\mathbf{C}} \cdot \mathbf{C} = \mathbf{1}. \tag{3.197}$$

The eigenvectors form Slater determinants. A determinant $|\Phi\rangle$ is associated with $\mathbf{C}$ and a determinant $\langle\tilde{\Phi}|$ is associated with $\tilde{\mathbf{C}}$. If the effective Hamiltonian is built from a FS-CCSD ansatz, the eigenvalues are the negative of the FS-CCSD IP's and

EA's. However, the question is if the orbitals are improved as well. As a measure of the quality of the orbitals the calculation of the kinetic energy and dipole moments are chosen.

With the correlation potential given in Fig. 3–12, the occupied and the unoccupied blocks of the effective Hamiltonian are decoupled. However, Fig. 3–15 and Fig. 3–16 show, that there is an indirect contribution from the virtual space to $\mathbf{V}_c^{IP}$, whenever an upwards pointing line is part of an IP diagram, and that there is an indirect contribution from the occupied space to $\mathbf{V}_c^{EA}$, whenever a downwards pointing line is part of an EA diagram. Because of the nonhermiticity of $\bar{\mathbf{H}}_{eff}$ its eigenvectors are biorthogonal, whereas Hartree-Fock orbitals are orthogonal, meaning that the CIP model has two sets of eigenvectors, whereas the Hartree-Fock model has one set. However, the eigenvectors of the CIP model are not expected to be very different from Hatree-Fock orbitals, obtained by a unitary transformation of canonical Hartree-Fock orbitals, since the occupied orbitals of the CIP model are obtained by a rotation within the occupied space, and the unoccupied orbitals of the CIP model are obtained by a rotation within the virtual space of the Hartree-Fock orbitals. Properties are therefore not expected to be very different from properties computed within the Hartree-Fock model either. In the following this hypothesis will be tested.

The calculation of the kinetic energy is chosen as an example that involves a differential operator. In contrast to a multiplicative operator, its expectation value depends on the density matrix instead of the density. The kinetic energy operator is given by

$$k = -\sum_{i=1}^{N} \frac{1}{2} \nabla_i^2. \tag{3.198}$$

The expectation value of the kinetic energy operator K within the CIP model can be written as

$$K = \langle \tilde{\Phi} | k | \Phi \rangle. \tag{3.199}$$

Since k is a one-electron operator, the kinetic energy is

$$K = \mathrm{Tr}(\mathbf{D}^1\mathbf{K}), \tag{3.200}$$

where the matrices $\mathbf{K}$ and $\mathbf{D}^1$ have to be given in a consistent basis. For instance, if $\mathbf{K}$ contains the kinetic energy integrals in the basis of the eigenvectors of Eq. 3.196 (i.e., $K_{mn} = \langle\tilde{\phi}_m|k|\phi_n\rangle$), then $\mathbf{D}^1$ is a diagonal matrix, whose diagonal elements are the occupation numbers in the CIP model, two for the occupied orbitals and zero otherwise, where the spin restricted case is assumed. $\mathbf{K}$ and $\mathbf{D}^1$ could have also both been given in the basis of atomic orbitals.

Table 3–5 lists the kinetic energies of several molecules. The geometries were optimized at the MBPT(2)/DZP level. The kinetic energies of the CIP model, column II, are compared to the Hartree-Fock kinetic energies, column I, and the CCSD kinetic energies, column VI. To obtain the Hartree-Fock kinetic energies, $\mathbf{K}$ in Eq. 3.200 is given in the basis of canonical Hartree-Fock orbitals, in which $\mathbf{D}^1$ is a diagonal matrix, containing the occupation numbers. The CCSD kinetic energies are calculated with the correlated density matrix in the basis of molecular orbitals. $\mathbf{K}$ is given in the basis of molecular orbitals as well. Further comparison is made with the kinetic energy obtained from the first natural configuration, column III. The natural orbitals are calculated by diagonalization of the correlated CCSD density matrix. The kinetic energy integrals are transformed into the basis of natural orbitals, and $\mathbf{D}^1$ is again a diagonal matrix, containing the occupation numbers two for the first N orbitals and zero otherwise. Also included in Table 3–5 are kinetic energies computed from a determinant of Brueckner orbitals, column IV, and kinetic energies of the CIP model, where Brueckner orbitals are used to formulate the effective Hamiltonian, column V. For a more detailed discussion on Brueckner orbitals see the following chapter.

Table 3–5. Kinetic energies in Hartree, DZP basis

	HF	CIP(HF)	1.NC	BR	CIP(BR)	CCSD
HF	100.03366	100.03166	99.98224	99.89852	99.87724	100.11853
H_2O	75.92108	75.91744	75.93392	75.90440	75.90061	76.11443
NH_3	56.17124	56.17032	56.20265	56.20408	56.20318	56.39030
CH_4	40.14029	40.14004	40.16510	40.17154	40.17145	40.33915
HCN	92.46336	92.32461	92.59806	92.66512	92.65981	92.90719

Table 3–5 shows that the kinetic energies in the CIP model are indeed very similar to the kinetic energies obtained from the reference determinant. That is true when Hartree-Fock orbitals are used to build the effective Hamiltonian (compare column I and II) and also when Brueckner orbitals are used to build the effective Hamiltonian (compare column IV and V). A clear statement, about which determinant yields the best kinetic energy, cannot be made from the examples shown. The Hartree-Fock determinant is slightly better for HF, for H_2O and CH_4; the different determinants yield similar kinetic energies, and for NH_3 and HCN the first natural configuration and the Brueckner determinant give better results for the kinetic energy, compared to the coupled-cluster kinetic energy.

As a second example, the calculation of dipole moments was chosen. The classical definition of the dipole moment is given by

$$\vec{\mu} = \sum_i q_i r_i, \tag{3.201}$$

where q_i is the charge with position vector r_i. Quantum mechanically, the electronic dipole operator is $-\sum_{i=1}^{N} r_i$. The total dipole moment in the CIP model can be written as

$$\vec{\mu} = -\sum_{i=1}^{N} \langle \tilde{\Phi} | r_i | \Phi \rangle + \sum_A Z_A R_A, \tag{3.202}$$

where the first term is the quantum mechanical contribution of the electrons and the second term is the classical contribution of the nuclei. The three vector components

Table 3–6. Dipole moments in Hartree, DZP basis

	HF	CIP(HF)	1.NC	BR	CIP(BR)	CCSD
HF	2.054	2.054	1.969	1.941	1.941	1.935
H_2O	2.102	2.102	2.025	2.010	2.010	1.993
NH_3	1.677	1.677	1.649	1.654	1.654	1.631
HCN	3.259	3.259	3.005	2.923	2.923	2.916

(x,y,z) of the electronic contribution to the dipole moment are given similar to Eq. 3.200, for example for μ_x

$$\mu_x = \mathrm{Tr}(\mathbf{D}^1 \boldsymbol{\mu}_x), \tag{3.203}$$

where $\boldsymbol{\mu}_x$ contains the integrals of the x component of the dipole moment, similar for y and z. The classical contribution of the nuclei is added afterwards.

The same calculations, as were done for the kinetic energy, were performed to obtain the components of the dipole moments, only with different property integrals. The results are given in Table 3–6. The example molecules have nonzero dipole moments only in one direction.

Table 3–6 shows, that the dipole moments in the CIP model are the same as the ones, obtained from the reference determinants. The dipole moments in the CIP model, which has the Hartree-Fock determinant as reference determinant, are the same as the Hartree-Fock dipole moments (compare column I and II) and the dipole moments in the CIP model, which has the Brueckner determinant as reference determinant, are the same as the Brueckner dipole moments (compare column IV and V). However, in the case of dipole moments, it becomes apparent that the dipole moments calculated from the first natural configuration and the Brueckner determinant are much closer to the coupled-cluster dipole moments than the Hartree-Fock dipole moments.

The results for the kinetic energies and the dipole moments indicate, that the orbitals, or the density matrix respectively, in the CIP model are only slightly modified, compared to the reference orbitals or the reference density matrix. The kinetic energies calculated from the Hartree-Fock determinant seem to be of about the same accuracy as from a first natural configuration or a Brueckner determinant, which is not very surprising, since the orbitals of the Hartree-Fock determinant are optimized with respect to the total energy, which is the sum of kinetic and potential energy. However, the better choice over the Hartree-Fock determinant for the calculation of dipole moments seems to be a determinant of Brueckner orbitals or the first natural configuration.

CHAPTER 4
SECOND-ORDER CORRELATION POTENTIAL

In the previous chapter possibilities, of how to obtain a correlation potential for the CIP model, which yields the negative of the exact IP's and EA's as orbital energies, were discussed. The partitioned equation-of-motion approach led to an energy-dependent correlation potential, where an eigenvalue equation has to be solved for each orbital with corresponding eigenvalue. If the Fock space coupled-cluster method is employed, the energy dependence is removed by virtue of the Rayleigh-Schrödinger expansion, which is implicit in the Fock space ansatz, or by using the eigenvectors of the full transformed Hamiltonian to build an effective Hamiltonian.

However, in the last section of the previous chapter, it was pointed out, that even though the IP's and EA's can be obtained at the accuracy of Fock space coupled-cluster, the orbitals, and consequently the density matrix, in the CIP model is not significantly improved, compared to that of the reference determinant. That is, because the occupied orbitals of the CIP model are obtained by a rotation of the occupied orbitals of the reference function, and the unoccupied orbitals of the CIP model are obtained by a rotation of the unoccupied orbitals of the reference function. Properties computed with the CIP model are therefore similar to properties computed with the reference function.

The correlation potential, shown in Fig. 3–12, has a sector that determines the IP's, and an independent sector that determines the EA's. This is naturally the case, since the FS-CC methods in the IP and in the EA sector, from which the correlation potential was derived, are two independent methods. The off-diagonal blocks (the ia-block and the ai-block) were both set to zero. It was shown for the

IP-EOM and the EA-EOM methods (Section 3.3) that the decoupling is correct for the eigenvalues, since the ia-block is zero and the ai-block is then arbitrary (i.e., any choice of ai-elements would lead to the same eigenvalues). Because the IP-EOM and the EA-EOM methods are equivalent to the FS-CC methods for the IP and the EA sector, the decoupling of the IP and the EA sector in the correlation potential, derived from the FS-CC ansatz according to Fig. 3–12, is correct as well.

Because of the independence of the IP and the EA sector for the FS-CC method, only the occupied-occupied and the virtual-virtual blocks are defined in the correlation potential. That was sufficient for the infinite-order correlation potential of the previous chapter, because the IP's and the EA's corresponding to the Fock space coupled-cluster values could be obtained by a single diagonalization. In this chapter the objective is to derive a finite-order correlation potential, which depends on the orbitals, used in an iterative procedure, where the orbitals are updated in each iteration. For such a procedure it is necessary to define the occupied-virtual and the virtual-occupied block of the correlation potential as well, since significant orbital changes are achieved by a rotation of the virtual into the occupied orbitals. Apart from the correctness of the eigenvalues being the negative of the IP's and EA's, the orbitals are desired to improve the orbitals of the reference function, chosen to be the Hartree-Fock determinant. In the last section of the previous chapter results for dipole moments were presented, which indicates that Brueckner orbitals are better than Hartree-Fock orbitals to calculate dipole moments, which was also found by Hesselmann and Jansen [114]. The Brueckner determinant has maximum overlap with the exact wave-function, and it can be expected in general that properties, calculated from a Brueckner determinant, are more accurate than properties calculated from a Hartree-Fock determinant. A second condition on the correlation potential is therefore invoked, which requires that the resulting orbitals are Brueckner orbitals. The condition of correctness of the IP's and EA's and the condition on the orbitals

are independent, since the Brillouin-Brueckner condition defines the partitioning of the space in occupied and virtual orbitals, whereas an arbitrary rotation within the occupied and within the virtual space is of no consequence for the partitioning. In this chapter the knowledge of the previous chapter is used to define the occupied-occupied block and the virtual-virtual block of the correlation potential, and the Brillouin-Brueckner condition is invoked to define the occupied-virtual block of the correlation potential.

In the first section of this chapter the Brueckner method is summarized, in the second section a second-order correlation potential is defined and in the last section it is applied to calculate IP's and EA's as well as properties of some sample molecules.

4.1 Brueckner Method

The Brueckner method originated in nuclear physics [40] for dealing with hard-core interaction in infinite nuclear matter. It was introduced in quantum chemistry circles by Nesbet [115] and by Löwdin [41]. Nesbet required the disappearance of single-excited clusters from a trial wave-function, which he called the Brueckner condition. Löwdin assumed the best-overlap condition to the exact wave-function in his "exact self-consistent theory", resulting in the vanishing of single-excitation contributions, which he called the Brillouin-Brueckner theorem.

The Brillouin-Brueckner condition was used as a starting point in the derivation of orbital equations, based on different types of correlated wave-functions. Larsson [42, 43] used pair functions to obtain Hartree-Fock like equations, but with an inhomogeneity term added. Kvasnička [116] used perturbation theory to obtain Brueckner orbitals. Chiles and Dykstra [44], Purvis and Bartlett [45] and Adamowicz and Bartlett [46], and Handy et al. [47] obtained Brueckner orbitals in coupled-cluster theory. Stolarczyk and Monkhorst [48, 117, 118] applied the maximum overlap condition to a coupled-cluster reference wave-function and formulated an effective

Hamiltonian, which has the form of the Fock operator plus a correlation potential. Scuseria [49, 50] implemented the Brueckner coupled-cluster method, employing the effective Brueckner Hamiltonian in a self consistent scheme. Further aspects of Brueckner theory were recently presented by Lindgren and Salomonson [51, 119], including its approximate relationship to DFT.

The Brillouin-Brueckner condition is only sufficient to determine the partition of the full space into occupied and virtual parts. For a complete specification of the corresponding eigenvalue problem, the one-particle operator also has to be defined in the occupied-occupied block and in the virtual-virtual block by applying an additional condition. Scuseria [49, 50] required that the total coupled-cluster energy is reproduced as a sum of orbital energies, whereas Kvasnička [116] and Lindgren [51] assumed that the orbital energies correspond to IP's and EA's.

The Brueckner single determinant $|\Phi^B\rangle$ is defined by requiring that the exact wave-function $|\Psi\rangle$ has maximum overlap with $|\Phi^B\rangle$

$$\langle\Psi|\Phi^B\rangle = \max. \tag{4.1}$$

If a reference determinant $|\Phi_0\rangle$ is chosen, then a determinant, different from $|\Phi_0\rangle$, is obtained by rotating the virtual orbitals into the occupied orbitals, represented by the operator $c_i^a\{a^\dagger i\}$, if only linear terms are considered. A general single determinant is then given by

$$|\Phi\rangle = (1 + c_i^a\{a^\dagger i\})|\Phi_0\rangle. \tag{4.2}$$

For the overlap to be maximal, it has to be stationary with respect to the rotation

$$\frac{\partial}{\partial c_i^a}\langle\Psi|(1 + c_i^a\{a^\dagger i\})|\Phi_0\rangle = 0 \quad \forall i, a, \tag{4.3}$$

which leads to

$$\langle\Psi|\Phi_i^a\rangle = 0 \quad \forall i, a. \tag{4.4}$$

If the orbital rotation is allowed to contribute beyond linear terms, then, according to the Thouless parameterization [120], any two nonorthogonal Slater determinants, within a given basis, are related by the transformation

$$|\Phi\rangle = e^{T_1}|\Phi_0\rangle, \tag{4.5}$$

with T_1 given in Eq. 3.9. For the overlap to be maximal, all T_1 amplitudes have to vanish, meaning that all effects of e^{T_1} must vanish as well, which is the difference between the Brueckner coupled-cluster method and the configuration interaction based Brueckner method.

In the Brueckner CC method the T_1 amplitudes can be rotated away iteratively[45, 46]. Solving first the coupled-cluster equations, the T_1 amplitudes are used to transform the orbitals, which give new integrals, with which a new coupled-cluster calculation is performed, yielding new T_1 amplitudes. The resulting T_1 amplitudes are used again to transform the orbitals. The procedure is repeated until the T_1 amplitudes reach a cut off. The orbitals of the last transformation are then the Brueckner orbitals.

Alternatively, a Brueckner effective Hamiltonian can be defined, as for instance by Scuseria [49, 50], who constructed an effective Hamiltonian by requiring that the coupled-cluster energy can be reproduced as a sum of expectation values of single-particle operators. If the truncation level of the coupled-cluster wave-function is chosen to be $T = T_1 + T_2$, and assuming the Brueckner condition $T_1 = 0$, the total energy is the sum of the reference energy and the correlation energy, Eq. 3.23,

$$E = E_0 + \Delta E_{CCSD} = \sum_i \langle i|h|i\rangle + \frac{1}{2}\sum_{i,j}\langle ij||ij\rangle + \frac{1}{4}\sum_{ijab}\langle ij||ab\rangle t_{ij}^{ab}. \tag{4.6}$$

The total energy can be rewritten as

$$E = \frac{1}{2}\sum_i (\langle i|h|i\rangle + F_{ii}), \tag{4.7}$$

Figure 4–1. Occupied-occupied block of the brueckner Hamiltonian

Figure 4–2. Virtual-virtual block of the brueckner Hamiltonian

which defines the Brueckner effective Hamiltonian for the occupied-occupied block,

$$F_{ij} = f_{ij} + \frac{1}{2}\sum_{kab}\langle ik||ab\rangle t_{jk}^{ab}, \tag{4.8}$$

where f_{ij} is the Fock matrix element. Particle-hole symmetry arguments lead then to the definition of the effective Hamiltonian in the virtual-virtual block

$$F_{ab} = f_{ab} - \frac{1}{2}\sum_{ijc}\langle ij||bc\rangle t_{ij}^{ac}, \tag{4.9}$$

The occupied-virtual block is chosen to be the T_1 equation, Fig. 3–5, where terms involving the T_1 amplitudes are zero

$$F_{ia} = f_{ia} + \sum_{jb} f_{jb}t_{ij}^{ab} + \frac{1}{2}\sum_{jbc}\langle aj||bc\rangle - \frac{1}{2}\sum_{jkb}\langle jk||ib\rangle t_{jk}^{ab}. \tag{4.10}$$

Convergence of the Brueckner coupled-cluster equations therefore enforces $t_i^a = F_{ia} = 0$. The different blocks of the Brueckner Hamiltonian are diagrammatically given in Fig. 4–1, in Fig. 4–2, and in Fig. 4–3. The equation for the T_2 amplitudes were given diagrammatically in Fig. 3–6, Fig. 3–7, and Fig. 3–8, where now all diagrams containing a T_1 amplitude are zero.

A calculation can be performed by starting with a set of T_2 amplitudes, from which the Brueckner Hamiltonian is constructed. It is then diagonalized to obtain

Figure 4–3. Occupied-virtual block of the brueckner Hamiltonian

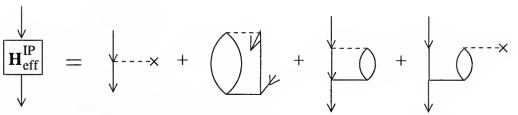

Figure 4–4. Effective Hamiltonian in the IP sector for the FS-CCSD method with $T_1 = 0$

a new set of orbitals, which define new integrals, which are used to calculate new T_2 amplitudes. The procedure is repeated until self-consistency.

However, instead of requiring that the couple-cluster energy can be reproduced,one can choose to employ an effective Hamiltonian, which yields the IP's and EA's as the negative of the eigenvalues. A correlation potential for the occupied-occupied block, Fig. 3–15, and for the virtual-virtual block, Fig. 3–16, were defined in the previous chapter, which does just that, if the Hartree-Fock terms are added. If the Brueckner condition is superimposed ($T_1 = 0$), the diagrams for the occupied-occupied and the virtual-virtual block of the effective Hamiltonian are given in Fig. 4–4 and Fig. 4–5, which contain Fock space amplitudes. Comparing those to Fig. 4–1 and to Fig. 4–2 shows that the difference lies in the last two diagrams in Fig. 4–4 and Fig. 4–5. If the coupled-cluster amplitudes and the Fock space amplitudes are given, the effective Hamiltonian, defined by Fig. 4–3, Fig. 4–4, and Fig. 4–5, yields Brueckner orbitals and exact FS-CC IP's and EA's as eigenvalues.

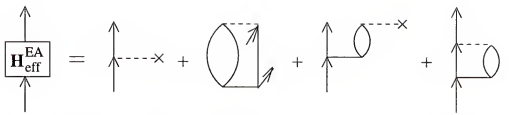

Figure 4–5. Effective Hamiltonian in the EA sector for the FS-CCSD method with $T_1 = 0$

4.2 Second-Order Brueckner Hamiltonian Yielding Second-Order IP's and EA's

In this section the Brueckner Hamiltonian yielding FS-CC IP's and EA's is expressed up to second order in perturbation, which yields second-order Brueckner orbitals as eigenfunctions and IP's and EA's, which are correct through second order as eigenvalues. Lindgren and Salomonson [51, 119] derived a second-order Brueckner potential, yielding correct second-order IP's and EA's, by minimizing the energy expectation value with respect to the partitioning of the Hamiltonian.

In order to derive a second-order Brueckner potential, the Hamiltonian has to be partitioned into an unperturbed part and a perturbation. The Hamiltonian in second quantization was given in Eq. 2.111

$$H = \sum_{pq} h_{pq} p^\dagger q + \frac{1}{4} \sum_{pqrs} \langle pq||rs\rangle p^\dagger q^\dagger sr. \tag{4.11}$$

A symmetric one-electron operator

$$U = \sum_{pq} u_{pq} p^\dagger q \tag{4.12}$$

can be added and subtracted to give

$$H = (H_1 + U) - U + H_2 = F - U + H_2, \tag{4.13}$$

where H_1 is the one-electron part and H_2 is the two-electron part of the Hamiltonian in Eq. 4.11. F is given by

$$F = H_1 + U = \sum_{pq}(h_{pq} + u_{pq})p^\dagger q = \sum_{pq} f_{pq}p^\dagger q, \tag{4.14}$$

where $f = h + u$. u is arbitrary but chosen to be

$$u = \sum_i (J_i - K_i), \tag{4.15}$$

so that

$$u_{pq} = \sum_i \langle pi||qi\rangle. \tag{4.16}$$

The coulomb and exchange operators are defined by

$$J_i(1)\phi(1) = \langle\psi_i(2)|\frac{1}{r_{12}}|\psi_i(2)\rangle\phi(1) \tag{4.17}$$

$$K_i(1)\phi(1) = \langle\psi_i(2)|\frac{1}{r_{12}}|\phi(2)\rangle\psi_i(1), \tag{4.18}$$

where it is integrated over the coordinates of electron 2 only. This definition does not restrict the orbitals to be Hartree-Fock orbitals. However, if Hartree-Fock orbitals are used, this choice makes the operator F equal to the Fock operator, in which case (canonical) $f_{pq} = 0$ for $p \neq q$. In general F is nondiagonal, with $f_{pq} \neq 0$.

In order to define the unperturbed Hamiltonian H_0, F is split into diagonal and off-diagonal parts

$$F = F^d + F^o. \tag{4.19}$$

The diagonal and off-diagonal parts are given by

$$F^d = \sum_p f^d_{pp}p^\dagger p \tag{4.20}$$

$$F^o = \sum_{p\neq q} f^o_{pq}p^\dagger q. \tag{4.21}$$

With these definitions the Hamiltonian takes the form

$$H = \sum_p f^d_{pp} p^\dagger p + \sum_{pq} (f^o_{pq} - u_{pq}) p^\dagger q + \frac{1}{4} \sum_{pqrs} \langle pq||rs\rangle p^\dagger q^\dagger sr = H_0 + V, \tag{4.22}$$

where

$$H_0 = F^d = \sum_p f^d_{pp} p^\dagger p \tag{4.23}$$

$$V = F^o - U + H_2 = \sum_{pq} (f^o_{pq} - u_{pq}) p^\dagger q + \frac{1}{4} \sum_{pqrs} \langle pq||rs\rangle p^\dagger q^\dagger sr. \tag{4.24}$$

Normal-ordered operators can be introduced by applying Wick's theorem, Section 3.1.1, which leads for the zero-order part to

$$\begin{aligned} H_0 &= \sum_p f^d_{pp} p^\dagger p = \sum_p f^d_{pp} \{p^\dagger p\} + \sum_i \epsilon_i \\ (H_0)_N &= H_0 - E^{(0)} = \sum_p f^d_{pp} \{p^\dagger p\}, \end{aligned} \tag{4.25}$$

where $E^{(0)} = \sum_i \epsilon_i$. The perturbation part, Eq. 4.24, gives

$$\begin{aligned} V &= \sum_{pq} (f^o_{pq} - u_{pq}) \{p^\dagger q\} - \sum_i u_{ii} + \frac{1}{4} \sum_{pqrs} \langle pq||rs\rangle \{p^\dagger q^\dagger sr\} \\ &+ \sum_{pq} \sum_i \langle pi||qi\rangle \{p^\dagger q\} + \frac{1}{2} \sum_{ij} \langle ij||ij\rangle \\ V &= F^o_N - U_N + W_N + U_N + \langle \Phi_0|V|\Phi_0\rangle \\ V &= F^o_N + W_N + \langle \Phi_0|V|\Phi_0\rangle, \end{aligned} \tag{4.26}$$

where

$$F^o_N = \sum_{pq} f^o_{pq} \{p^\dagger q\} \tag{4.27}$$

$$U_N = \sum_{pq} u_{pq} \{p^\dagger q\} = \sum_{pq} \sum_i \langle pi||qi\rangle \{p^\dagger q\} \tag{4.28}$$

$$W_N = \frac{1}{4} \sum_{pqrs} \langle pq||rs\rangle \{p^\dagger q^\dagger sr\} \tag{4.29}$$

$$\langle \Phi_0|V|\Phi_0\rangle = -\sum_i u_{ii} + \frac{1}{2} \sum_{ij} \langle ij||ij\rangle. \tag{4.30}$$

The normal-ordered perturbation operator is then

$$\begin{aligned} V_N &= V - \langle \Phi_0 | V | \Phi_0 \rangle \\ &= F_N^o + W_N \\ &= \sum_{p \neq q} f_{pq} \{ p^\dagger q \} + \frac{1}{4} \sum_{pqrs} \langle pq || rs \rangle \{ p^\dagger q^\dagger sr \}. \end{aligned} \tag{4.31}$$

The particular partitioning of the Hamiltonian, defined in Eq. 4.25 and Eq. 4.31, is referred to as partitioning I. Diagrammatically the operators F_N and W_N were given in Fig. 3–1 and Fig. 3–2. In order to express the effective Hamiltonian, defined in Fig. 4–3, Fig. 4–4, and Fig. 4–5, up to second-order in perturbation, all diagrams have to be collected that contain up to two vertices. Expressing the T_1 equation up to second order, ensures that the sum $T_1^{(1+2)} = T_1^{(1)} + T_1^{(2)} = 0$. The individual terms are not necessarily zero, and terms containing $T_1^{(1)}$ have to be included, even though terms that contain T_1 disappear in the infinite-order expressions.

The virtual-occupied block of the second-order effective Hamiltonian for partitioning I is given in Fig. 4–6. The horizontal lines symbolize the denominators. The algebraic interpretation of the diagrams can be found in Table 4–1. For closed-shell systems, the spin-restricted form can be used, which is obtained by spin integration. Since the $\alpha\alpha$ effective Hamiltonian is equivalent to the $\beta\beta$ effective Hamiltonian, only one of them needs to be constructed. The spin-restricted expressions can be found in Table 4–1 as well, where capital letters refer to spatial-orbital indices. Note that the occupied-virtual block is defined as the adjoint of the virtual-occupied block.

The occupied-occupied and virtual-virtual block of the effective Hamiltonian are derived by expanding the amplitudes in Fig. 3–15 and Fig. 3–16 in orders of perturbation. The terms up to second order are identified as the Fock matrix elements and all diagrams that contain two interaction vertices. The resulting diagrams are given in Fig. 4–7 and Fig. 4–8. Table 4–2 and Table 4–3 contain the algebraic expressions of the diagrams. With the exception of the diagrams I and III

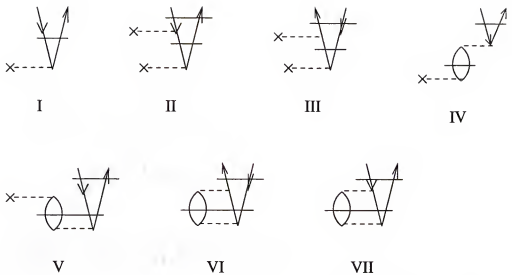

Figure 4–6. Occupied-virtual block of the second-order effective Hamiltonian, partitioning I

in Fig. 4–7 and Fig. 4–8, all other diagrams have a nonhermitian contribution. In order to obtain a hermitian effective Hamiltonian, each term is multiplied by $\frac{1}{2}$, and the corresponding term, where i and j and a and b respectively are exchanged, is added. Table 4–2 and Table 4–3 also show the spin-integrated expressions.

The second-order Brueckner Hamiltonian according to partitioning I, defined in Fig. 4–6, Fig. 4–7, and Fig. 4–8, is the same as the effective Hamiltonian Lindgren and Salomonson [51, 119] derived by minimizing the energy expectation value with respect to the partitioning of the Hamiltonian.

However, if the Hamiltonian is partitioned according to Eq. 4.25 and Eq. 4.31 (partitioning I), then $(H_0)_N$ is not invariant with respect to a transformation of the orbitals within the occupied or the virtual space; a necessity for any consistent theory of electron correlation. If the Hamiltonian is partitioned, so that the occupied-occupied and the virtual-virtual off-diagonal Fock matrix elements are part of the unperturbed Hamiltonian $(H_0)_N$, and not V_N, as in partitioning I, $(H_0)_N$ is invariant

Table 4–1. Algebraic interpretation of the diagrams in Fig. 4–6

	spin orbital expressions	spatial orbital expressions
I	$\frac{f_{ai}}{f_{ii}-f_{aa}}$	$\frac{f_{AI}}{f_{II}-f_{AA}}$
II	$\sum_{b\neq a}\frac{f_{ab}f_{bi}}{(f_{ii}-f_{bb})(f_{ii}-f_{aa})}$	$\sum_{B\neq A}\frac{f_{AB}f_{BI}}{(f_{II}-f_{BB})(f_{II}-f_{AA})}$
III	$-\sum_{j\neq i}\frac{f_{ji}f_{aj}}{(f_{ii}-f_{aa})(f_{jj}-f_{aa})}$	$-\sum_{J\neq I}\frac{f_{JI}f_{AJ}}{(f_{II}-f_{AA})(f_{JJ}-f_{AA})}$
IV	$\sum_{jb}\frac{\langle ja\|\|bi\rangle f_{bj}}{(f_{jj}-f_{bb})(f_{ii}-f_{aa})}$	$\sum_{JB}\frac{(2\langle JA\|BI\rangle-\langle JA\|IB\rangle)f_{BJ}}{(f_{JJ}-f_{BB})(f_{II}-f_{AA})}$
V	$\sum_{jb}\frac{\langle ab\|\|ij\rangle f_{jb}}{(f_{ii}+f_{jj}-f_{aa}-f_{bb})(f_{ii}-f_{aa})}$	$\sum_{JB}\frac{(2\langle AB\|IJ\rangle-\langle AB\|JI\rangle)f_{JB}}{(f_{II}+f_{JJ}-f_{AA}-f_{BB})(f_{II}-f_{AA})}$
VI	$-\frac{1}{2}\sum_{jkb}\frac{\langle jk\|\|ib\rangle\langle ab\|\|jk\rangle}{(f_{ii}+f_{kk}-f_{aa}-f_{bb})(f_{ii}-f_{aa})}$	$-\frac{1}{2}\sum_{JKB}\left[\frac{(2\langle JK\|IB\rangle-\langle JK\|BI\rangle)\langle AB\|JK\rangle}{(f_{II}+f_{KK}-f_{AA}-f_{BB})(f_{II}-f_{AA})}\right.$ $\left.+\frac{(2\langle JK\|BI\rangle-\langle JK\|IB\rangle)\langle AB\|KJ\rangle}{(f_{II}+f_{KK}-f_{AA}-f_{BB})(f_{II}-f_{AA})}\right]$
VII	$\frac{1}{2}\sum_{jbc}\frac{\langle aj\|\|bc\rangle\langle bc\|\|ij\rangle}{(f_{ii}+f_{jj}-f_{bb}-f_{cc})(f_{ii}-f_{aa})}$	$\frac{1}{2}\sum_{jbc}\left[\frac{(2\langle AJ\|BC\rangle-\langle AJ\|CB\rangle)\langle BC\|IJ\rangle}{(f_{II}+f_{JJ}-f_{BB}-f_{CC})(f_{II}-f_{AA})}\right.$ $\left.+\frac{(2\langle AJ\|CB\rangle-\langle AJ\|BC\rangle)\langle BC\|JI\rangle}{(f_{II}+f_{JJ}-f_{BB}-f_{CC})(f_{II}-f_{AA})}\right]$

to an orbital transformation within those subspaces. Partitioning II is given by

$$(H_0)_N = F^d = \sum_p f^d_{pp}\{p^\dagger p\} + \sum_{p,q\in occ} f^o_{pq}\{p^\dagger q\} + \sum_{p,q\in vir} f^o_{pq}\{p^\dagger q\} \qquad (4.32)$$

$$V_N = {\sum_{p,q}}' f^o_{pq}\{p^\dagger q\} + \frac{1}{4}\sum_{pqrs}\langle pq||rs\rangle\{p^\dagger q^\dagger sr\}. \qquad (4.33)$$

The prime in the sum means, that if p is an index of an occupied orbital, then q is an index of a virtual orbital, and if p is an index of a virtual orbital, then q is an index of an occupied orbital.

Since the off-diagonal f_{ij} and f_{ab} elements are included to *all orders* in the unperturbed Hamiltonian in partitioning II, the counting of orders becomes slightly different. Diagram II in Fig. 4–6, diagram III in Fig. 4–7 and Fig. 4–8 are first-order diagrams for partitioning II, instead of second-order diagrams for partitioning I. Partitioning II also implies, that a first-order in V_N solution for the amplitudes, which includes the off-diagonal f_{ij} and f_{ab} elements to infinite-order, has to be

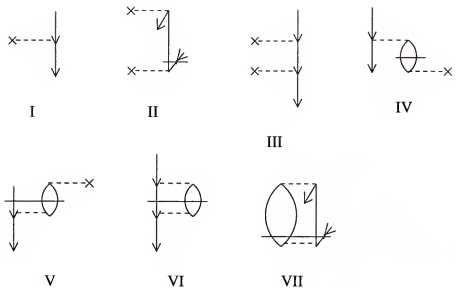

Figure 4–7. Occupied-occupied block of the second-order effective Hamiltonian, partitioning I

found, before the second-order terms can be built. Fig. 4–9 shows the iterative equations for the first-order single excitation and double excitation amplitudes. The algebraic interpretation can be found in Table 4–4, together with the spin-integrated expressions. For the $T_2^{(1)}$ amplitudes, the permutation of i and j in diagram V and a and b in diagram VI has to be taken into account. Table 4–4 therefore shows two terms for diagram V and two terms for diagram VI. The spin integration of the $T_1^{(1)}$ amplitudes is similar to the spin integration of the effective Hamiltonian, only the $\alpha\alpha$ part needs to be considered. The spin integration of the doubly excited amplitudes leads to two different types of amplitudes: $\alpha\alpha\alpha\alpha$, denoted by $T_2^{(1)}$, and $\alpha\alpha\beta\beta$, denoted by $[T_2^{(1)}]'$, which are iterated separately. For simplicity, the superscript (1) is omitted in the algebraic expressions.

Fig. 4–10 shows the virtual-occupied block of the second-order effective Hamiltonian, employing partitioning II in terms of the first-order amplitudes. The occupied-virtual block is again its adjoint. The interpretation of the diagrams in spin-orbital and spin-integrated form is given in Table 4–5.

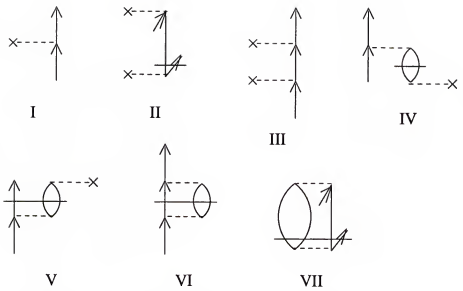

Figure 4–8. Virtual-virtual block of the second-order effective Hamiltonian, partitioning I

In principle, the first-order Fock space amplitudes should be iterated to include all zeroth-order terms, as has been done for the coupled-cluster amplitudes. However, since the $T_2^{(1)}$ does not change significantly during the iteration, the first-order Fock space amplitudes are simply given as in Fig. 4–11, with the algebraic interpretation in Table 4–6. The spin integration leads, as for the $T_2^{(1)}$ amplitudes, to two different types of Fock space amplitudes: $S_2^{(1)}$ denotes the $\alpha\alpha\alpha\alpha$ spin case and $[S_2^{(1)}]'$ denotes the $\alpha\alpha\beta\beta$ spin case.

Fig. 4–12 shows the occupied-occupied block of the second-order Hamiltonian according to partitioning II, Fig. 4–13 shows the virtual-virtual block. The algebraic interpretations are given in Table 4–7 and Table 4–8 in the spin-orbital and the spin-integrated from. In order to obtain an hermitian effective Hamiltonian, each diagram, except diagram I, in Fig. 4–12 and Fig. 4–13 is multiplied by a factor of one half, and the diagram, in which i and j and a and b respectively is exchanged, is added.

Table 4–2. Algebraic interpretation of the diagrams in Fig. 4–7

	spin orbital expressions	spatial orbital expressions
I	f_{ij}	f_{IJ}
II	$\sum_a \frac{f_{ia}f_{aj}}{f_{jj}-f_{aa}}$	$\sum_A \frac{f_{IA}f_{AJ}}{f_{JJ}-f_{AA}}$
III	$-\sum_{k\neq i,j} f_{ik}f_{kj}$	$-\sum_{K\neq I,J} f_{IK}f_{KJ}$
IV	$\sum_{ka} \frac{\langle ik\|\|ja\rangle f_{ak}}{f_{kk}-f_{aa}}$	$\sum_{KA} \frac{(2\langle IK\|JA\rangle-\langle IK\|AJ\rangle)f_{AK}}{f_{KK}-f_{AA}}$
V	$\sum_{ka} \frac{\langle ia\|\|jk\rangle f_{ka}}{f_{kk}+f_{jj}-f_{aa}-f_{ii}}$	$\sum_{KA} \frac{(2\langle IA\|JK\rangle-\langle IA\|KJ\rangle)f_{KA}}{f_{KK}+f_{JJ}-f_{AA}-f_{II}}$
VI	$-\frac{1}{2}\sum_{kla} \frac{\langle kl\|\|ja\rangle\langle ia\|\|kl\rangle}{f_{kk}+f_{ll}-f_{aa}-f_{ii}}$	$-\frac{1}{2}\sum_{KLA}\left[\frac{(2\langle KL\|JA\rangle-\langle KL\|AJ\rangle)\langle IA\|KL\rangle}{f_{KK}+f_{LL}-f_{AA}-f_{II}}\right.$ $\left.+\frac{(2\langle KL\|AJ\rangle-\langle KL\|JA\rangle)\langle IA\|LK\rangle}{f_{KK}+f_{LL}-f_{AA}-f_{II}}\right]$
VII	$\frac{1}{2}\sum_{kab} \frac{\langle ki\|\|ba\rangle\langle ba\|\|kj\rangle}{f_{kk}+f_{jj}-f_{aa}-f_{bb}}$	$\frac{1}{2}\sum_{KAB}\left[\frac{(2\langle KI\|BA\rangle-\langle KI\|AB\rangle)\langle BA\|KJ\rangle}{f_{KK}+f_{JJ}-f_{AA}-f_{BB}}\right.$ $\left.+\frac{(2\langle KI\|AB\rangle-\langle KI\|BA\rangle)\langle BA\|JK\rangle}{f_{KK}+f_{JJ}-f_{AA}-f_{BB}}\right]$

Depending on the choice of the partitioning of the Hamiltonian, two second-order effective Hamiltonians were derived. Its eigenfunctions are second-order Brueckner orbitals and its eigenvalues are the negative of the ionization potentials and electron affinities, correct through second-order

$$\mathbf{H}^{(2)}_{eff}\mathbf{C}^{(2)} = \mathbf{C}^{(2)}\boldsymbol{\varepsilon}^{(2)} \tag{4.34}$$

The effective Hamiltonian depends on the orbitals, which leads to an iterative scheme. Starting with Hartree-Fock orbitals, the effective Hamiltonian is built and diagonalized. The new orbitals are used to build new integrals and a new Fock matrix, with which a new effective Hamiltonian is built. Its eigenfunctions are again used to transform the integrals and to build a Fock matrix. The procedure is repeated until self-consistency.

Table 4–3. Algebraic interpretation of the diagrams in Fig. 4–8

	spin orbital expressions	spatial orbital expressions
I	f_{ab}	f_{AB}
II	$-\sum_i \frac{f_{ai}f_{ib}}{f_{ii}-f_{aa}}$	$-\sum_I \frac{f_{AI}f_{IB}}{f_{II}-f_{AA}}$
III	$\sum_{c\neq a,b} f_{ac}f_{cb}$	$\sum_{C\neq A,B} f_{AC}f_{CB}$
IV	$\sum_{ic} \frac{\langle ai\|\|bc\rangle f_{ci}}{f_{ii}-f_{cc}}$	$\sum_{IC} \frac{(2\langle AI\|BC\rangle-\langle AI\|CB\rangle)f_{CI}}{f_{II}-f_{CC}}$
V	$\sum_{ic} \frac{\langle ac\|\|bi\rangle f_{ci}}{f_{ii}+f_{bb}-f_{aa}-f_{cc}}$	$\sum_{IC} \frac{(2\langle AC\|BI\rangle-\langle AC\|IB\rangle)f_{CI}}{f_{II}+f_{BB}-f_{AA}-f_{CC}}$
VI	$\frac{1}{2}\sum_{icd} \frac{\langle ai\|\|cd\rangle\langle cd\|\|bi\rangle}{f_{ii}+f_{bb}-f_{cc}-f_{dd}}$	$\frac{1}{2}\sum_{ICD}\left[\frac{(2\langle AI\|CD\rangle-\langle AI\|DC\rangle)\langle CD\|BI\rangle}{f_{II}+f_{BB}-f_{CC}-f_{DD}}\right.$ $\left.+\frac{(2\langle AI\|DC\rangle-\langle AI\|CD\rangle)\langle CD\|IB\rangle}{f_{II}+f_{BB}-f_{CC}-f_{DD}}\right]$
VII	$-\frac{1}{2}\sum_{ijc} \frac{\langle ji\|\|ca\rangle\langle cb\|\|ji\rangle}{f_{ii}+f_{jj}-f_{cc}-f_{bb}}$	$-\frac{1}{2}\sum_{IJC}\left[\frac{(2\langle JI\|CA\rangle-\langle JI\|AC\rangle)\langle CB\|JI\rangle}{f_{II}+f_{JJ}-f_{CC}-f_{BB}}\right.$ $\left.+\frac{(2\langle JI\|AC\rangle-\langle JI\|CA\rangle)\langle CB\|IJ\rangle}{f_{II}+f_{JJ}-f_{CC}-f_{BB}}\right]$

4.3 Numerical Results

In the previous section it was shown, how to obtain second-order Brueckner Hamiltonians, which yield second-order IP's and EA's, according to two different partitioning schemes. For practical reasons, the second-order CIP model is implemented slightly differently. Since the Brueckner condition defines the orbitals, and diagonalization of the occupied-occupied and the virtual-virtual block is merely a unitary transformation of the orbitals, the procedure is implemented in a two-step scheme. First, the second-order Brueckner orbitals are determined iteratively, second, the occupied-occupied and the virtual-virtual blocks of the effective Hamiltonians are built with the previously obtained orbitals. Diagonalization yields then the second-order IP's and EA's.

For partitioning I the orbital determination consist of the following steps:

1. transformation of the one-electron integrals
2. transformation of the two-electron integrals

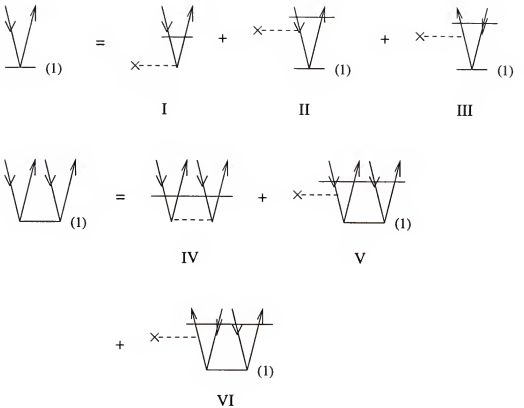

Figure 4–9. Iterative equations of the first-order single and double excitation amplitudes, partitioning II

3. construction of the Fock matrix
4. construction of the second-order $T_1^{(2)}$ amplitudes, as given in Fig. 4–6 and Table 4–1
5. rotation of the orbitals
6. check if the orbitals are converged; if yes, stop; if no, go back to 1.

For partitioning II the orbital determination is slightly different, since the first-order amplitudes have to be determined iteratively as well:

1. transformation of the one-electron integrals
2. transformation of the two-electron integrals
3. construction of the Fock matrix
4. iteration of the first-order $T_1^{(1)}$ amplitudes, according to Fig. 4–9 and Table 4–4

Table 4–4. Algebraic interpretation of the diagrams in Fig. 4–9

	spin orbital expressions	spatial orbital expressions
I	$\frac{f_{ai}}{f_{ii}-f_{aa}}$	$\frac{f_{AI}}{f_{II}-f_{AA}}$
II	$-\sum_{j\neq i}\frac{f_{aj}f_{ji}}{f_{ii}-f_{aa}}t_j^a$	$-\sum_{J\neq I}\frac{f_{AJ}f_{JI}}{f_{II}-f_{AA}}t_J^A$
III	$\sum_{b\neq a}\frac{f_{ab}f_{bi}}{f_{ii}-f_{aa}}t_j^b$	$\sum_{B\neq A}\frac{f_{AB}f_{BI}}{f_{II}-f_{AA}}t_J^B$
IV	$\frac{\langle ab\|ij\rangle}{f_{ii}+f_{jj}-f_{aa}-f_{bb}}$	$T_2^{(1)}$: $\frac{(AB\|IJ)-\langle AB\|JI\rangle}{f_{II}+f_{JJ}-f_{AA}-f_{BB}}$
		$[T_2^{(1)}]'$: $\frac{(AB\|IJ\rangle}{f_{II}+f_{JJ}-f_{AA}-f_{BB}}$
V	$-\sum_{k\neq j}\frac{f_{kj}}{f_{ii}+f_{jj}-f_{aa}-f_{bb}}t_{ik}^{ab}$	$T_2^{(1)}$:$-\sum_{K\neq J}\frac{f_{KJ}}{f_{II}+f_{JJ}-f_{AA}-f_{BB}}t_{IK}^{AB}$
		$[T_2^{(1)}]' = T_2^{(1)}$
	$\sum_{k\neq i}\frac{f_{ki}}{f_{ii}+f_{jj}-f_{aa}-f_{bb}}t_{jk}^{ab}$	$T_2^{(1)}$:$\sum_{K\neq I}\frac{f_{KI}}{f_{II}+f_{JJ}-f_{AA}-f_{BB}}t_{JK}^{AB}$
		$[T_2^{(1)}]' = 0$
VI	$\sum_{c\neq b}\frac{f_{bc}}{f_{ii}+f_{jj}-f_{aa}-f_{bb}}t_{ij}^{ac}$	$T_2^{(1)}$:$\sum_{C\neq B}\frac{f_{BC}}{f_{II}+f_{JJ}-f_{AA}-f_{BB}}t_{IJ}^{AC}$
		$[T_2^{(1)}]' = T_2^{(1)}$
	$-\sum_{c\neq a}\frac{f_{ac}}{f_{ii}+f_{jj}-f_{aa}-f_{bb}}t_{ij}^{bc}$	$T_2^{(1)}$:$-\sum_{C\neq A}\frac{f_{AC}}{f_{II}+f_{JJ}-f_{AA}-f_{BB}}t_{IJ}^{BC}$
		$[T_2^{(1)}]' = 0$

5. iteration of the first-order $T_2^{(1)}$ amplitudes for the $\alpha\alpha\alpha\alpha$ spin case, according to Fig. 4–9 and Table 4–4
6. iteration of the first-order $[T_2^{(1)}]'$ amplitudes for the $\alpha\alpha\beta\beta$ spin case, according to Fig. 4–9 and Table 4–4
7. construction of the second-order $T_1^{(2)}$ amplitudes, as given in Fig. 4–10 and Table 4–5
8. rotation of the orbitals
9. check if the orbitals are converged; if yes, stop; if no, go back to 1.

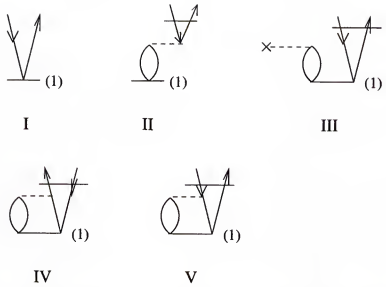

Figure 4–10. Virtual-occupied block of the second-order effective Hamiltonian, partitioning II

The orbital rotation step is carried out in such a way, that the new occupied orbitals i' are orthogonal to the new virtual orbitals a'

$$\begin{aligned} |i'\rangle &= |i\rangle + \sum_a t_i^a |a\rangle \\ |a'\rangle &= |a\rangle - \sum_i t_i^a |i\rangle. \end{aligned} \tag{4.35}$$

However, the occupied orbitals and the virtual orbitals are not orthogonal among themselves. To obtain orthogonal orbitals m'', the orbitals n' are transformed, according to

$$|m''\rangle = \sum_n X_{nm} |n'\rangle, \tag{4.36}$$

where $\mathbf{X} = \mathbf{S}^{-\frac{1}{2}}$, and $\mathbf{S}$ is the overlap matrix $\mathbf{S} = (\mathbf{C}')^\dagger \mathbf{C}'$. It can be easily verified, that this transformation indeed orthogonalizes the orbitals

$$\begin{aligned} (\mathbf{C}'')^\dagger \mathbf{C}'' &= \left(\mathbf{C}'\mathbf{S}^{-\frac{1}{2}}\right)^\dagger \mathbf{C}'\mathbf{S}^{-\frac{1}{2}} \\ \mathbf{S}^{-\frac{1}{2}} (\mathbf{C}')^\dagger \mathbf{C}' \mathbf{S}^{-\frac{1}{2}} &= \mathbf{S}^{-\frac{1}{2}} \mathbf{S} \mathbf{S}^{-\frac{1}{2}} = \mathbf{1}. \end{aligned} \tag{4.37}$$

Table 4–5. Algebraic interpretation of the diagrams in Fig. 4–10

	spin orbital expressions	spatial orbital expressions
I	t_i^a	t_I^A
II	$\sum_{jb} \frac{\langle ja\|\|bi\rangle}{f_{ii}-f_{aa}} t_j^b$	$\sum_{JB} \frac{(2\langle JA\|BI\rangle - \langle JA\|IB\rangle}{f_{II}-f_{AA}} t_J^B$
III	$\sum_{jb} \frac{f_{jb}}{f_{ii}-f_{aa}} t_{ij}^{ab}$	$\sum_{JB} \frac{f_{JB}}{f_{II}-f_{AA}} \left(t_{IJ}^{AB} + [t_{IJ}^{AB}]'\right)$
IV	$\frac{1}{2}\sum_{jbc} \frac{\langle aj\|\|cb\rangle}{f_{ii}-f_{aa}} t_{ij}^{cb}$	$\frac{1}{2}\sum_{JBC} \left[\frac{\langle AJ\|CB\rangle}{f_{II}-f_{AA}} \left(t_{IJ}^{CB} + [t_{IJ}^{CB}]'\right)\right.$
		$\left. + \frac{\langle AJ\|BC\rangle}{f_{II}-f_{AA}} \left(t_{JI}^{CB} + [t_{JI}^{CB}]'\right)\right]$
v	$-\frac{1}{2}\sum_{jkb} \frac{\langle jk\|\|ib\rangle}{f_{ii}-f_{aa}} t_{jk}^{ab}$	$-\frac{1}{2}\sum_{JKB} \left[\frac{\langle JK\|IB\rangle}{f_{II}-f_{AA}} \left(t_{JK}^{AB} + [t_{JK}^{AB}]'\right)\right.$
		$\left. \frac{\langle JK\|BI\rangle}{f_{II}-f_{AA}} \left(t_{KJ}^{AB} + [t_{KJ}^{AB}]'\right)\right]$

As a measurement of the quality of the orbitals, the calculation of the dipole moment is chosen, Section 3.4.3. In Table 4–9 the dipole moments of some sample molecules are given. For comparison, the dipole moments obtained from the Hartree-Fock, the MBPT(2), and the CCSD density matrices are included, together with the results, obtained from the second-order Brueckner orbitals, when partitioning I and partitioning II is used, as well as the results after the first step of the iteration, which is the same for partitioning I and II, indicated by nonit. The DZP basis set was used for all calculations. The geometry of the molecules was optimized at the MBPT(2)/DZP level of theory.

Fig. 4–14 shows the differences of the CCSD dipole moments to the dipole moments, obtained from the other methods, included in Table 4–9. The dipole moments, obtained from the Brueckner determinant, are closest to the CCSD results. The second-order Brueckner approximations are a significant improvement over Hartree-Fock, and close, but somewhat worse, than the MBPT(2) results. This is not surprising, since in the MBPT(2) method the dipole moments are calculated from a second-order correlated density matrix, whereas in the second-order

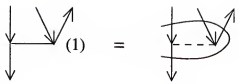

I

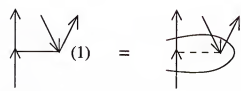

II

Figure 4–11. first-order Fock space amplitudes, partitioning II

Table 4–6. Algebraic interpretation of the diagrams in Fig. 4–11

	spin orbital expressions	spatial orbital expressions
I	$\frac{\langle ia\|\|jk\rangle}{f_{jj}+f_{kk}-f_{aa}-f_{ii}}$	$S_2^{(1)}$: $\frac{\langle IA\|JK\rangle-\langle IA\|KJ\rangle}{f_{JJ}+f_{KK}-f_{AA}-f_{II}}$
		$[S_2^{(1)}]'$: $\frac{\langle IA\|KJ\rangle}{f_{JJ}+f_{KK}-f_{AA}-f_{II}}$
II	$\frac{\langle ac\|\|bi\rangle}{f_{ii}+f_{bb}-f_{aa}-f_{cc}}$	$S_2^{(1)}$: $\frac{\langle AC\|BI\rangle-\langle AC\|IB\rangle}{f_{II}+f_{BB}-f_{AA}-f_{CC}}$
		$[S_2^{(1)}]'$: $\frac{\langle AC\|BI\rangle}{f_{II}+f_{BB}-f_{AA}-f_{CC}}$

Brueckner methods, the 1-particle functions are approximated up to second order in perturbation, and the dipole moments are calculated from an idempotent density matrix. The calculation of the dipole moment of CO is a particular difficult case, and the errors are big compared to the other test cases; but all approximations correctly change the sign of the dipole moment, which is predicted wrong by the Hartree-Fock method. In order to view the differences between the second-order Brueckner approximations better, in Fig. 4–15 the dipole moment differences are given, where CO is taken out, and the Hartree-Fock errors for HCN and H_2CO are

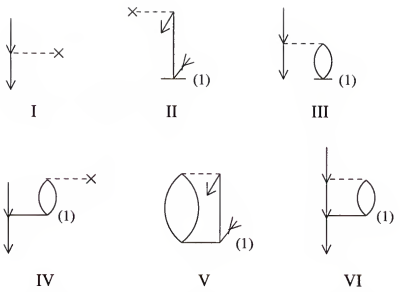

Figure 4–12. Occupied-occupied block of the second-order effective Hamiltonian, partitioning II

cut off at 0.15 Deb. The graph shows, that the second-order Brueckner orbitals, obtained by calculating them from Hartree-Fock orbitals, according to Fig. 4–6 or Fig. 4–10, are close to the iterative solutions. Partitioning II yields usually better results than partitioning I.

After the orbitals are determined, the occupied-occupied and the virtual-virtual blocks of the second-order Brueckner Hamiltonians are built and diagonalized to obtain the negative of the second-order IP's and EA's as eigenvalues. Table 4–10, Table 4–11, Table 4–12, Table 4–13, Table 4–14, Table 4–15, and Table 4–16 show the eigenvalues of the second-order Brueckner Hamiltonians, according to partitioning I and II for some sample molecules. The IP's and EA's in the tables are given in Hartree to avoid numbers with large magnitude. Also included in the tables are the eigenvalues when Hartree-Fock orbitals are used to build the second-order Hamiltonian (nonit.), which is identical for the two partitioning schemes. The eigenvalues are compared to Hartree-Fock values, as well as IP-EOM-CCSD and EA-EOM-CCSD results. The infinite-order EA-EOM-CCSD results are chosen as reference values in

Table 4–7. Algebraic interpretation of the diagrams in Fig. 4–12

	spin orbital expressions	spatial orbital expressions
I	f_{ij}	f_{IJ}
II	$\sum_a f_{aj} t_j^a$	$\sum_A f_{AJ} t_J^A$
III	$\sum_{ka} \langle ik \| ja \rangle t_k^a$	$\sum_{KA} \left(2\langle IK \| JA \rangle - \langle IK \| AJ \rangle\right) t_K^A$
IV	$\sum_{ka} f_{ka} s_{jk}^{ia}$	$\sum_{KA} f_{KA} \left(s_{JK}^{IA} + [s_{JK}^{IA}]'\right)$
V	$\frac{1}{2} \sum_{kab} \langle ki \| ba \rangle t_{kj}^{ba}$	$\frac{1}{2} \sum_{KAB} \left[\langle KI \| BA \rangle \left(t_{KJ}^{BA} + [t_{KJ}^{BA}]'\right) + \langle KI \| AB \rangle \left(t_{JK}^{BA} + [t_{JK}^{BA}]'\right)\right]$
VI	$-\frac{1}{2} \sum_{kla} \langle kl \| ja \rangle s_{kl}^{ia}$	$-\frac{1}{2} \sum_{KLA} \left[\langle KL \| JA \rangle \left(s_{KL}^{IA} + [s_{KL}^{IA}]'\right) + \langle KL \| AJ \rangle \left(s_{LK}^{IA} + [s_{LK}^{IA}]'\right)\right]$

the L^2 space for the second-order approximations, even though we don't claim that those unbound states exist (some might in the continuum). The DZP basis set was used, and the geometries were optimized at the MBPT(2)/DZP level of theory.

In Fig. 4–16, Fig. 4–18, Fig. 4–20 and Fig. 4–22 the differences in eV between the negative of the IP-EOM-CCSD results for the IP's and the eigenvalues of the different independent particle models, included in the tables, for HF, H_2O, NH_3, and CH_4 (Table 4–10, Table 4–11, Table 4–12, Table 4–13) are shown. The core IP's are not given, since the energy differences are relatively large, because of their large absolute values. All energy differences in the graphs are presented in eV (IP's are commonly reported in eV). Fig. 4–17, Fig. 4–19, Fig. 4–21, and Fig. 4–23 show the differences in eV between EA-EOM-CCSD results for the EA's and the eigenvalues of the independent particle models. Each cluster of columns belongs to a particular IP or EA, for which the EOM-CCSD result in eV is given next to the cluster. The first observation to be made, is that the second-order Hamiltonians generally overcorrect Koopmans' values for IP's and EA's. While the eigenvalues of the occupied orbitals

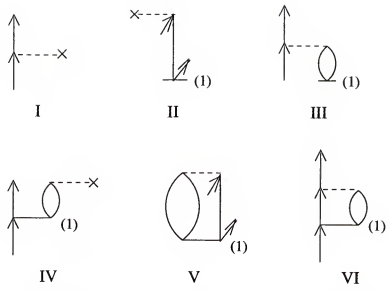

Figure 4–13. Virtual-virtual block of the second-order effective Hamiltonian, partitioning II

are too low and the eigenvalues of the virtual orbitals are too high for the Hartree-Fock model, the second-order Hamiltonians predict eigenvalues for the occupied orbitals that are too high, and for the virtual orbitals that are too low. The second-order approximations for IP's and EA's are often very close. However, for the EA's of H_2O at 5.3 eV and 21.5 eV partitioning I shows particular large deviations from the EA-EOM-CCSD results. A large deviation from the EA-EOM-CCSD result occurs for the noniterative scheme for H_2O at 21.5 eV. The values for IP's and EA's, obtained from partitioning scheme II, are of relatively stable quality and in most cases an improvement over the Hartree-Fock values. In general, the EA's are better described by the second-order approximation than the IP's, compared to the Hartree-Fock values, which is the result of the error cancellation occurring for Koopmans' IP's.

However, the second-order IP's and EA's for CO, H_2CO, and HCN, Table 4–14, Table 4–15, and Table 4–16, are of rather poor quality. It becomes difficult to correlate the second-order values with the EOM-CCSD results, even the wrong

Table 4–8. Algebraic interpretation of the diagrams in Fig. 4–13

	spin orbital expressions	spatial orbital expressions
I	f_{ab}	f_{AB}
II	$-\sum_i f_{ib} t_i^a$	$-\sum_I f_{IB} t_I^A$
III	$\sum_{ic} \langle ai \| bc \rangle t_i^c$	$\sum_{IC} \left(2\langle AI \| BC\rangle - \langle AI \| CB\rangle\right) t_I^C$
IV	$\sum_{ic} f_{ic} s_{bi}^{ac}$	$\sum_{IC} f_{IC} \left(s_{BI}^{AC} + [s_{BI}^{AC}]'\right)$
V	$-\frac{1}{2}\sum_{ijc} \langle ji \| ca\rangle t_{ji}^{cb}$	$-\frac{1}{2}\sum_{IJC} \left[\langle JI \| CA\rangle \left(t_{JI}^{CB} + [t_{JI}^{CB}]'\right) + \langle JI \| AC\rangle \left(t_{IJ}^{CB} + [t_{IJ}^{CB}]'\right)\right]$
VI	$\frac{1}{2}\sum_{icd} \langle ai \| cd\rangle s_{bi}^{cd}$	$\frac{1}{2}\sum_{ICD} \left[\langle AI \| CD\rangle \left(s_{BI}^{CD} + [s_{BI}^{CD}]'\right) + \langle AI \| DC\rangle \left(s_{IB}^{CD} + [s_{IB}^{CD}]'\right)\right]$

signs are predicted. The difference between those molecules and the ones discussed before, is that they all contain multiple bonds, which means the probability of intruder state problems increases. Intruder state problems are common in Fock space coupled-cluster and were discussed briefly in Section 3.4.1. For instance, with a standard Fock space coupled-cluster code only 3 roots of H_2O can be converged in a DZP basis set. The second-order approximations seem to be less sensitive to intruder state problems, but they still are apparent.

Having a closer look at the IP's of CO, Table 4–14 column 3, one can see, that the two eigenvalues with value -1.30494 H for partitioning II do not seem to fit. Assuming that those are intruder states, leaving them out, and changing the order of the two eigenvalues at -0.58524 H and the eigenvalue at -0.57059 H, a correlation between eigenvalues of the different methods and the EOM-CCSD results can be found. Fig. 4–24 shows for the six lowest IP's the difference in eV between the IP-EOM-CCSD values and the other approximate methods. The experimental order of the lowest states confirms the IP-EOM-CCSD results (5σ 14.01 eV, 1π 16.91 eV, 4σ 19.72 eV) [121]. The usual trend is found, that the second-order approximations

overcorrect the Hartree-Fock values. Focusing on the partitioning scheme II, the overcorrection leads for the IP's at 19.4 eV and 13.9 eV to a larger difference to IP-EOM-CCSD than Hartree-Fock.

The same can be done for the IP's of H_2CO, Table 4–15 column 3. Leaving the eigenvalue for partitioning II at -1.59545 H out, leads to the energy differences in eV, shown in Fig. 4–25. The lowest IP-EOM-CCSD results are confirmed by experiment (b_2 10.9 eV, b_1 14.5 eV, b_1 16.1 eV, b_2 17.0 eV, b_1 21.4 eV) [121]. Again, the Hartree-Fock values are generally overcorrected, with larger differences to IP-EOM-CCSD for the second-order approximations at 10.4 eV, 14.2 eV, and 15.7 eV than Hartree-Fock.

For HCN, Table 4–16, it is very difficult to see which eigenvalues belong to which IP and it was not attempted to correlate the different states.

Fig. 4–24 and Fig. 4–25 show, that when intruder states are taken into account, it is possible to make the connection between the EOM-CCSD values and the second-order approximations. However, the intruder states also influence the other eigenvalues through the diagonalization of the Hamiltonians [122]. Included in all the tables are the percentages of singles. If the percentage is high, the corresponding IP root has mainly one-hole character. The smaller the percentage gets, the more two-hole one-particle character the root has (i.e. an intruder state gains influence), which lowers the quality of the root. A high percentage of singles for EA's means, that the character of the root is mainly one-particle character, a low percentage indicates an increasing influence of a two-particle one-hole state.

In Table 4–10, Table 4–12, and Table 4–13 the percentage of singles is high for all roots of HF, NH_3, and CH_4. In relation, the second-order IP's and EA's consistently improve Koopmans' values. For H_2O (Table 4–11) the percentage of singles for the second highest IP's is only 60.4%. Consequently, inconsistencies in the second-order eigenvalues, especially for the EA's, occur. For CO the third highest IP has only a

Table 4–9. Dipole moments in Deb

	HF	part. I	part. II	nonit.	Brueckner	MBPT(2)	CCSD
HF	2.054	1.948	1.937	1.947	1.941	1.945	1.935
H_2O	2.102	2.023	2.013	2.026	2.010	2.012	1.993
NH_3	1.677	1.665	1.661	1.664	1.654	1.655	1.631
HCN	3.259	2.937	2.901	2.939	2.923	2.894	2.916
CO	0.369	-0.439	-0.376	-0.357	-0.188	-0.310	-0.064
H_2CO	2.934	2.310	2.285	2.353	2.366	2.326	2.387

value of 53.2% singles, for H_2CO that value is 43.8%, and for HCN 43.8% (Table 4–14, Table 4–15, Table 4–16) and significant errors occur in the IP and the EA spectra.

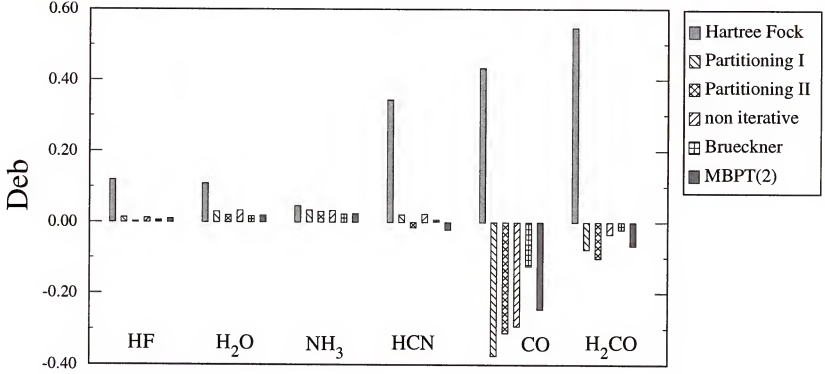

Figure 4–14. Dipole moment differences from CCSD dipole moments in Deb

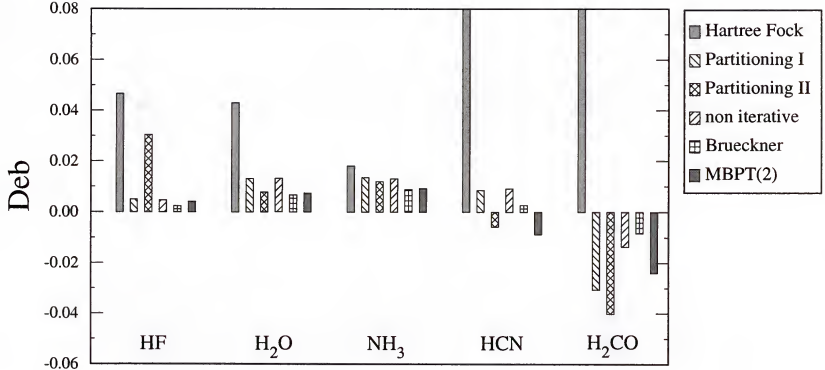

Figure 4–15. Dipole moment differences from CCSD dipole moments in Deb, the Hartree-Fock values for HCN and H_2CO are cut off

Table 4–10. Negative IP's and EA's in Hartree for HF/DZP

HF	part. I	part. II	nonit.	IP/EA-EOM-CCSD	%S
-26.28539	-25.05174	-25.08629	-25.08724	-25.65810	85.7
-1.59133	-1.39889	-1.41129	-1.40721	-1.43576	82.9
-0.75860	-0.66569	-0.67669	-0.67275	-0.71583	95.7
-0.64098	-0.50330	-0.51584	-0.51080	-0.56560	94.9
-0.64098	-0.50330	-0.51584	-0.51080	-0.56560	94.9
0.22143	0.20110	0.19894	0.20041	0.20349	98.7
0.98659	0.91893	0.91275	0.91538	0.92105	94.5
1.05931	1.01886	1.01039	1.01504	1.01912	96.7
1.05931	1.01886	1.01039	1.01504	1.01912	96.7
1.14869	1.10746	1.10342	1.10536	1.10492	95.2
1.50856	1.47320	1.47204	1.47277	1.46872	91.3

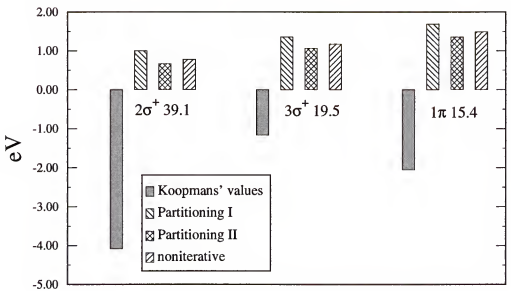

Figure 4–16. IP differences from IP-EOM-CCSD in eV for HF/DZP

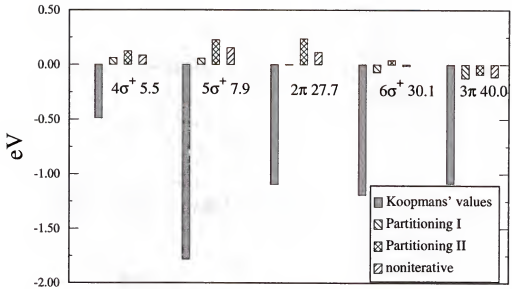

Figure 4–17. EA differences from EA-EOM-CCSD in eV for HF/DZP

Table 4–11. Negative IP's and EA's in Hartree for H_2O/DZP

HF	part. I	part. II	nonit.	IP/EA-EOM-CCSD	%S
-20.55751	-19.43178	-19.44382	-19.45110	-19.96103	84.2
-1.33196	-1.15820	-1.16357	-1.16282	-1.17460	60.4
-0.71173	-0.65495	-0.65948	-0.65786	-0.68814	95.8
-0.56036	-0.46204	-0.46725	-0.46518	-0.51003	94.7
-0.49922	-0.38784	-0.39324	-0.39024	-0.43616	94.4
0.22131	-0.04088	0.16231	0.18866	0.19516	97.9
0.31264	0.28087	0.27742	0.27987	0.28496	97.4
0.85080	0.72253	0.77832	0.73692	0.78943	93.2
0.86854	0.81350	0.81067	0.81641	0.82683	88.5
0.91033	0.86318	0.85997	0.86132	0.86787	90.4
1.02785	0.96681	0.96572	0.96528	0.97146	92.0

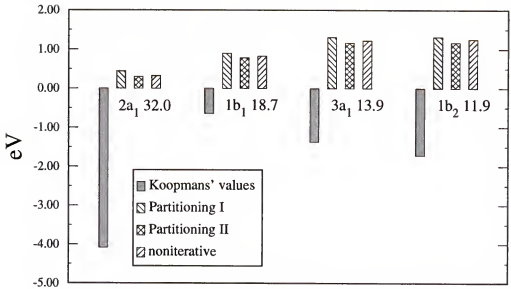

Figure 4–18. IP differences from IP-EOM-CCSD in eV for H_2O/DZP

Table 4–12. Negative IP's and EA's in Hartree for NH_3/DZP

HF	part. I	part. II	nonit.	IP/EA-EOM-CCSD	%S
-15.54241	-14.64534	-14.63836	-14.64866	-15.00636	83.3
-1.13735	-1.00089	-0.99994	-1.00092	-1.01459	81.3
-0.62069	-0.57526	-0.57474	-0.57445	-0.59681	95.4
-0.62069	-0.57526	-0.57474	-0.57445	-0.59681	95.4
-0.42676	-0.35657	-0.35561	-0.35522	-0.38400	94.6
0.23629	0.19716	0.19732	0.19810	0.20678	97.6
0.34430	0.30176	0.30179	0.30253	0.31181	96.9
0.34430	0.30176	0.30179	0.30253	0.31181	96.9
0.65714	0.60481	0.60487	0.60580	0.60868	92.8
0.65714	0.60481	0.60487	0.60580	0.60868	92.8
0.68698	0.63031	0.63087	0.63160	0.63969	94.8

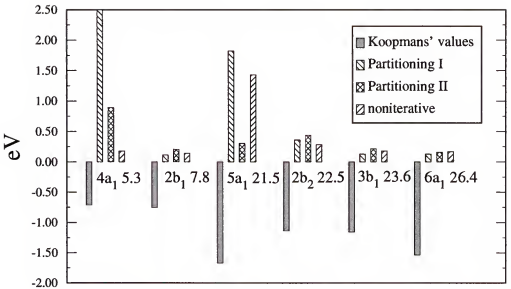

Figure 4–19. EA differences from EA-EOM-CCSD in eV for H_2O/DZP, value for partitioning I at 5.3 eV is cut off

Table 4–13. Negative IP's and EA's in Hartree for CH_4/DZP

HF	part. I	part. II	nonit.	IP/EA-EOM-CCSD	%S
-11.21049	-10.57459	-10.56399	-10.57498	-10.76674	82.8
-0.94181	-0.84581	-0.84338	-0.84531	-0.85393	88.0
-0.54314	-0.51003	-0.50799	-0.50877	-0.52187	95.2
-0.54314	-0.51003	-0.50799	-0.50877	-0.52187	95.2
-0.54314	-0.51003	-0.50799	-0.50877	-0.52187	95.2
0.29706	0.24337	0.24321	0.25162	0.26196	94.3
0.31397	0.29064	0.29102	0.29129	0.29531	94.3
0.31397	0.29064	0.29102	0.29129	0.29531	98.3
0.31397	0.29064	0.29102	0.29129	0.29531	98.3
0.48072	0.41598	0.41752	0.41722	0.42371	98.3
0.48072	0.41598	0.41752	0.41722	0.42371	96.8

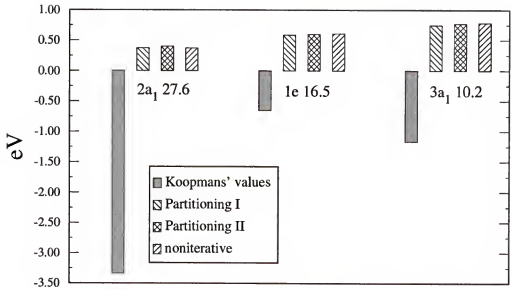

Figure 4–20. IP differences from IP-EOM-CCSD in eV for NH_3/DZP

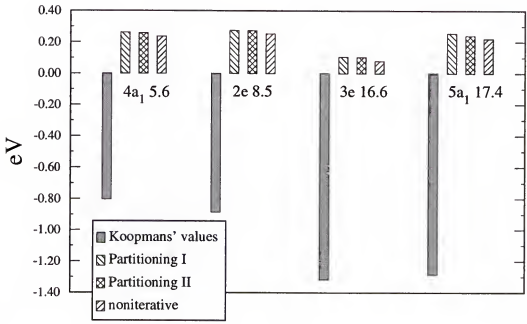

Figure 4–21. EA differences from EA-EOM-CCSD in eV for NH_3/DZP

Table 4–14. Negative IP's and EA's in Hartree for CO/DZP

HF	part. I	part. II	nonit.	IP/EA-EOM-CCSD	%S
-20.67026	-19.33478	-19.40594	-19.44733	-20.07916	84.1
-11.38191	-10.91112	-10.85325	-10.88541	-10.98422	83.2
-1.50623	-1.22295	-1.30494	-1.19841	-1.31468	53.2
-0.80078	-0.57478	-1.30494	-0.58294	-0.71333	89.3
-0.62837	-0.57151	-1.23034	-0.57827	-0.60624	93.5
-0.62837	-0.57151	-0.58524	-0.57827	-0.60624	93.5
-0.55387	-0.45701	-0.58524	-0.45615	-0.51021	92.9
0.12943	0.09083	-0.57059	0.00011	0.10827	96.0
0.12943	0.09083	-0.45935	0.00011	0.10827	96.0
0.30366	0.23445	0.28225	0.28378	0.28706	98.5
0.47417	0.40781	0.33601	0.40863	0.42348	93.7
0.47417	0.40781	0.33601	0.40863	0.42348	93.7
0.55891	0.48128	0.42509	0.50598	0.51555	91.0

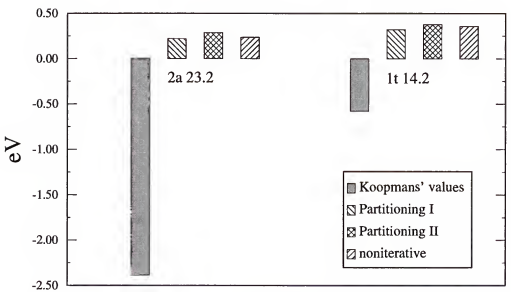

Figure 4–22. IP differences from IP-EOM-CCSD in eV for CH_4/DZP

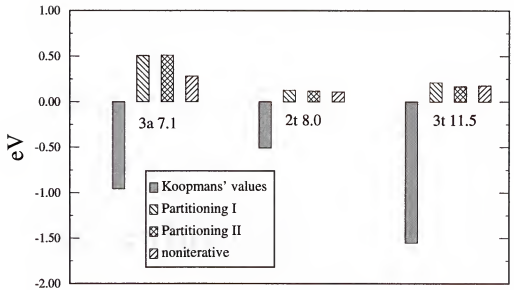

Figure 4–23. EA differences from EA-EOM-CCSD in eV for CH_4/DZP

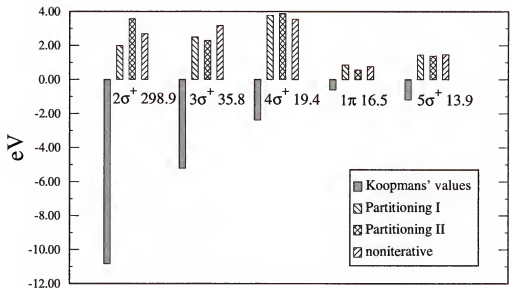

Figure 4–24. IP differences from IP-EOM-CCSD in eV for CO/DZP

Table 4–15. Negative IP's and EA's in Hartree for H_2CO/DZP

HF	part. I	part. II	nonit.	IP/EA-EOM-CCSD	%S
-20.57847	-19.24650	-19.29043	-19.32706	-19.97270	83.3
-11.35315	-10.78168	-10.74734	-10.76450	-10.91576	82.3
-1.39698	-1.20105	-1.59545	-1.10494	-1.17432	43.8
-0.86952	-0.77683	-1.14507	-0.77595	-0.79056	88.5
-0.68874	-0.60810	-0.76830	-0.60098	-0.62874	91.3
-0.64665	-0.49467	-0.59752	-0.50779	-0.57800	92.5
-0.52887	-0.48516	-0.50529	-0.49653	-0.52248	93.5
-0.44189	-0.31004	-0.50235	-0.32206	-0.38357	93.5
0.11400	0.04509	-0.32395	-0.20172	0.08035	95.4
0.27621	0.18690	0.05441	-0.00165	0.24624	96.8
0.28903	0.24561	0.23365	0.23336	0.26362	98.0
0.37970	0.33207	0.25326	0.32630	0.35703	96.9
0.44520	0.36889	0.35501	0.34276	0.40746	89.9
0.46922	0.39745	0.36789	0.36954	0.40942	92.2

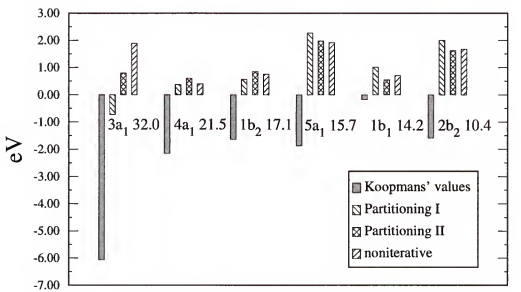

Figure 4–25. IP differences from IP-EOM-CCSD in eV for H_2CO/DZP

Table 4–16. Negative IP's and EA's in Hartree for HCN/DZP

HF	part. I	part. II	nonit.	IP/EA-EOM-CCSD	%S
-15.61928	-14.57737	-84.58809	-14.60710	-15.07147	82.1
-11.31547	-10.69301	-14.57316	-10.68916	-10.88826	82.8
-1.22330	-8.91337	-10.69232	-5.25436	-1.05901	47.4
-0.81278	-5.26210	-10.33742	-0.70557	-0.74736	90.7
-0.58113	-0.71036	-0.69820	-0.48857	-0.50258	91.1
-0.48710	-0.49220	-0.48794	-0.48857	-0.49657	95.7
-0.48710	-0.49220	-0.48794	0.08215	-0.49657	95.7
0.15607	0.08370	-0.30914	0.08215	0.13216	95.5
0.15607	0.08370	0.08208	0.13958	0.13216	95.5
0.22862	0.16644	0.08208	0.35395	0.19493	96.6
0.41458	0.32914	0.27179	0.38467	0.38976	96.7
0.47164	0.37629	0.33715	0.38467	0.42234	93.6
0.47164	0.37629	0.33715	0.42320	0.42234	93.6

CHAPTER 5
CONCLUSION

In this dissertation the correlated independent particle (CIP) model is discussed. The CIP model can be regarded as a generalized Hartree-Fock model, which includes correlation, or as an approximation to density matrix functional theory.

A correlated independent particle (CIP) model is formulated, which has the general form $(f + v_c)\phi_p = \varepsilon_p \phi_p$, where f is the Fock operator and v_c is the correlation potential to be determined, while the ϕ_p are the one-particle solutions. The first question to be answered is, what conditions should be imposed leading to the construction of the correlation potential. That condition is chosen to be the exactness of the ionization potentials and electron affinities, which correspond to the eigenvalues of the model. This choice is inspired and supported by the extended Koopman's theorem.

In Chapter 2, following the introduction, the basic principles and ideas, leading to the formulation of the CIP model, are discussed. Theorems and proofs are summarized, which are essential to density matrix functional theory (DMFT). In DMFT the total energy is written as a functional of the density matrix, and the energy is minimized with respect to the density matrix. Even though DMFT is similar in spirit to density functional theory, where local potentials are employed, the potentials used in DMFT are general, giving the possibility for nonlocal potentials. While the kinetic energy and the exchange term are known in DMFT, the correlation energy functional is unknown.

The extended Koopmans' theorem is summarized in Chapter 2 as well. While Koopmans' theorem provides a simple one-electron model for ionization and electron

attachment, the extended Koopmans' theorem is a generalization, which uses a correlated wave-function to describe the unionized or unattached system. The extended Koopmans' theorem employs a nonlocal and nonhermitian effective one-particle operator, whose eigenvalues are the variationally optimized energy differences between the ionic and parent species, i.e. the ionization potentials and the negative of the electron affinities.

In Chapter 3 the condition of exactness of the ionization potentials and electron affinities as eigenvalues is exploited to obtain correlation potentials. If no truncation is introduced, the equation-of-motion coupled-cluster method for ionization potentials and electron affinities (IP-EOM-CC/EA-EOM-CC) yields exact ionization potentials and electron affinities. An energy-dependent correlation potential is obtained from a partitioned equation-of-motion approach, which reproduces IP-EOM-CC and EA-EOM-CC results as orbital energies. As a consequence of the energy dependence of the correlation potential, a different effective Hamiltonian corresponds to each orbital and each eigenvalue. An eigenvalue equation has therefore to be solved for each eigenvalue separately. The resulting orbitals are nonorthogonal, and the density matrix is not idempotent, even though the general form of the CIP model as shown above is maintained.

The energy dependence is regarded as a disadvantage, but can be removed by using the Fock space coupled-cluster method to extract a correlation potential. The Fock space coupled-cluster method for the one-hole and one-particle sector and the IP-EOM-CC/EA-EOM-CC method are equivalent, and the eigenvalues of the effective Hamiltonians are the same, if the same truncation level is used. The correlation potential is constructed from the Fock space coupled-cluster amplitudes. Since those are difficult to converge for all ionization potentials and electron affinities, an alternative route to build the correlation potential is shown, which uses the eigenvectors

of the transformed Hamiltonian in the full configuration space. The resultant correlation potential is energy-independent and universal for all orbitals. In a one-step procedure the exact FS-CC results for ionization potentials and electron affinities are obtained within the CIP model, using the correlation potential derived from the Fock space coupled-cluster method.

Also, in Chapter 3 the electron-propagator method is discussed. In contrast to the EOM-CC and Fock space methods, the one-hole and the one-particle sectors are in general not decoupled, but described simultaneously. From the electron-propagator method a formally exact one-electron theory can be derived, where an energy-dependent effective Hamiltonian is employed, which is the sum of the Fock operator and the energy-dependent self-energy. It is shown, that if the coupled-cluster wave-function is used as the ground state wave-function, the one-hole and one-particle sector decouple with respect to the eigenvalues. The self-energy is then shown to be equivalent to the correlation potential, derived from the partitioned equation-of-motion coupled-cluster method.

In Chapter 4 the infinite-order correlation potential, derived from the Fock space coupled-cluster approach, is approximated by a potential correct through second order in perturbation. Since the one-hole and the one-particle sectors are decoupled in the Fock space coupled-cluster method, the orbitals, obtained from the CIP model, are rotations within the occupied-occupied space and rotations within the virtual-virtual space and are therefore not an improvement over Hartree-Fock orbitals. To improve the orbitals, an additional condition has to be applied. The Brillouin-Brueckner condition is used to assure, that the single determinant, that is formed by the orbitals, has maximum overlap with the exact wave-function. The Brueckner condition is ensured through second order in perturbation.

Two different partitioning schemes of the Hamiltonian were used, leading to two different second-order Hamiltonians. Results for ionization potentials, electron

affinities, and dipole moments are given for some sample molecules. The dipole moments show significant improvement over the Hartree-Fock values, if the second-order Brueckner determinant is used.

The second-order IP's and EA's show mostly an improvement over Koopmans' values. However, it became apparent that intruder state problems are severe; in certain cases intruder states from the shake-up eigenspectrum even occur among the principal IP's. Certainly, the quality of the IP's and EA's is influenced by intruder states. In Section 3.4.2 it was shown, how to obtain Fock space amplitudes through EOM-CC amplitudes. In order to ensure, that intruder states do not occur in the principal IP and EA spectra of the second-order effective Hamiltonian, the EOM-CC problem could be expressed up to second order in perturbation, and the second-order Fock space amplitudes could be calculated through the second-order EOM-CC amplitudes, as has been shown for the infinite-order expressions.

REFERENCES

[1] P. Hohenberg and W. Kohn, Phys. Rev. B **136**, 864 (1964).

[2] W. Kohn and L. J. Sham, Phys. Rev. **140**, 1133 (1965).

[3] S. H. Vosko, L. Wilk, and M. Nusair, Can. J. Phys. **58**, 1200 (1980).

[4] C. T. Lee, W. T. Yang, and R. G. Parr, Phys. Rev. B **37**, 785 (1988).

[5] J. P. Perdew, Phys. Rev. Lett. **55**, 1665 (1985).

[6] J. P. Perdew and W. Yue, Phys. Rev. B **33**, 8800 (1986).

[7] A. D. Becke, J. Chem. Phys. **84**, 4524 (1986).

[8] R. G. Parr and W. Yang, *Density Functional Theory of Atoms and Molecules* (Oxford University Press, Oxford, 1989).

[9] S. Ivanov, S. Hirata, and R. J. Bartlett, Phys. Rev. Lett. **83**, 5455 (1999).

[10] A. Görling, Phys. Rev. Lett. **83**, 5459 (1999).

[11] I. Grabowski, S. Hirata, S. Ivanov, and R. J. Bartlett, J. Chem. Phys. **116**, 4415 (2002).

[12] A. Szabo and N. S. Ostlund, *Modern Quantum Chemistry* (Dover Publications, New York, 1989).

[13] J. A. Koopmans, Physica **1**, 104 (1933).

[14] R. J. Bartlett, Ann. Rev. Phys. Chem. **32**, 359 (1981).

[15] I. Lindgren and J. Morrison, *Atomic Many-Body Theory* (Springer, Berlin, 1982).

[16] R. J. Bartlett, J. Phys. Chem. **93**, 1697 (1989).

[17] P.-O. Löwdin, Adv. Chem. Phys. **2**, 207 (1959).

[18] Y. Öhrn and G. Born, Adv. Quantum Chem. **13**, 1 (1981).

[19] J. Schirmer, L. S. Cederbaum, and O. Walter, Phys. Rev. A **28**, 1237 (1983).

[20] J. V. Ortiz, Adv. Quantum Chem. **35**, 33 (1999).

[21] O. Dolgounitcheva, V. G. Zakrzewski, and J. V. Ortiz, Int. J. Quantum Chem. **90**, 1547 (2000).

[22] J. V. Ortiz, J. Phys. Chem. A **106**, 5924 (2002).

[23] O. Dolgounitcheva, V. G. Zakrzewski, and J. V. Ortiz, J. Phys. Chem. A **106**, 8411 (2002).

[24] J. D. Doll and W. P. Reinhardt, J. Chem. Phys. **57**, 1169 (1972).

[25] T. L. Gilbert, Phys. Rev. B **12**, 2111 (1975).

[26] G. Csányi and T. A. Arias, Phys. Rev. B **61**, 7348 (2000).

[27] M. A. Buijse and E. J. Bärends, Mol. Phys. **100**, 401 (2002).

[28] S. Gödecker and C. J. Umrigar, Phys. Rev. Lett. **81**, 866 (1998).

[29] J. Cioslowski and K. Pernal, J. Chem. Phys. **111**, 3396 (1999).

[30] J. Cioslowski and K. Pernal, Phys. Rev. A **61**, 034503 (2000).

[31] J. Cioslowski, P. Ziesche, and K. Pernal, Phys. Rev. B **63**, 205105 (2001).

[32] V. N. Staroverov and G. E. Scuseria, J. Chem. Phys. **117**, 2489 (2002).

[33] J. M. Herbert and J. E. Harriman, Int. J. Quantum Chem. **90**, 355 (2002).

[34] K. Yasuda, Phys. Rev. A **63**, 032517 (2001).

[35] D. A. Mazziotti, Chem. Phys. Lett. **338**, 323 (2001).

[36] K. Yasuda, Phys. Rev. Lett. **88**, 053001 (2002).

[37] P. Ziesche, Int. J. Quantum Chem. **90**, 342 (2002).

[38] J. Cioslowski and R. Lopez-Boada, J. Chem. Phys. **109**, 4156 (1998).

[39] J. Cioslowski and R. Lopez-Boada, Chem. Phys. Lett. **307**, 445 (1999).

[40] K. A. Brueckner, Phys. Rev. **96**, 508 (1954).

[41] P.-O. Löwdin, J. Math. Phys. **3**, 1171 (1962).

[42] S. Larsson, Chem. Phys. Lett. **7**, 165 (1970).

[43] S. Larsson, J. Chem. Phys. **58**, 5049 (1973).

[44] R. A. Chiles and C. E. Dykstra, J. Chem. Phys. **74**, 4544 (1981).

[45] G. D. Purvis and R. J. Bartlett, J. Chem. Phys. **76**, 1910 (1982).

[46] L. Adamowicz and R. J. Bartlett, Intern. J. Quantum Chem. Symposium **19**, 217 (1986).

[47] N. C. Handy *et al.*, Chem. Phys. Lett. **164**, 185 (1989).

[48] L. Z. Stolarczyk and H. J. Monkhorst, Intern. J. Quantum Chem. Symposium **18**, 267 (1984).

[49] G. E. Scuseria, Chem. Phys. Lett. **226**, 251 (1994).

[50] G. E. Scuseria, Int. J. Quantum Chem. **55**, 165 (1995).

[51] I. Lindgren and S. Salomonson, Int. J. Quantum Chem. **90**, 294 (2002).

[52] O. W. Day, D. W. Smith, and C. Garrod, Intern. J. Quantum Chem. Symposium **8**, 501 (1974).

[53] M. M. Morrell, R. G. Parr, and M. Levy, J. Chem. Phys. **62**, 549 (1975).

[54] J. Katriel and E. R. Davidson, Proc. Natl. Acad. Sci. USA **77**, 4403 (1980).

[55] J. Olsen and D. Sundholm, Chem. Phys. Lett. **288**, 282 (1998).

[56] R. C. Morrison, J. Chem. Phys. **96**, 3718 (1992).

[57] D. Sundholm and J. Olsen, J. Chem. Phys. **98**, 3999 (1993).

[58] D. Sundholm and J. Olsen, J. Chem. Phys. **99**, 6222 (1993).

[59] J. M. O. Matos and O. W. Day, Int. J. Quantum Chem. **31**, 871 (1987).

[60] A. Messiah, *Quantum Mechanics* (North-Holland Publishing Company, Amsterdam, 1961), Vol. I.

[61] A. J. Coleman and V. I. Yukalov, *Reduced Density Matrices: Coulson's Challenge* (Springer, New York, 2000).

[62] M. Berrondo and O. Goscinski, Intern. J. Quantum Chem. Symposium **9**, 67 (1975).

[63] R. A. Donnelly and R. G. Parr, J. Chem. Phys. **69**, 4431 (1978).

[64] M. Levy, Proc. Natl. Acad. Sci. USA **76**, 6062 (1979).

[65] A. J. Coleman, Rev. Modern Phys. **35**, 668 (1963).

[66] P.-O. Löwdin, Phys. Rev. **97**, 1474 (1955).

[67] S. M. Valone, J. Chem. Phys. **73**, 1344 (1980).

[68] E. V. Ludeña and A. Sierraalta, Phys. Rev. A **32**, 19 (1985).

[69] T. T. Nguyen-Dang, E. V. Ludeña, and Y. Tal, J. Mol. Struct. (Theochem) **120**, 247 (1985).

[70] G. Zumbach and K. Maschke, J. Chem. Phys. **82**, 5604 (1985).

[71] E. M. Zoueva, V. I. Galkin, and A. R. Cherkasov, J. Mol. Struct. (Theochem) **501-502**, 133 (2000).

[72] E. H. Lieb, Int. J. Quantum Chem. **24**, 243 (1983).

[73] M. Nooijen, J. Chem. Phys. **111**, 8356 (1999).

[74] E. H. Lieb, Phys. Rev. Lett. **46**, 457 (1981).

[75] D. W. Smith and O. W. Day, J. Chem. Phys. **62**, 113 (1975).

[76] O. W. Day, D. W. Smith, and R. C. Morrison, J. Chem. Phys. **62**, 115 (1975).

[77] B. T. Pickup and J. G. Snijders, Chem. Phys. Lett. **153**, 69 (1988).

[78] K. Pernal and J. Cioslowski, J. Chem. Phys. **114**, 4359 (2001).

[79] A. Holas, Phys. Rev. A **59**, 3454 (1999).

[80] M. A. Buijse, Ph.D. thesis, Vrije Universiteit, Amsterdam, 1991.

[81] G. Csányi, S. Gödecker, and T. A. Arias, Phys. Rev. A **65**, 032510 (2002).

[82] A. J. Cohen and E. J. Baerends, Chem. Phys. Lett. **364**, 409 (2002).

[83] L. Cohen and C. Frishberg, Phys. Rev. A **13**, 927 (1976).

[84] H. Nakatsuji, Phys. Rev. A **14**, 41 (1976).

[85] M. Levy, in *Density Matrices and Density Functionals*, edited by R. Erdahl and V. H. Smith (D. Reidel Pub. Co., Boston, 1987).

[86] J. Cioslowski, P. Ziesche, and K. Pernal, J. Chem. Phys. **115**, 8725 (2001).

[87] J. Cioslowski and K. Pernal, J. Chem. Phys. **117**, 67 (2002).

[88] J. P. Perdew and Y. Wang, Phys. Rev. B **45**, 13244 (1992).

[89] A. L. Fetter and J. D. Walecka, *The Quantum Theory of Many-Particle Systems* (Mcgraw-Hill, New York, 1971).

[90] J. Cizek, J. Chem. Phys. **45**, 4256 (1966).

[91] J. Cizek, Adv. Chem. Phys. **14**, 35 (1669).

[92] I. Lindgren, Intern. J. Quantum Chem. Symposium **12**, 33 (1978).

[93] B. H. Brandow, Rev. Modern Phys. **39**, 771 (1967).

[94] H. Sekino and R. J. Bartlett, Intern. J. Quantum Chem. Symposium **18**, 255 (1984).

[95] J. F. Stanton and R. J. Bartlett, J. Chem. Phys. **98**, 7029 (1993).

[96] R. J. Bartlett, in *Modern Electronic Structure Theory, Part I*, edited by D. R. Yarkony (World Scientific Publishing Co., Singapore, 1995).

[97] R. P. Mattie, Ph.D. thesis, University of Florida, Gainesville, USA, 1995.

[98] M. Nooijen and R. J. Bartlett, J. Chem. Phys. **102**, 3629 (1995).

[99] J. F. Stanton, J. Chem. Phys. **101**, 8928 (1994).

[100] P.-O. Löwdin, J. Mol. Spectr. **10**, 12 (1963).

[101] J. Geertsen, M. Rittby, and R. J. Bartlett, Chem. Phys. Lett. **164**, 57 (1989).

[102] S. R. Gwaltney, M. Nooijen, and R. J. Bartlett, Chem. Phys. Lett. **248**, 189 (1996).

[103] M. Nooijen, S. A. Perera, and R. J. Bartlett, Chem. Phys. Lett. **266**, 456 (1997).

[104] B. T. Pickup and O. Goscinski, Mol. Phys. **26**, 1013 (1973).

[105] G. D. Purvis and Y. Öhrn, Intern. J. Quantum Chem. Symposium **11**, 359 (1977).

[106] P.-O. Löwdin, Phys. Rev. **139**, A357 (1965).

[107] L. Meissner and R. J. Bartlett, Int. J. Quantum Chem. **27**, 67 (1993).

[108] M. Nooijen and J. G. Snijders, Int. J. Quantum Chem. **26**, 55 (1992).

[109] M. Nooijen and J. G. Snijders, Int. J. Quantum Chem. **48**, 15 (1993).

[110] D. Mukherjee and S. Pal, Adv. Quantum Chem. **20**, 292 (1989).

[111] M. A. Haque and D. Mukherjee, J. Chem. Phys. **80**, 5058 (1984).

[112] D. Mukherjee, Intern. J. Quantum Chem. Symposium **20**, 409 (1986).

[113] L. Meissner and R. J. Bartlett, J. Chem. Phys. **94**, 6670 (1991).

[114] A. Hesselmann and G. Jansen, Chem. Phys. Lett. **315**, 248 (1999).

[115] R. K. Nesbet, Phys. Rev. **109**, 1632 (1958).

[116] V. Kvasnička, Theoret. Chim. Acta **36**, 297 (1975).

[117] L. Z. Stolarczyk and H. J. Monkhorst, Phys. Rev. A **32**, 725 (1985).

[118] L. Z. Stolarczyk and H. J. Monkhorst, Phys. Rev. A **32**, 743 (1985).

[119] I. Lindgren, Phys. Rev. A **31**, 1273 (1985).

[120] D. J. Thouless, *The Quantum Mechanics of Many-Body Systems* (Academic, New York, 1961).

[121] K. Kimura *et al.*, *Handbook of Photoelectron Spectra of Fundamental Organic Molecules* (Halsted, New York, 1981).

[122] M. Nooijen and V. Lotrich, J. Chem. Phys. **113**, 494 (2000).

BIOGRAPHICAL SKETCH

Ariana Beste was born on June 28th, 1973, in Naumburg/Saale, Germany. Ariana is the daughter of Gudrun Beste and Herbert Beste. She graduated from high school in June 1992. In September 1994, she received her B.S. degree in chemistry from the Philipps-Universität Marburg, Germany. During the last year of her graduate education, she specialized in computational chemistry under the supervision of Dr. Gernot Frenking, in the field of theoretical investigations of reaction mechanisms of transition metal complexes. Ariana received her M.S. in chemistry in April 1999. Also in April 1999, she received a first academic degree in computer science as a postgraduate degree. Ariana spent the next three months doing research at the Universidad de Barcelona, Spain, performing theoretical analysis of chemical bonds on surfaces.

Ariana came to the USA in August of 1999 and joined the Physical Chemistry Division of the Chemistry Department at the University of Florida. After completing her written and oral examinations in September 2001, Ariana was admitted to the Ph.D. program and started her research on the theoretical and computational aspects of independent particle models, which include electron correlation, under the supervision of Dr. Rodney J. Bartlett.

I certify that I have read this study and that in my opinion it conforms to acceptable standards of scholarly presentation and is fully adequate, in scope and quality, as a dissertation for the degree of Doctor of Philosophy.

Rodney J. Bartlett, Chair
Graduate Research Professor of Chemistry

I certify that I have read this study and that in my opinion it conforms to acceptable standards of scholarly presentation and is fully adequate, in scope and quality, as a dissertation for the degree of Doctor of Philosophy.

Jeffrey L. Krause
Associate Professor of Chemistry

I certify that I have read this study and that in my opinion it conforms to acceptable standards of scholarly presentation and is fully adequate, in scope and quality, as a dissertation for the degree of Doctor of Philosophy.

Philip J. Brucat
Associate Professor of Chemistry

I certify that I have read this study and that in my opinion it conforms to acceptable standards of scholarly presentation and is fully adequate, in scope and quality, as a dissertation for the degree of Doctor of Philosophy.

Samuel B. Trickey
Professor of Physics

I certify that I have read this study and that in my opinion it conforms to acceptable standards of scholarly presentation and is fully adequate, in scope and quality, as a dissertation for the degree of Doctor of Philosophy.

Dmitrii Maslov
Associate Professor of Physics

This dissertation was submitted to the Graduate Faculty of the College of Liberal Arts and Sciences and to the Graduate School and was accepted as partial fulfillment of the requirements for the degree of Doctor of Philosophy.

May 2004

Dean, Graduate School